HOLTEC
INTERNATIONAL

Holtec Center, 555 Lincoln Drive West, Marlton, NJ 08053
Telephone (856) 797- 0900
Fax (856) 797 - 0909

SPENT FUEL POOL RACKS MODIFICATIONS WITH POISON MATERIAL INSERTS IN ANO UNIT 1

FOR

ENTERGY

Holtec Report No: HI-2022867

Holtec Project No: 1196

Report Class : SAFETY RELATED

THIS DOCUMENT IS NOT PROPRIETARY
SEE PAGE 4 OF 4

8-10-06

HOLTEC INTERNATIONAL

DOCUMENT NUMBER: HI-2022867

PROJECT NUMBER: 1196

DOCUMENT ISSUANCE AND REVISION STATUS

DOCUMENT NAME: SPENT FUEL POOL RACKS MODIFICATIONS WITH POISON MATERIAL INSERTS IN ANO UNIT-1

DOCUMENT CATEGORY: ☐ GENERIC ☒ PROJECT SPECIFIC

No.	Document Portion††	REVISION No. 0			REVISION No. 1			REVISION No. 2		
		Author's Initials	Date Approved	VIR #	Author's Initials	Date Approved	VIR #	Author's Initials	Date Approved	VIR #
1.	CHAP01	DMM	11/16/02	202651	-	-		DMM	1/17/02	726911
2.	CHAP02	CWB	11/16/02	871854	-	-		CWB	1/17/02	807558
3.	CHAP03	CWB	11/16/02	504354	-	-		CWB	1/17/02	711269
4.	CHAP04	ST	11/16/02	788335	ST	11/21/02	816617	DMM	1/17/02	734332
5.	CHAP05	EBR	11/16/02	691366	-	-		EBR	1/17/02	980931
6.	CHAP06	CWB	11/16/02	406182	CWB	11/21/02	623799	CWB	1/17/02	14788
7.	CHAP07	JZ	11/16/02	458172	-	-		JZ	1/17/02	886712

†† Chapter or section number.

HOLTEC INTERNATIONAL

DOCUMENT NUMBER: HI-2022867 PROJECT NUMBER: 1196

DOCUMENT ISSUANCE AND REVISION STATUS

DOCUMENT NAME: SPENT FUEL POOL RACKS MODIFICATIONS WITH POISON MATERIAL INSERTS IN ANO UNIT-1

DOCUMENT CATEGORY: ☐ GENERIC ☒ PROJECT SPECIFIC

No.	Document Portion††	REVISION No. 3			REVISION No. 4			REVISION No. 5		
		Author's Initials	Date Approved	VIR #	Author's Initials	Date Approved	VIR #	Author's Initials	Date Approved	VIR #
1.	CHAP01	DMM	2/25/03	686344	-	-	-	DMM	12/19/03	701998
2.	CHAP02	AK	2/25/03	195327	-	-	-	DMM	12/19/03	754039
3.	CHAP03	AK	2/25/03	962934	-	-	-	DMM	12/19/03	968723
4.	CHAP04	DMM	2/25/03	266472	DMM	11/18/03	165227	DMM	12/19/03	122189
5.	CHAP05	EBR	2/25/03	138108	-	-	-	-	-	-
6.	CHAP06	AK	2/25/03	531949	-	-	-	CWB	12/19/03	905606
7.	CHAP07	JZ	-	-	-	-	-	-	-	-

†† Chapter or section number.

HOLTEC INTERNATIONAL

DOCUMENT NUMBER: HI-2022867 PROJECT NUMBER: 1196

DOCUMENT ISSUANCE AND REVISION STATUS

DOCUMENT NAME: SPENT FUEL POOL RACKS MODIFICATIONS WITH POISON MATERIAL INSERTS IN ANO UNIT-1

DOCUMENT CATEGORY: ☐ GENERIC ☒ PROJECT SPECIFIC

No.	Document Portion††	REVISION No. 6			REVISION No. 7			REVISION No. 8		
		Author's Initials	Date Approved	VIR #	Author's Initials	Date Approved	VIR #	Author's Initials	Date Approved	VIR #
1.	CHAP01	SPA	7/5/06	620228	-	-	-	-	-	-
2.	CHAP02	SPA	7/5/06	700869	-	-	-	-	-	-
3.	CHAP03	SPA	7/5/06	723072	KC	7/17/06	558104	-	-	-
4.	CHAP04	KC	7/5/06	245294	KC	7/17/06	622989	KC	7/24/06	799666
5.	CHAP05	EBR	7/5/06	378241	-	-	-	-	-	-
6.	CHAP06	SPA	7/5/06	382403	DMM	7/17/06	296072	KC	7/24/06	527550

†† Chapter or section number.

DOCUMENT CATEGORIZATION

In accordance with the Holtec Quality Assurance Manual and associated Holtec Quality Procedures (HQPs), this document is categorized as a:

☐ Calculation Package[3] (Per HQP 3.2) ☒ Technical Report (Per HQP 3.2)(Such as a Licensing Report)

☐ Design Criterion Document (Per HQP 3.4) ☐ Design Specification (Per HQP 3.4)

☐ Other (Specify):

DOCUMENT FORMATTING

The formatting of the contents of this document is in accordance with the instructions of HQP 3.2 or 3.4 except as noted below:

DECLARATION OF PROPRIETARY STATUS

☒ Nonproprietary ☐ Holtec Proprietary ☐ Privileged Intellectual Property (PIP)

Documents labeled Privileged Intellectual Property contain extremely valuable intellectual/commercial property of Holtec International. They cannot be released to external organizations or entities without explicit approval of a company corporate officer. The recipient of Holtec's proprietary or Top Secret document bears full and undivided responsibility to safeguard it against loss or duplication.

Notes:

1. This document has been subjected to review, verification and approval process set forth in the Holtec Quality Assurance Procedures Manual. Password controlled signatures of Holtec personnel who participated in the preparation, review, and QA validation of this document are saved in the N-drive of the company's network. The Validation Identifier Record (VIR) number is a random number that is generated by the computer after the specific revision of this document has undergone the required review and approval process, and the appropriate Holtec personnel have recorded their password-controlled electronic concurrence to the document.

2. A revision to this document will be ordered by the Project Manager and carried out if any of its contents is materially affected during evolution of this project. The determination as to the need for revision will be made by the Project Manager with input from others, as deemed necessary by him.

3. Revisions to this document may be made by adding supplements to the document and replacing the "Table of Contents", this page and the "Revision Log".

SUMMARY OF REVISIONS

Revision 0 contains the following pages:	
COVER PAGE	1 page
QA AND ADMINISTRATIVE INFORMATION LOG	2 page
SUMMARY OF REVISIONS	1 pages
TABLE OF CONTENTS	8 pages
1.0 INTRODUCTION	5 pages
2.0 SPENT FUEL RACK FLUX TRAP GAP POISON INSERTS	10 pages
3.0 MATERIAL CONSIDERATIONS	6 pages
4.0 CRITICALITY SAFETY EVALUATION	43 pages
-- APPENDIX 4A	25 pages
5.0 THERMAL-HYDRAULIC CONSIDERATIONS	23 pages
6.0 STRUCTURAL/SEISMIC CONSIDERATIONS	56 pages
7.0 MECHANICAL ACCIDENTS	2 pages
TOTAL	182 pages

Revision 1

The changes made are

1. Revised table 4.2.2 and 4.2.3 to reflect change of burnup requirement for 2.0% enrichment fuel (from 0 to 0.5 MWD/MTU) for spent fuel storage in Unit 1 Region 1 racks. As a result Figure 4.1.1 is also revised.

2. Editorial changes to Section 6 .6.2 (iii) a).

The number of pages in the documents remains unchanged from revision 0.

Revision 2

Per verbal request from ANO, editorial changes were made to align the document closely with the Unit 2 licensing submittal (HI-20222868). All the changes are marked via revision bars.

Revision 3

Incorporate editorial changes as per the E-Mail by C Walker (ANO) to Debu Mitra-Majumdar (Holtec) dated Feb 17, 2003.Only sections 1 to 6 were modified. The e-mail is stored in the Holtec server at \projects\1196\e-mail\ANO-U1-2022867rev2-Comments

Revision 2 contains the following pages:

COVER PAGE	1 page
QA AND ADMINISTRATIVE INFORMATION LOG	3 page
SUMMARY OF REVISIONS	2 pages
TABLE OF CONTENTS	8 pages
1.0 INTRODUCTION	5 pages
2.0 SPENT FUEL RACK FLUX TRAP GAP POISON INSERTS	9 pages
3.0 MATERIAL CONSIDERATIONS	6 pages
4.0 CRITICALITY SAFETY EVALUATION	43 pages
-- APPENDIX 4A	26 pages
5.0 THERMAL-HYDRAULIC CONSIDERATIONS	22 pages
6.0 STRUCTURAL/SEISMIC CONSIDERATIONS	54 pages
7.0 MECHANICAL ACCIDENTS	2 pages
TOTAL	181 pages

Revision 4

Changes made to address comments from ANO. These were transmitted via e-mails from Christopher Walker (ANO) to D. Mitra-Majumdar (Holtec) on 11/10/03 and 11/11/03 and from Dana Miller (ANO) to D. Mitra-Majumdar (Holtec) on 11/10/03. Also, changes to the Region 3 racks criticality analysis, with stainless steel poison insert components, were also incorporated. All the changes are annotated by revision bars. Changes were made to Chapter 4 only.

Revision 5

Editorial changes made to chapters 1, 2, 3 and 4. Changes to chapter 6 include the addition of 2 new WPMR cases as described in Section 6.7. Subsections 6.8.4.3, 6.9.3.a, 6.9.4.c, and Table 6.9.1 have also been revised to reflect the additional cases. All changes are identified via revision bars.

Revision 5 contains the following pages:	
COVER PAGE	1 page
QA AND ADMINISTRATIVE INFORMATION LOG	3 page
SUMMARY OF REVISIONS	2 pages
TABLE OF CONTENTS	7 pages
1.0 INTRODUCTION	5 pages
2.0 SPENT FUEL RACK FLUX TRAP GAP POISON INSERTS	9 pages
3.0 MATERIAL CONSIDERATIONS	6 pages
4.0 CRITICALITY SAFETY EVALUATION	41 pages
-- APPENDIX 4A	25 pages
5.0 THERMAL-HYDRAULIC CONSIDERATIONS	22 pages
6.0 STRUCTURAL/SEISMIC CONSIDERATIONS	54 pages
7.0 MECHANICAL ACCIDENTS	2 pages
TOTAL	177 pages

Revision 6

The principal changes in this revision are the addition of a new fuel type (HTP fuel), removal of Chapter 6, and incorporation of client comments. Editorial changes are made to chapters 1, 2, 3. Chapter 4 is replaced in its entirety. Editorial changes are made to Chapter 5, and results are updated in this chapter to reflect the new fuel type. Previous Chapter 7 is now Chapter 6, with editorial changes.

Revision 6 contains the following pages:	
COVER PAGE	1 page
QA AND ADMINISTRATIVE INFORMATION LOG	4 pages
SUMMARY OF REVISIONS	3 pages
TABLE OF CONTENTS	7 pages
1.0 INTRODUCTION	5 pages
2.0 SPENT FUEL RACK FLUX TRAP GAP POISON INSERTS	9 pages
3.0 MATERIAL CONSIDERATIONS	6 pages
4.0 CRITICALITY SAFETY EVALUATION	85 pages
-- APPENDIX 4A	25 pages
5.0 THERMAL-HYDRAULIC CONSIDERATIONS	22 pages
6.0 MECHANICAL ACCIDENTS	2 pages
TOTAL	169 pages

Revision 7

The principal change in this revision is the evaluation of the Region 3 fuel storage in 3 of 4 arrangement (3 fresh and 1 spent in a 2x2 array) under the assumption that all of the Metamic panels are damaged. Also, the boron dilution analyses were modified to show dilution times for normal storage conditions only. Changes are made to chapters 4 to reflect these. Editorial changes were also made to chapter 3 and 4 per client comments.

Revision 7 contains the following pages:	
COVER PAGE	1 page
QA AND ADMINISTRATIVE INFORMATION LOG	4 pages
SUMMARY OF REVISIONS	3 pages
TABLE OF CONTENTS	7 pages
1.0 INTRODUCTION	5 pages
2.0 SPENT FUEL RACK FLUX TRAP GAP POISON INSERTS	9 pages
3.0 MATERIAL CONSIDERATIONS	6 pages
4.0 CRITICALITY SAFETY EVALUATION	85 pages
-- APPENDIX 4A	25 pages
5.0 THERMAL-HYDRAULIC CONSIDERATIONS	22 pages
6.0 MECHANICAL ACCIDENTS	2 pages
TOTAL	169 pages

Revision 8

Editorial changes are made to chapters 4 and 6.

Revision 8 contains the following pages:	
COVER PAGE	1 page
QA AND ADMINISTRATIVE INFORMATION LOG	4 pages
SUMMARY OF REVISIONS	4 pages
TABLE OF CONTENTS	7 pages
1.0 INTRODUCTION	5 pages
2.0 SPENT FUEL RACK FLUX TRAP GAP POISON INSERTS	9 pages
3.0 MATERIAL CONSIDERATIONS	6 pages
4.0 CRITICALITY SAFETY EVALUATION	85 pages
-- APPENDIX 4A	25 pages
5.0 THERMAL-HYDRAULIC CONSIDERATIONS	22 pages
6.0 MECHANICAL ACCIDENTS	2 pages
TOTAL	170 pages

TABLE OF CONTENTS

1.0 INTRODUCTION 1-1
1.1 References 1-4

2.0 SPENT FUEL RACK FLUX TRAP GAP POISON INSERT ASSEMBLY DESIGN 2-1
2.1 Introduction 2-1
2.2 Summary of Principal Design Criteria 2-1
2.3 Applicable Codes and Standards 2-2
2.4 Quality Assurance Program 2-7
2.5 Mechanical Design 2-7
2.6 Fabrication 2-9
2.7 Installation 2-9

3.0 MATERIAL CONSIDERATIONS 3-1
3.1 Introduction 3-1
3.2 Structural Materials 3-1
3.3 Neutron Absorbing Material 3-1
3.3.1 METAMIC® Material Characteristics 3-3
3.4 Compatibility with Environment 3-3
3.5 Heavy Load Considerations 3-4
3.6 References 3-4

4.0 CRITICALITY SAFETY ANALYSIS 4-1
4.1 Introduction and Summary 4-1
4.2 Methodology 4-3
4.3 Acceptance Criteria 4-5
4.4 Assumptions 4-6
4.5 Input Data 4-6
4.5.1 Fuel Assembly Specification 4-6
4.5.2 Core Operating Parameters 4-7
4.5.3 Axial Burnup Distribution 4-7
4.5.4 Core Inserts 4-7
4.5.5 ANO Unit 1 Storage Rack Specification 4-7
4.5.5.1 Region 1 Style Storage Racks 4-7
4.5.5.2 Region 2 Style Storage Racks 4-8
4.5.5.3 Region 3 Style Storage Racks 4-8
4.5.5.4 Gaps Between Adjacent Racks 4-9
4.6 Computer Codes 4-9
4.7 Analysis 4-9
4.7.1 Calculational Methodologies Applicable to Region 1, Region 2 & Region 3 4-10
4.7.1.1 Moderator Temperature Effect 4-10
4.7.1.2 Reactivity Effect of Inserts During Depletion 4-10
4.7.1.3 Reactivity Effect of Axial Burnup Distribution 4-11
4.7.1.4 Isotopic Compositions 4-11
4.7.1.5 Uncertainty in Depletion Calculations 4-12
4.7.2 Region 1 4-12

TABLE OF CONTENTS

4.7.2.1 Identification of Reference Fuel Assembly 4-12
4.7.2.2 Eccentric Fuel Assembly Positioning 4-12
4.7.2.3 Uncertainties Due to Manufacturing Tolerances 4-13
4.7.2.4 Temperature and Water Density Effects 4-14
4.7.2.5 Calculation of Maximum k_{eff} 4-14
4.7.2.6 Determination of Burnup versus Enrichment Values 4-15
4.7.2.7 Soluble Boron Concentration for Maximum k_{eff} of 0.95 4-15
4.7.3 Region 2 4-15
4.7.3.1 Identification of Reference Fuel Assembly 4-15
4.7.3.2 Eccentric Fuel Assembly Positioning 4-16
4.7.3.3 Uncertainties Due to Manufacturing Tolerances 4-16
4.7.3.4 Temperature and Water Density Effects 4-17
4.7.3.5 Calculation of Maximum k_{eff} 4-17
4.7.3.6 Determination of Burnup versus Enrichment Values 4-18
4.7.3.7 Soluble Boron Concentration for Maximum k_{eff} of 0.95 4-18
4.7.4 Region 3 4-18
4.7.4.1 Identification of Reference Fuel Assembly 4-18
4.7.4.2 Eccentric Fuel Assembly Positioning 4-19
4.7.4.3 Uncertainties Due to Manufacturing Tolerances 4-19
4.7.4.4 Temperature and Water Density Effects 4-20
4.7.4.5 Calculation of Maximum k_{eff} 4-20
4.7.4.6 Determination of the Minimum Burnup for a Single Spent Assembly in the 3 of 4 Loading Pattern 4-21
4.7.4.7 Soluble Boron Concentration for Maximum k_{eff} of 0.95 4-21
4.7.5 Abnormal and Accident Conditions for Region 1, 2 & 3 Racks 4-21
4.7.5.1 Abnormal Temperature 4-22
4.7.5.2 Dropped Assembly - Horizontal 4-22
4.7.5.3 Dropped Assembly - Vertical 4-22
4.7.5.4 Abnormal Location of a Fuel Assembly 4-23
4.7.5.4.1 Misloaded Fresh Fuel Assembly 4-23
4.7.5.4.2 Mislocated Fresh Fuel Assembly 4-23
4.7.5.5 Loss of all Metamic 4-24
4.7.6 Interfaces Within and Between Racks 4-24
4.7.6.1 Normal Conditions 4-24
4.7.6.2 Rack Lateral Motion – Seismic Event 4-25
4.7.7 Boron Dilution Evaluation 4-25
4.7.7.1 Low Flow Rate Dilution 4-26
4.7.7.2 High Flow Rate Dilution 4-26
4.8 New Fuel Storage Racks Criticality Analysis 4-28
4.9 Fuel Handling Equipment 4-29
4.10 References 4-30

Appendix 4A Benchmark Calculations 4A-1
4A.1 Introduction and Summary 4A-1
4A.2 Effect of Enrichment 4A-3
4A.3 Effect of ^{10}B Loading 4A-4
4A.4 Miscellaneous and Minor Parameters 4A-5

TABLE OF CONTENTS

4A.4.1	Reflector Material and Spacings	4A-5
4A.4.2	Fuel Pellet Diameter and Lattice Pitch	4A-5
4A.4.3	Soluble Boron Concentration Effects	4A-5
4A.5	MOX Fuel	4A-6
4A.6	References	4A-7
5.0	THERMAL-HYDRAULIC CONSIDERATIONS	5-1
5.1	Introduction	5-1
5.2	Cooling System Description	5-2
5.3	Spent Fuel Pool Decay Heat Loads	5-3
5.4	Minimum Time-to-Boil and Maximum Boiloff Rate	5-4
5.5	Maximum SFP Local Water Temperature	5-5
5.6	Fuel Rod Cladding Temperature	5-7
5.7	Results	5-9
5.7.1	Decay Heat	5-9
5.7.2	Minimum Time-to-Boil and Maximum Boiloff Rate	5-9
5.7.3	Local Water and Fuel Cladding Temperatures	5-9
5.8	References	5-10
6.0	MECHANICAL ACCIDENTS	6-1
6.1	Introduction	6-1
6.2	Description of Mechanical Accidents	6-1
6.3	Evaluation of Mechanical Accidents	6-1
6.4	Conclusion	6-2
6.5	References	6-2

Tables

3.3.1 Chemical Composition and Physical Properties of Aluminum (6061 Alloy) 3-5
3.3.2 Chemical Composition and Physical Properties of Boron Carbide 3-6

4.5.1 PWR Fuel Assembly Specifications 4-31
4.5.2 Core Operating Parameters for Depletion Analysis 4-32
4.5.3 Axial Burnup Profile 4-33
4.5.4 BPRA Data 4-34
4.5.5 Weight Percents of BPRA Material (3.5wt% B_4C) 4-34
4.5.6 APSR Data 4-34
4.5.7 Fuel Rack Specifications – Region 1 Racks 4-35
4.5.8 Fuel Rack Specifications – Region 2 Racks 4-36
4.5.9 Fuel Rack Specifications – Region 3 Racks 4-37
4.5.10 Identification of Possible Rack Interaction and Minimum Distances Between Racks.. 4-38
4.7.1 Summary of the Criticality Safety Analyses for Region 1 without Soluble Boron at 0 Years Cooling Time 4-39
4.7.2 Summary of the Criticality Safety Analyses for Region 1 with Soluble Boron at 0 Years Cooling Time 4-40
4.7.3 Summary of the Criticality Safety Analyses for Region 1 without Soluble Boron for a 2x2 Checkerboard of Fresh Fuel and Empty Cells 4-41
4.7.4 Summary of the Criticality Safety Analyses for Region 1 with Soluble Boron for a 2x2 Checkerboard of Fresh Fuel and Empty Cells 4-42
4.7.5 Summary of the Criticality Safety Analyses for Region 2 without Soluble Boron at 0 Years Cooling Time 4-43
4.7.6 Summary of the Criticality Safety Analyses for Region 2 with Soluble Boron at 0 Years Cooling Time 4-44
4.7.7 Summary of the Criticality Safety Analyses for Region 2 without Soluble Boron for a 2x2 Checkerboard of Fresh Fuel and Empty Cells 4-45
4.7.8 Summary of the Criticality Safety Analyses for Region 2 with Soluble Boron for a 2x2 Checkerboard of Fresh Fuel and Empty Cells 4-46
4.7.9 Summary of the Criticality Safety Analyses for Region 3 without Soluble Boron for a 2x2 Checkerboard of 3 Fresh Fuel Assemblies and 1 Spent Fuel Assembly at 0 Years Cooling Time 4-47
4.7.10 Summary of the Criticality Safety Analyses for Region 3 with Soluble Boron for a 2x2 Checkerboard of 3 Fresh Fuel Assemblies and 1 Spent Fuel Assembly at 0 Years Cooling Time 4-48
4.7.11 Summary of the Criticality Safety Analyses for Region 3 without Soluble Boron 4-49
4.7.12 Summary of the Criticality Safety Analyses for Region 3 with Soluble Boron 4-50
4.7.13 Burnup Value at which APSRs and BPRAs have Equivalent Reactivity Effect 4-51
4.7.14 Maximum Burnup versus Enrichment Values for Region 1 Racks with Spent Fuel 4-52
4.7.15 Maximum Burnup versus Enrichment Values for Region 2 Racks with Spent Fuel 4-53
4.7.16 Reactivity Effect of Insert Type, Enrichment 5.0 wt% ^{235}U, 0 Cooling Time 4-54
4.7.17 Reactivity Effect of Fuel and Rack Tolerances for Region 1 Racks 4-55
4.7.18 Reactivity Effect of Temperature Variation in Region 1 Racks 4-56
4.7.19 Reactivity Effect of Fuel and Rack Tolerances for Region 2 Racks 4-57

4.7.20 Reactivity Effect of Temperature Variation in Region 2 Racks 4-58
4.7.21 Reactivity Effect of Fuel and Rack Tolerances for Region 3 Racks 4-59
4.7.22 Reactivity Effect of Temperature Variation in Region 3 Racks 4-60
4.7.23 Region 1 Accident Conditions 4-61
4.7.24 Region 2 Accident Conditions 4-62
4.7.25 Region 3 Accident Conditions 4-63
4.7.26 Interface Calculations 4-64
4.8.1 Summary of New Fuel Vault Criticality Safety Analysis 4-65

4A.1 Summary of Criticality Benchmark Calculations ..... 4A-9 thru 4A-13
4A.2 Comparison of MCNP4a and Keno5a Calculated Reactivities for Various Enrichments 4A-14
4A.3 MCNP4a Calculated Reactivities for Critical Experiments with Neutron Absorbers 4A-15
4A.4 Comparison of MCNP4a and KENO5a Calculated Reactivities for Various ^{10}B Loadings 4A-16
4A.5 Calculations for Critical Experiments with Thick Lead and Steel Reflectors 4A-17
4A.6 Calculations for Critical Experiments with Various Soluble Boron Concentrations 4A-18
4A.7 Calculations for Critical Experiments with MOX Fuel 4A-19

5.3.1 Key Input Data for Decay Heat Computations 5-11
5.3.2 Offload Schedule 5-12
5.4.1 Key Input Data for Time-To-Boil Evaluation 5-13
5.5.1 Key Input Data for Local Temperature Evaluation 5-14
5.7.1 Result of SFP Decay Heat Calculations 5-15
5.7.2 Results of Loss-of-Forced Cooling Evaluations 5-16
5.7.3 Results of Maximum Local Water and Fuel Cladding Temperature Evaluations 5-17

TABLE OF CONTENTS

Figures

1.1 Location of the Different Rack Types in the Spent Fuel Pool

2.5.1 Schematic of the Poison Insert Assembly Mechanism
2.5.2 Lead-in Device

4.5.1 A Two-Dimensional Representation of the Actual Calculational Model Used for the Region 1 Rack Analysis for Uniform Loading of Spent Fuel. This Figure was Drawn (To Scale) with the Two-Dimensional Plotter in MCNP4a.
4.5.2 A Two-Dimensional Representation of the Actual Calculational Model Used for the Region 1 Rack Analysis for Checkerboard Loading of Fresh Fuel. This Figure was Drawn (To Scale) with the Two-Dimensional Plotter in MCNP4a.
4.5.3 A Two-Dimensional Representation of the Actual Calculational Model Used for the Region 2 Rack Analysis for Uniform Loading of Spent Fuel. This Figure was drawn (To Scale) with the Two-Dimensional Plotter in MCNP4a.
4.5.4 A Two-Dimensional Representation of the Actual Calculational Model Used for the Region 2 Rack Analysis for Checkerboard Loading of Fresh Fuel. This Figure was Drawn (To Scale) with the Two-Dimensional Plotter in MCNP4a.
4.5.5 A Two-Dimensional Representation of the Actual Calculational Model Used for the Region 3 Rack Analysis for Uniform Loading of Fresh Fuel. This Figure was drawn (To Scale) with the Two-Dimensional Plotter in MCNP4a.
4.5.6 A Two-Dimensional Representation of the Actual Calculational Model Used for the Region 3 Rack Analysis for "3 of 4" Loading of Spent and Fresh Fuel. This Figure was drawn (To Scale) with the Two-Dimensional Plotter in MCNP4a.
4.5.7 A Two-Dimensional Representation of the ANO Unit 1 Spent Fuel Pool Layout with Rack Region Layout and Gaps between Adjacent Racks.
4.5.8 Sketch Illustrating Locations of Measurements of Water Gaps Between Adjacent Racks.
4.5.9 Sketch of Region 1 Racks, Detailing Important Dimensions and Tolerances.
4.5.10 Sketch of Region 2 Racks, Detailing Important Dimensions and Tolerances.
4.5.11 Sketch of Region 3 Racks, Detailing Important Dimensions and Tolerances.
4.7.1 Interface Calculation for Adjacent Region 1 Racks Containing Fresh Fuel Checkerboards with Fresh Fuel Assemblies Facing Across the Gap.
4.7.2 Fresh Fuel Checkerboard and Spent Fuel in same Region 1 Rack.
4.7.3 Interface Calculation for Adjacent Region 2 Racks Containing Fresh Fuel Checkerboards with Fresh Fuel Assemblies Facing Across the Gap.
4.7.4 Fresh Fuel Checkerboard and Spent Fuel in same Region 2 Rack.
4.7.5 Interface Calculation for Adjacent Region 3 Racks with 3 of 4 Pattern and Fresh Fuel Facing Across the Gap.
4.7.6 Interface Calculation for Region 3 Racks. Fresh Fuel in one Region 3 Rack Facing Fresh and Spent Fuel in the Adjacent Rack.
4.7.7 Interface Calculation for Region 3 Racks. All Fresh Fuel (4.35 wt%) in one Rack, 3 of 4 Pattern with Fresh Fuel Facing Gap in Adjacent Rack.
4.7.8 Interface Calculation for Region 3 Racks. All Fresh Fuel (4.35 wt%) in one Rack, 3 of 4 Pattern with Fresh and Spent Fuel Facing Gap in Adjacent Rack.
4.7.9 Interface Calculation for Region 1 and Region 3 Racks. Fresh Fuel Checkerboard in Region 1 Rack, 3 of 4 pattern in Region 3 Rack with Fresh Fuel Facing Gap.

4.7.10 Interface Calculation for Region 1 and Region 3 Racks. Spent Fuel in Region 1 Rack, 3 of 4 Pattern in Region 3 Rack with Fresh Fuel Facing Gap.
4.7.11 Interface Calculation for Region 2 and Region 3 Racks. Fresh Fuel Checkerboard in Region 2 Rack, 3 of 4 pattern in Region 3 Rack with Fresh Fuel Facing Gap.
4.7.12 Interface Calculation for Region 2 and Region 3 Racks. Spent Fuel in Region 2 Rack, 3 of 4 Pattern in Region 3 Rack with Fresh Fuel Facing Gap.
4.7.13 3 of 4 Loading Pattern and Fresh Fuel (4.35 wt%) in same Region 3 Rack, All fresh 5.0 wt% facing all fresh 4.35 wt%.
4.7.14 3 of 4 Loading Pattern and Fresh Fuel (4.35 wt%) in same Region 3 Rack, Fresh and Spent 5.0 wt% facing all fresh 4.35 wt%.
4.8.1 Reactivity of the New Fuel Vault as a Function of Moderator Density for 4.95 wt% Fuel.
4.8.2 Acceptable New Fuel Storage Vault Configuration for up to 4.95 wt% Enrichment Fresh Fuel.
4.8.3 Acceptable New Fuel Storage Vault Configuration for up to 4.2 wt% Enrichment Fresh Fuel.

4A.1 MCNP Calculated k-eff Values for Various Values of the Spectral Index
4A.2 KENO5a Calculated k-eff Values for Various Values of the Spectral Index
4A.3 MCNP Calculated k-eff Values at Various U-235 Enrichments
4A.4 KENO Calculated k-eff Values at Various U-235 Enrichments
4A.5 Comparison of MCNP and KENO5a Calculations for Various Fuel Enrichments
4A.6 Comparison of MCNP and KENO5a Calculations for Various Boron-10 Areal Densities

5.5.1 Schematic of the CFD Model of the ANO-1 SFP
5.7.1 Partial Core Offload Bounding Spent Fuel Pool Heat Load
5.7.2 Full Core Offload Bounding Spent Fuel Pool Heat Load
5.7.3 Contours of Static Temperature in a Vertical Plane Through the Center of the SFP
5.7.4 Velocity Vector Plot in a Vertical Plane Through the Center of the SFP

1.0 INTRODUCTION

Arkansas Nuclear One, Unit 1 (ANO-1), operated by Entergy Operations, is located approximately 70 miles northwest of Little Rock, Arkansas and about five miles west of Russellville. ANO-1 is a Babcock & Wilcox (B&W) pressurized water reactor and has been in commercial operation since 1974. The ANO-1 reactor is licensed for a thermal power level of 2568 megawatts. The reactor core contains 177 fuel assemblies and the spent fuel pool (SFP) is licensed for the storage of 968 assemblies.

The Westinghouse designed racks in the ANO-1 SFP are free-standing and self supporting racks. The principal fabrication materials are ASTM A-240, Type 304 stainless steel for the structural members and shapes. "Boraflex," a product of BISCO (a division of Brand, Inc.) was originally used to augment reactivity control.

The ANO-1 SFP was designed to hold spent fuel assemblies (or control rod assemblies) in underwater storage for long-term decay after their removal from the reactor core. The structure is a seismic Category I, heavy walled, reinforced concrete pool, located on grade outside the containment structure. The interior of the pool is lined with stainless steel plate (Type 304L).

The ANO-1 spent fuel racks consist of individual cells with a square pitch of 10.65 inches, each of which accommodates a single B&W 15x15 fuel assembly or equivalent. The ANO-1 SFP is divided into two regions, designated as Region 1 and Region 2. Region 1 racks employ Boraflex as the poison material and are presently qualified to store fresh fuel assemblies with enrichments of up to 4.1 weight percent (wt%) ^{235}U. Region 2 racks are designed with flux-traps and are currently used to store spent fuel assemblies with various initial enrichments that have accumulated certain minimum burnups. The Region 2 racks do not have any poison material. Two of the Region 2 racks will be modified by the insertion of Metamic® poison insert assemblies into the flux trap region to create a new region, which will be designated as Region 3. The locations of Regions 1 and 2 and proposed Region 3 in the SFP are depicted in Figure 1-1.

The poison insert assemblies have been designed to contain two borated Aluminum (Metamic®) panels for neutron absorbers. The insertion of the Metamic® poison assemblies into Region 3, as shown by analyses later in this report, will enable storage of fresh fuel with a maximum enrichment up to 5.0 wt% in the ANO-1 SFP. Region 3 racks have been analyzed to establish their capability for fresh fuel storage in a 4 of 4 configuration for enrichments up to 4.35 wt% and a 3 of 4 configuration (3 fresh fuel

assemblies and 1 spent fuel assembly) for enrichments up to 5.0 wt%. The Region 3 flux traps will be fitted with lead-ins on the top of the flux traps, which will act to prevent any possible uplifting of the poison panel insert assembly. The lead-in devices will also help guide the fuel assemblies into the storage cells.

The existing Region 1 racks have been reanalyzed to establish new fuel storage requirements without crediting the presence of Boraflex. The Region 2 racks were also re-analyzed to establish more flexible fuel storage requirements. The racks in Region 1 and 2 have been re-analyzed to establish their capability for fresh fuel storage in a 2-of-4 checkerboard (2 fresh fuel assemblies and 2 empty cells in a 2x2 storage space) arrangement or to store spent fuel assemblies of specified enrichment-burnup limits. The New Fuel Vault and fuel handling equipment were also analyzed to confirm acceptability of fuel with initial enrichment up to 5.0 wt% ^{235}U.

Sections 2.0 and 3.0 of this report provide an abstract of the design and material information about the poison insert assemblies.

Section 4.0 provides a summary of the methods and results of the criticality evaluations performed for the SFP storage racks in all designated Regions of the SFP, including interfacing analysis between the Regions. Credit for soluble boron in the pool has been taken, in accordance with 10CFR50.68, to assure the criticality safety of the spent fuel storage racks. The analyses show that the neutron multiplication factor (k_{eff}) for the stored fuel array is subcritical under an assumed condition of the loss of all soluble boron in the pool water. Additional analyses have been performed to demonstrate that the soluble boron requirements to maintain k_{eff} below 0.95 for both normal storage and accident conditions are satisfied. The criticality safety analysis sets the requirements on the Metamic® poison insert panel length and the amount of B_4C (i.e., loading density) of the Metamic® inserts for the Region 3 SFP racks.

Section 4.0 also includes a summary of the criticality evaluation performed for the New Fuel Vault racks and the fuel handling equipment.

Thermal-hydraulic analyses verify that fuel cladding will not fail due to excessive thermal stress. The thermal-hydraulic analyses, which support the modification of two of the existing Region 2 racks, are described in Section 5.0.

The structural qualification requires that the subcriticality of the stored fuel be maintained under all postulated mechanical accident scenarios and is presented in Section 6.0 of this report.

Results of the analyses presented in this report establish acceptable restrictions on combinations of initial enrichment and discharge burnups for Region 1 and Region 2, and show that the insertion of poison insert assemblies into the newly defined Region 3 racks will permit storage of fresh fuel assemblies in these racks. The storage racks meet all requirements of the applicable USNRC guidelines and regulations, and applicable ANSI/ANS standards (References 2 – 6). The analysis methodologies employed are a direct evolution of previous license applications reviewed and approved by the USNRC, including nuclear subcriticality, thermal-hydraulic safety and integrity following a mechanical accident.

All computer programs utilized to perform the analyses documented in Sections 2.0 through 6.0 are benchmarked and verified. These programs have been utilized by Holtec International in numerous license applications over the past decade. The analyses presented herein clearly demonstrate that the rack module arrays with the addition of the poison insert assemblies and the lead-ins possess wide margins of safety in respect to all considerations of safety specified in the OT Position Paper [3], namely, nuclear subcriticality, thermal-hydraulic safety, and mechanical integrity.

1.1 REFERENCES

[1] American Society of Mechanical Engineers (ASME), Boiler & Pressure Vessel Code, Section III, 1989 Edition, Subsection NF, and Appendices.

[2] General Design Criterion 62, Prevention of Criticality in Fuel Storage and Handling.

[3] USNRC, "OT Position for Review and Acceptance of Spent Fuel Storage and Handling Applications," April 14, 1978, and Addendum dated January 18, 1979.

[4] Code of Federal Regulations 10CFR50.68, Criticality Accident Requirements

[5] ANSI-8.17-1984, Criticality Safety Criteria for the Handling, Storage and Transportation of LWR Fuel Outside Reactors.

[6] L. I. Kopp, "Guidance on the Regulatory Requirements for Criticality Analysis Of Fuel Storage At Light-Water Reactor Plants," USNRC Internal Memorandum L. Kopp to Timothy Collins, August 19 1998.

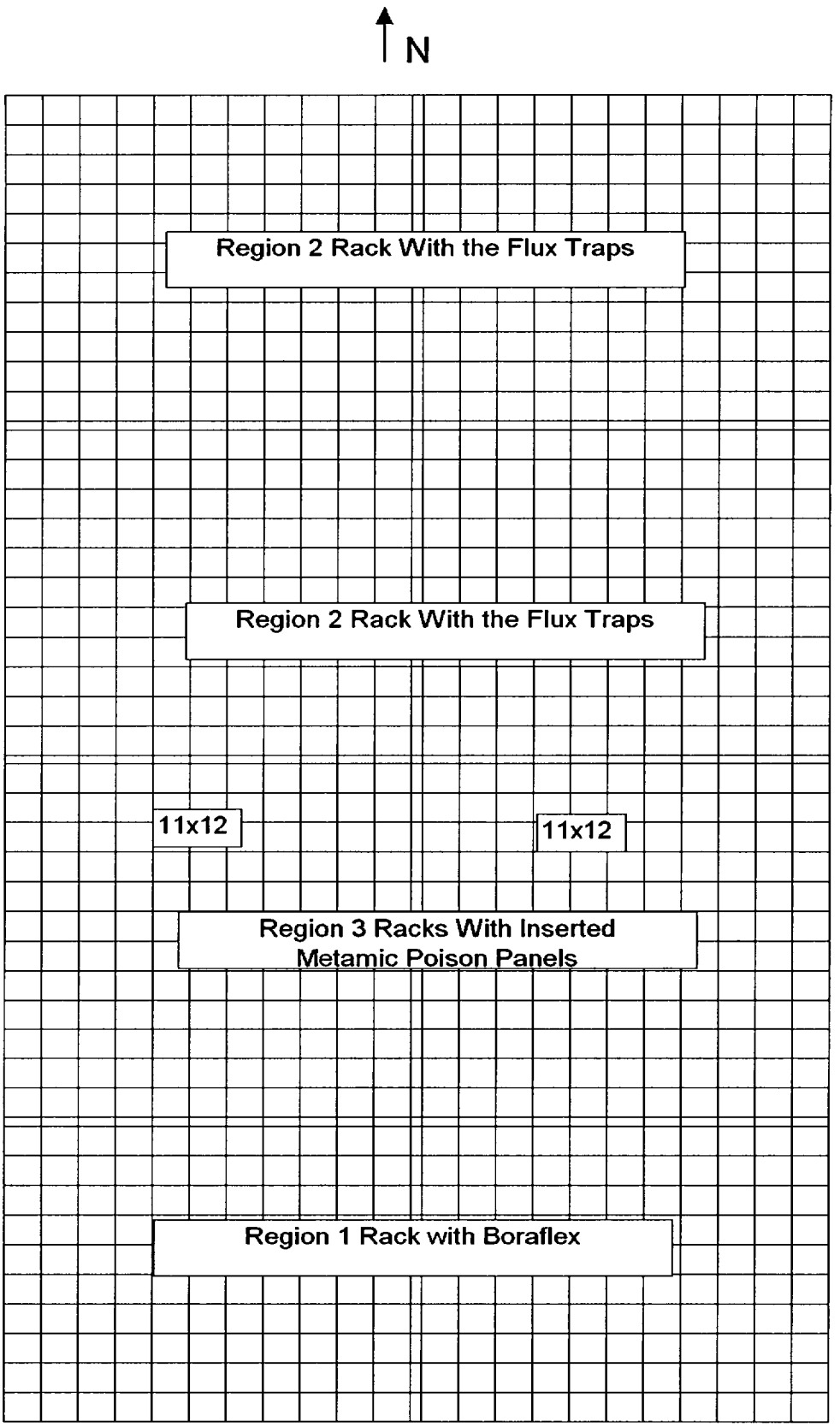

Figure 1.1: Location of the Different Rack Types in the Spent Fuel Pool.

2.0 SPENT FUEL RACK FLUX TRAP GAP POISON INSERT ASSEMBLY DESIGN

2.1 INTRODUCTION

Metamic poison insert assemblies containing a high loading of the B_4C (nominally 25% by weight) will be inserted into the flux traps of the Region 3 storage racks to provide appropriate neutron attenuation between adjacent storage cells. Design inputs and overview applicable to the Metamic poison insert assemblies and lead-in devices are addressed within this Section. A brief description of the poison insert assembly fabrication and installation is also provided in this Section.

2.2 SUMMARY OF PRINCIPAL DESIGN CRITERIA

The key design criteria for the spent fuel racks are set forth in the USNRC memorandum entitled "OT Position for Review and Acceptance of Spent Fuel Storage and Handling Applications," dated April 14, 1978 as modified by amendment dated January 18, 1979. The individual sections of this report expound on the specific design bases derived from the above-mentioned "OT Position Paper." The thermal-hydraulic, criticality safety and mechanical accidents design bases for the spent fuel racks with the poison insert assemblies in them are summarized below:

a. Thermal-Hydraulic Compliance: The spatial average bulk pool temperature is required to remain below 150 °F. No localized boiling is permitted.

b. Criticality Compliance: The New Fuel Storage Racks (NFSR) and Spent Fuel Storage Racks (SFSR) must be able to store fuel of 5.0 weight percent maximum enrichment while maintaining the reactivity (k_{eff}) less than the applicable regulatory limit. For fuel in the SFSR, appropriate credit is taken for soluble boron as allowed by 10CFR 50.68.

c. Accident Events: In the event of postulated drop events (uncontrolled lowering of a fuel assembly, for instance), it is necessary to demonstrate that the racks containing fuel assemblies remain subcritical.

The foregoing design bases are further articulated in Sections 4.0 through 6.0 of this report.

2.3 APPLICABLE CODES AND STANDARDS

The following codes, standards and practices are used as applicable for the design, construction, and assembly of the poison insert assemblies and lead-in devices. Additional specific references related to detailed analyses are given in each section.

a. Design Codes

(1) American Society for Nondestructive Testing SNT-TC-1A, June 1984, Recommended Practice for Personnel Qualifications and Certification in Non-destructive Testing.

(2) American Society of Mechanical Engineers (ASME) Y14.5M, Dimensioning and Tolerancing

(3) ASME B & PV Code, Section II-Part D, 1998 Edition.

(4) ASME, Boiler and Pressure Vessel Code, Section III, Subsection NF, 1983 Edition, No Addenda.

(5) ASME, Boiler and Pressure Vessel Code, Section II - Parts A and C, 1983 Edition, No Addenda.

b. Standards of American Society for Testing and Materials (ASTM)

(1) ASTM A240 - Standard Specification for Heat-Resisting Chromium and Chromium-Nickel Stainless Steel Plate, Sheet and Strip for Pressure Vessels.

(2) ASTM A262 - Standard Practices for Detecting Susceptibility to Intergranular Attack in Austenitic Stainless Steel.

(3) ASTM C750 - Standard Specification for Nuclear-Grade Boron Carbide Powder.

(4) ASTM A380 - Standard Practice for Cleaning, Descaling, and Passivation of Stainless Steel Parts, Equipment and Systems.

(5) ASTM C992 - Standard Specification for Boron-Based Neutron Absorbing Material Systems for Use in Nuclear Spent Fuel Storage Racks.

(6) ASTM E3 - Standard Practice for Preparation of Metallographic Specimens.

(7) ASTM E190 - Standard Test Method for Guided Bend Test for Ductility of Welds.

c. Welding Code

(1) ASME B & PV Code, Section IX - Welding and Brazing Qualifications, latest applicable edition and addenda.

(2) ASME, Boiler and Pressure Vessel Code, Section III, Subsection NF, 1989 Edition, No Addenda.

d. Quality Assurance, Cleanliness, Packaging, Shipping, Receiving, Storage, and Handling

(1) ANSI N45.2.1 - Cleaning of Fluid Systems and Associated Components during Construction Phase of Nuclear Power Plants - 1980 (Regulatory Guide (RG) 1.37).

(2) ANSI N45.2.2 - Packaging, Shipping, Receiving, Storage and Handling of Items for Nuclear Power Plants - 1978 (RG 1.38).

(3) ANSI N45.2.6 - Qualifications of Inspection, Examination, and Testing Personnel for the Construction Phase of Nuclear Power Plants - 1973. (RG 1.58).

(4) ANSI N45.2.8 - Supplementary Quality Assurance Requirements for Installation, Inspection and Testing of Mechanical Equipment and Systems for the Construction Phase of Nuclear Plants - 1975 (RG 1.116).

(5) ANSI N45.2.11 - Quality Assurance Requirements for the Design of Nuclear Power Plants - 1978 (RG 1.64).

(6) ANSI N45.2.12 - Requirements for Auditing of Quality Assurance Programs for Nuclear Power Plants - 1977 (RG 1.144).

(7) ANSI N45.2.13 - Quality Assurance Requirements for Control of Procurement of Items and Services for Nuclear Power Plants - 1976 (RG 1.123).

(8) ANSI N45.2.23 - Qualification of Quality Assurance Program Audit Personnel for Nuclear Power Plants - 1978 (RG 1.146).

(9) ASME B & PV Code, Section V, Nondestructive Examination, 1983 Edition.

(10) ANSI N16.9-75 - Validation of Calculation Methods for Nuclear Criticality Safety.

(11) ASME NQA-1 – Quality Assurance Program Requirements for Nuclear Facilities.

(12) ASME NQA-2 – Quality Assurance Requirements for Nuclear Power Plants.

e. USNRC Documents

(1) "OT Position for Review and Acceptance of Spent Fuel Storage and Handling Applications," dated April 14, 1978, and the modifications to this document of January 18, 1979.

(2) NUREG 0612, "Control of Heavy Loads at Nuclear Power Plants," USNRC, Washington, D.C., July, 1980.

(3) NUREG 0800, "Standard Review Plan for the Review of Safety Analysis Reports for Nuclear Power Plants," USNRC, Washington, D.C., July 1981.

(4) NUREG-1233, Seismic Design Criteria.

f. Other ANSI Standards (not listed in the preceding)

(1) ANSI/ANS 8.1/N16.1 - Nuclear Criticality Safety in Operations with Fissionable Materials Outside Reactors, 1975.

(2) ANSI N45.2.9 - Requirements for Collection, Storage and Maintenance of Quality Assurance Records for Nuclear Power Plants - 1974.

(3) ANSI N45.2.10 - Quality Assurance Terms and Definitions - 1973.

(4) ANSI/ASME N626-3 – Qualification and Duties of Specialized Professional Engineers, 1977.

g. Code-of-Federal Regulations (CFR)

(1) 10 CFR 20 - Standards for Protection Against Radiation.

(2) 10 CFR 21 - Reporting of Defects and Non-compliance.

(3) 10 CFR 50 Appendix A - General Design Criteria for Nuclear Power Plants.

(4) 10 CFR 50 Appendix B - Quality Assurance Criteria for Nuclear Power Plants and Fuel Reprocessing Plants.

(5) 10 CFR 100 – Reactor Site Criteria

h. Regulatory Guides (RG)

(1) RG 1.13 - Spent Fuel Storage Facility Design Basis (Revision 2 Proposed).

(2) RG 1.25 - Assumptions Used for Evaluating the Potential Radiological Consequences of a Fuel Handling Accident in the Fuel Handling and Storage Facility for Boiling and Pressurized Water Reactors, Rev. 0 - March, 1972.

(3) RG 1.28 - Quality Assurance Program Requirements - Design and Construction, Rev. 2 - February 1979 (endorses ANSI N45.2).

(4) RG 1.33 – Quality Assurance Program Requirements.

(5) RG 1.31 - Control of Ferrite Content in Stainless Steel Weld Metal, Rev. 3.

(6) RG 1.37 - Cleaning of Fluid Systems and Associated Components during Construction Phase of Nuclear Power Plants.

(7) RG 1.38 - Quality Assurance Requirements for Packaging, Shipping, Receiving, Storage and Handling of Items for Water-Cooled Nuclear Power Plants, Rev. 2 - May, 1977 (endorses ANSI N45.2.2).

(8) RG 1.44 - Control of the Use of Sensitized Stainless Steel.

(9) RG 1.58 – Qualification of Nuclear Power Plant Inspection, Examination, and Testing Personnel, Rev. 1 – September 1980 (endorses ANSI N45.2.6)

(10) RG 1.64 - Quality Assurance Requirements for the Design of Nuclear Power Plants, Rev. 2 - June, 1976 (endorses ANSI N45.2.11).

(11) RG 1.71 - Welder Qualifications for Areas of Limited Accessibility.

(12) RG 1.74 - Quality Assurance Terms and Definitions, Rev. 2 - February, 1974 (endorses ANSI N45.2.10).

(13) RG 1.85 - Materials Code Case Acceptability - ASME Section III, Division 1.

(14) RG 1.88 - Collection, Storage and Maintenance of Nuclear Power Plant Quality Assurance Records, Rev. 2 - October, 1976 (endorses ANSI N45.2.9).

(15) RG 1.116 - Quality Assurance Requirements for Installation, Inspection and Testing of Mechanical Equipment and Systems, Rev. 0-R - May,1977 (endorses ANSI N45.2.8-1975)

(16) RG 1.123 - Quality Assurance Requirements for Control of Procurement of Items and Services for Nuclear Power Plants, Rev. 1 - July, 1977 (endorses ANSI N45.2.13).

(17) RG 1.144 - Auditing of Quality Assurance Programs for Nuclear Power Plants, Rev.1 - September, 1980 (endorses ANSI N45.2.12-1977)

(18) RG 8.8 - Information Relative to Ensuring that Occupational Radiation Exposures at Nuclear Power Stations will be as Low as Reasonably Achievable (ALARA).

(19) RG 8.38 - Control of Access to High and Very High Radiation Areas in Nuclear Power Plants, June, 1993.

i. Branch Technical Position

(1) CPB 9.1-1 - Criticality in Fuel Storage Facilities.

j. American Welding Society (AWS) Standards

(1) AWS D1.1 - Structural Welding Code - Steel.

(2) AWS D1.3 - Structure Welding Code - Sheet Steel.

(3) AWS D9.1 - Sheet Metal Welding Code.

(4) AWS A2.4 - Standard Symbols for Welding, Brazing and Nondestructive Examination.

(5) AWS A3.0 - Standard Welding Terms and Definitions.

(6) AWS A5.12 - Specification for Tungsten and Tungsten Alloy Electrodes for Arc-Welding and Cutting

(7) AWS QC1 - Standard for AWS Certification of Welding Inspectors.

(8) AWS 5.4 – Specification for Stainless Steel Electrodes for Shielded Metal Arc Welding.

(9) AWS 5.9 – Specification for Bare Stainless Steel Welding Electrodes and Rods.

k. Other References

(1) ANO Unit 1 Operating License and Technical Specifications, License No. DPR-51.

(2) ANO Unit 1 Updated Final Safety Analysis Report (UFSAR).

(3) IE Information Notice 83-29 - Fuel Binding Caused by Fuel Rack Deformation.

2.4 QUALITY ASSURANCE PROGRAM

The governing quality assurance requirements for design and fabrication of the poison insert assemblies are stated in 10 CFR 50 Appendix B. Holtec's Nuclear Quality Assurance program complies with this regulation and is designed to provide a system for the design, analysis, and licensing of customized components in accordance with various codes, specifications, and regulatory requirements. The lead-in devices are classified as not important to safety and are not subject to a 10 CFR 50 Appendix B program.

The Quality Assurance System that will be used by Entergy Operations to install the poison insert assemblies and lead-in devices is controlled by the Entergy Quality Assurance Program.

2.5 MECHANICAL DESIGN

The mechanical design of the poison insert assembly consists of two poison panels separated by a mechanism to maintain the water gap specified by criticality considerations. The poison panels are independent flat panels sized to cover the active fuel region. The poison panels will extend all the way to the SFP rack base plate. The poison panel will be nominally 0.10 inches thick 6061 aluminum metal matrix composite (MMC) with ASTM C-750 isotopically-graded boron carbide (B_4C) manufactured by Metamic®.

The poison panels will be held together with a frame that is fabricated from SA240-304 stainless steel. A schematic of the arrangement is shown in Figure 2.5.1. Each poison insert assembly is composed of two interconnected rectangular Metamic poison panel assemblies. Each Metamic poison panel assembly includes a Metamic poison panel protected and held in place by stainless steel sheathing bands. Full-length sheathing covers the side of the Metamic panel facing the flux trap wall. This will prevent any direct contact between the Metamic panel and the flux trap wall. Additional stainless steel bands connect the two Metamic poison panel sub-assemblies together. The poison insert assembly includes a hook/wedge mechanism. The hook/wedge mechanism along with some metallic shims, connecting the full-length sheathings covering the Metamic pieces, maintains the required poison insert assembly width prior to and after installation in the flux trap. The poison insert assemblies are designed based on worst-

case measured dimensions of the flux trap and maximizing use of the allowable space in each flux trap for criticality safety purposes.

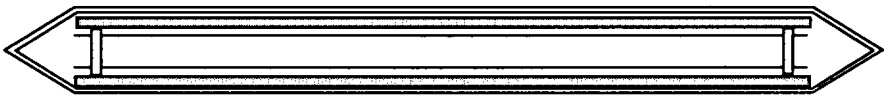

Figure 2.5.1 Schematic of the Poison Insert Assembly Mechanism

The lead-in device, which is depicted in Figure 2.5.2, is fabricated from SA240-304L stainless steel. The device is designed to rest on top of the flux trap, and it is secured in place by two slotted plates, which straddle the cell wall at the corners external to the flux trap. The size and shape of the lead-in is such that it will not interfere with the square opening of the cell. The lead-in contains flow holes in the mounting plate to provide an uninterrupted flow path for the water entering at the bottom of the flux trap and exiting at the top of the flux trap. Each poison insert assembly and lead-in device together weighs less than 50 lbs.

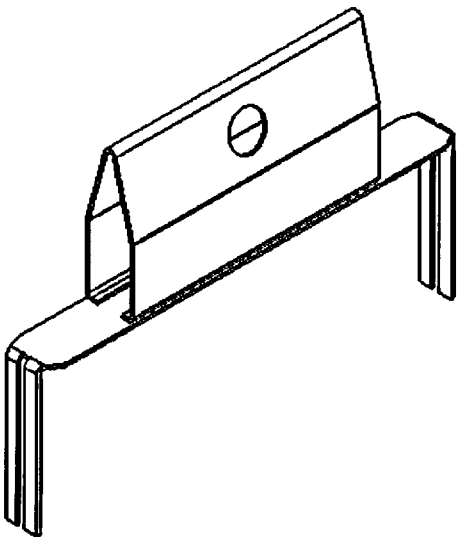

Figure 2.5.2 Lead-in Device

2.6 FABRICATION

This section provides a brief description of the poison insert assembly construction activities. The pertinent methods used in manufacturing the poison insert assemblies may be stated as follows:

1. The poison panels are extruded and rolled from a powder metallurgy billet then cut to the specified rectangular size.

2. The fabrication process involves operational sequences that permit immediate accessibility for verification by the inspection staff.

3. The poison insert assemblies are fabricated per the manufacturer's Appendix B Quality Assurance program, which ensures and documents that the fabricated poison insert assemblies meet all of the requirements of the design and fabrication documents.

2.7 INSTALLATION

The poison insert assembly is placed in an upending cradle on the fuel bridge. The poison insert assembly is then upended and connected to the poison insert assembly handling tool. All installation activities will be performed remotely, from the fuel bridge, using long handled installation tools. Subsequent to the upending process, the poison insert assembly is lowered into the spent fuel pool and guided into the appropriate flux trap with installation tools. Then, the lead-ins are installed onto a flux trap that received a poison insert assembly.

3.0 MATERIAL CONSIDERATIONS

3.1 INTRODUCTION

Safe storage of nuclear fuel in the pool requires that the materials utilized in the poison inserts be of proven durability and compatible with the pool water environment. This section provides a synopsis of the considerations with regard to long-term design service life of 40 years.

3.2 STRUCTURAL MATERIALS

The only structural material utilized in the fabrication of the poison inserts is SA240 Type 304 stainless steel.

3.3 NEUTRON ABSORBING MATERIAL

In addition to the structural materials, the poison inserts employ Metamic®, a patented product of Metamic®, Inc., as the neutron absorber material. Metamic® has been approved by USNRC for use in spent fuel pool applications [3.3.4]. A brief description of Metamic® follows.

Metamic® is a neutron absorber material developed by the Reynolds Aluminum Company in the mid-1990s for spent fuel reactivity control in dry and wet storage applications [3.3.1]. Metallurgically, Metamic® is a metal matrix composite (MMC) consisting of a high purity 6061 aluminum matrix reinforced with Type 1 ASTM C750-89, isotopically graded boron carbide (B_4C). Metamic® is characterized by an extremely fine aluminum spherical powder (325 mesh or better) and boron carbide powder (average particle size under 25 microns). The high performance reliability of Metamic® derives from the particle size distribution of its constituents, namely, high purity aluminum 6061 alloy powder and isotopically graded B_4C particulate, rendered into an isotropic metal matrix composite state by the powder metallurgy process which yields excellent homogeneity, and which prevents B_4C from clustering in the final product.

The powders are carefully blended together without binders, chelating agents, or other additives that could potentially become retained in the final product and deleteriously influence performance. The nominal percentage of B_4C that will be dispersed in the aluminum alloy 6061 matrix is 25% by weight.

The pure blend of powders is isostatically compacted to form a high density "green" billet. This green billet is then vacuum sintered to produce the final hard billet of nearly full theoretical density.[1] Once the aluminum and the boron carbide powders are thoroughly mixed, pressed, and sintered, there is no credible mechanism that could alter the composition of Metamic®. An extrusion process is used to bring the matrix into final density. Billets can vary in diameter, size and weight depending on a number of variables including loading and final panel dimensions.

Metamic® has been subjected to an extensive array of tests sponsored by the Electric Power Research Institute (EPRI) that evaluated the functional performance of the material at elevated temperatures (up to 900 °F) and radiation levels (1E+11 rads gamma). The results of the tests documented in an EPRI report [3.3.2] indicate that Metamic® maintains its physical and neutron absorption properties with little variation in its properties from the unirradiated state. The main conclusions provided in the above-referenced EPRI report are summarized below:

- The isotropic metal matrix configuration produced by the powder metallurgy process with a complete absence of interconnected internal porosity in Metamic® ensures that its density is essentially equal to the maximum theoretical density.

- Measurements of boron carbide particle distribution show extremely small particle-to-particle distance[2] and near-perfect homogeneity.

- The physical and neutronic properties of Metamic® are essentially unaltered under exposure to elevated temperatures (750 °F – 900 °F).

- No detectable change in the neutron attenuation characteristics under accelerated test conditions has been observed.

[1] The density of Metamic® before hot work is 82% to 98% of theoretical density depending on B_4C content.
[2] Medium measured neighbor-to-neighbor distance is 10.08 microns according to the article, "METAMIC Neutron Shielding" [3.3.3].

Independent tests and investigations by Holtec International [3.3.5] confirm the conclusions summarized above, and present additional data on the fundamental characteristics of Metamic® and the applicability of the material in wet storage applications.

Holtec International's Q.A. program ensures that Metamic® is manufactured under the control and surveillance of a Quality Assurance/Quality Control Program that conforms to the requirements of 10 CFR 50 Appendix B, "Quality Assurance Criteria for Nuclear Power Plants."

3.3.1 METAMIC® Material Characteristics

Aluminum: Aluminum is a silvery-white, ductile metallic element. The 6061 alloy aluminum is used extensively in heat exchangers, pressure and storage tanks, chemical equipment, reflectors, and sheet metal work.

It has high resistance to corrosion in industrial and marine atmospheres. Aluminum has atomic number of 13, atomic weight of 26.98, specific gravity of 2.69 and valence of 3. The physical, mechanical and chemical properties of the 6061 alloy aluminum are listed in Table 3.3.1.

The excellent corrosion resistance of the 6061 alloy aluminum is provided by the protective oxide film that quickly develops on its surface from exposure to the atmosphere or water. This film prevents the loss of metal from general corrosion or pitting corrosion.

Boron Carbide: The boron carbide contained in Metamic® is a fine granulated powder that conforms to ASTM C750-89 nuclear grade Type I. The material conforms to the chemical composition and properties listed in Table 3.3.2.

References [3.3.1] and [3.3.2] provide further discussion as to the suitability of these materials for use in spent fuel storage applications.

3.4 COMPATIBILITY WITH ENVIRONMENT

All materials used in the construction of the poison inserts have been determined to be compatible with the ANO-1 SFP, and have an established history of in-pool usage. Austenitic stainless steel (e.g., Type

304) is a widely used stainless alloy in nuclear power plants, and it has an established history of in-pool usage. Metamic® is likewise an excellent material for spent fuel applications based on its high resistance to corrosion and its functional performance at elevated temperatures and radiation levels.

3.5 HEAVY LOAD CONSIDERATIONS

There are no heavy loads involved in the proposed installation of poison inserts. The weight of a single poison insert and a lead-in is less than 50 pounds.

3.6 REFERENCES

[3.3.1] "Use of METAMIC in Fuel Pool Applications," Holtec International, HI-2022871, Revision 1, August 2002.

[3.3.2] "Qualification of METAMIC for Spent Fuel Storage Application," EPRI, 1003137, Final Report, October 2001.

[3.3.3] K. Anderson et al., "METAMIC Neutron Shielding," EPRI Boraflex Conference, November 19-20, 1998.

[3.3.4] Safety Evaluation By The Office Of Nuclear Reactor Regulation Related To Holtec International Report HI-2022871 Regarding Use Of Metamic• In Fuel Pool Applications, Facility Operating License Nos. DPR-51 and NPF-6, Entergy Operations, Inc., Arkansas Nuclear One, Unit Nos. 1 and 2, Docket Nos. 50-313 and 50-368

[3.3.5] "Sourcebook for Metamic Performance Assessment", Holtec International, HI-2043215, Revision 1, February 2005

Table 3.3.1 Chemical Composition and Physical Properties of Aluminum (6061 Alloy)	
Chemical Composition	
0.8-1.2%	Magnesium
0.40-0.8%	Silicone
0.15-0.40%	Copper
0.15% max.	Iron
0.25% max.	Zinc
0.15% max.	Titanium
50 ppm max.	Nickel
10 ppm max.	Cobalt
10 ppm max.	Manganese
10 ppm max.	Chromium
0.15% max.	Other
Remainder	Aluminum
Physical Properties	
Density	0.098 lb/in^3 2.71 g/cm^3
Melting Range	1080 °F – 1205 °F 582 °C – 652 °C
Thermal Conductivity (77 °F)	1250 BTU/hr-ft^2-°F/in 1.55 kcal/hr-cm^2-°C/cm

Table 3.3.2 Chemical Composition and Physical Properties of Boron Carbide	
Chemical Composition (Weight Percent)	
Total boron	76.5 min.
B^{10} isotope	19.9 ± 0.30 a/o
HNO_3 soluble boron	0.59* max.
Water soluble boron	0.29* max.
Fluoride	25 ppm max.
Chloride	57 ppm max.
Calcium	0.3 max.
Iron	0.5 max.
Total boron plus total carbon	98.0 min.
Physical Properties	
Chemical formula	B_4C
Crystal structure	rhombohedral
Density	0.0907 lb/in^3 2.51 g/cm^3
Melting Point	4442 °F 2450 °C
Boiling Point	6332 °F 3500 °C

* From tests presented in Reference 3.3.1

4.0 CRITICALITY SAFETY ANALYSIS

4.1 Introduction and Summary

This section documents the criticality safety evaluation for the storage of PWR fresh and spent nuclear fuel in Region 1, 2 & 3 style high-density spent fuel storage racks at the ANO Unit 1 nuclear power plant operated by Entergy. This section also documents the criticality safety evaluation for the storage of fresh fuel in the new fuel vault (NFV) at the ANO Unit 1 nuclear power plant.

The objective of the spent fuel pool analysis is to ensure that the effective neutron multiplication factor (k_{eff}) is less than or equal to 0.95 with the storage racks fully loaded with fuel of the highest permissible reactivity and the pool flooded with borated water at a temperature corresponding to the highest reactivity. In addition, it is demonstrated that k_{eff} is less than 1.0 under the assumed loss of soluble boron in the pool water, i.e., assuming unborated water in the spent fuel pool. The maximum calculated reactivities include a margin for uncertainty in reactivity calculations, including manufacturing tolerances, and are calculated with a 95% probability at a 95% confidence level [4.1]. Reactivity effects of abnormal and accident conditions have also been evaluated to assure that under all credible abnormal and accident conditions, the reactivity will not exceed the regulatory limit of 0.95.

The ANO Unit 1 spent fuel pool currently contains two unique types of racks:

1. Region 1 racks: These racks were originally designed with Boraflex as the poison material in a flux-trap configuration.
2. Region 2 racks: These racks are designed to store spent fuel assemblies of a specified combination of initial enrichment and discharge burnup. These racks do not currently contain neutron absorber material.

Due to the Boraflex degradation in the Region 1 racks, future credit for Boraflex in these racks is not feasible. The proposed resolution is to re-evaluate the criticality safety of the Region 1 racks without credit for Boraflex. Additionally, some of the Region 2 racks will be modified by placing a neutron absorbing poison insert assembly into the existing Region 2 rack water gaps between storage cells. These modified Region 2 racks are identified as Region 3 racks. The new Region 3 racks will enable unrestricted storage of fresh fuel up to 4.35 wt% ^{235}U or a "3 of 4" pattern with 3 fresh fuel assemblies with enrichments up to 5.0 wt% ^{235}U and a single assembly with a maximum nominal initial enrichment of 5.0 wt% ^{235}U and a specified minimum burnup requirement.

Specifically, the following evaluations were performed for the ANO Unit 1 spent fuel pool:

- The Region 1 racks were evaluated for storage of spent fuel assemblies with specific burnup requirements as a function of initial enrichment between 2.0 wt% and 5.0 wt%

^{235}U and decay times between 0 and 20 years. Results are summarized in Table 4.7.14 and calculation of the maximum k_{eff} for 5.0 wt% ^{235}U at 0 years cooling time is given in Table 4.7.1 with no soluble boron and Table 4.7.2 with soluble boron.

- The Region 1 racks were evaluated for storage of fresh fuel assemblies with a maximum nominal enrichment of 5.0 wt% ^{235}U in a checkerboard configuration with empty storage cells. Calculation of the maximum k_{eff} is presented in Table 4.7.3 for the case without soluble credit and in Table 4.7.4 for the case with soluble boron credit.
- The Region 2 racks were evaluated for storage of spent fuel assemblies with specific burnup requirements as a function of initial enrichment between 2.0 wt% and 5.0 wt% ^{235}U and decay times between 0 and 20 years. Results are summarized in Table 4.7.15 and calculation of the maximum k_{eff} for 5.0 wt% ^{235}U at 0 years cooling time is given in Table 4.7.5 with no soluble boron and Table 4.7.6 with soluble boron.
- The Region 2 racks were evaluated for storage of fresh fuel assemblies with a maximum nominal enrichment of 5.0 wt% ^{235}U in a checkerboard configuration with empty storage cells. Calculation of the maximum k_{eff} is presented in Table 4.7.7 for the case without soluble credit and in Table 4.7.8 for the case with soluble boron credit.
- The Region 3 racks were evaluated for storage of fresh and spent fuel assemblies in a 3 of 4 configuration of 3 fresh fuel assemblies with a maximum nominal enrichment of 5.0 wt% ^{235}U and 1 spent fuel assembly with a maximum nominal initial enrichment of 5.0 wt% ^{235}U that has accumulated a minimum specified burnup. Calculation of the maximum k_{eff} is given in Table 4.7.9 with no soluble boron and Table 4.7.10 with soluble boron.
- The Region 3 racks were evaluated for unrestricted storage of fresh fuel assemblies with a maximum nominal enrichment of 4.35 wt% ^{235}U. Calculation of the maximum k_{eff} is presented in Table 4.7.11 for the case without soluble credit and in Table 4.7.12 for the case with soluble boron credit.

Reactivity effects of abnormal and accident conditions have also been evaluated. A summary of the types of accidents analyzed and the soluble boron required to ensure that the maximum k_{eff} remains below 0.95 are shown in Table 4.7.23, Table 4.7.24 and Table 4.7.25 for Region 1, Region 2 and Region 3, respectively. The most limiting accident condition involves placing a fresh fuel assembly, enriched to 5.0 wt% ^{235}U, outside the storage rack, adjacent to other fuel assemblies in the rack. A minimum soluble boron concentration of 889 ppm must be maintained in the spent fuel pool to ensure that the maximum k_{eff} is less than 0.95 under accident conditions.

In addition to the analysis for each individual rack detailed above, the possibility of an increased reactivity effect due to the rack interfaces within and between the racks was analyzed. Table 4.7.26 provides a summary of the various interface calculations performed for the ANO Unit 1 spent fuel pool. Interfaces within the rack include spent and fresh fuel loading patterns within the same rack to determine acceptability. Interface calculations between racks include Region 1-Region 1, Region 2-Region 2, Region 3-Region 3, Region 1-Region 3 and Region 2-Region 3. The calculated reactivity from the interface calculation is then compared to the calculated reactivity from the reference infinite array calculations. From the summary of the results in

Table 4.7.26 the following conclusions may be drawn regarding the reactivity effect of the interfaces:

- In the Region 1 and Region 2 racks, a fresh fuel checkerboard and uniform spent fuel loading may be placed in the same rack.
- In Region 1 and Region 2 racks, if adjacent racks contain a checkerboard of fresh fuel assemblies, the checkerboard must be maintained across the gap, i.e., fresh fuel assemblies may not face each other across a gap.
- In Region 3, uniform loading of fresh fuel at 4.35 wt% ^{235}U may be combined with 3 of 4 loading in the same rack as long as a row of fresh and spent fuel in the 3 of 4 loading pattern faces the uniform loading of all fresh fuel at 4.35 wt% ^{235}U.
- If adjacent Region 3 racks contain different loading patterns (one rack contains all fresh fuel at 4.35 wt% and the other rack contains a 3 of 4 loading pattern), both fresh and spent fuel must be in the outer row of the rack containing the 3 of 4 pattern.
- If adjacent Region 3 racks both contain 3 of 4 loading patterns, both racks may not have fresh fuel facing the other rack. Calculations with both Region 3 racks containing 3 of 4 patterns with all fresh fuel in the outer row of one rack and fresh and spent fuel in the outer row of the second rack shows a slight increase in reactivity ($\Delta k = +0.0017$) compared to the reference case. This increase is accommodated by the margin in the calculations (max k_{eff} for Region 3 racks with 3 of 4 pattern is 0.9958). Therefore, this condition is allowed.
- All interfaces between dissimilar racks (Region 1-Region 3 and Region 2-Region 3) do not result in an increase in the reactivity, and therefore, are permitted. Calculations were performed with a 3 of 4 loading pattern in the Region 3 racks, with fresh fuel (5.0 wt% ^{235}U) in the outer row facing the other rack. This is bounding for the Region 3 rack containing all fresh fuel at 4.35 wt%, because the analyzed cases have higher reactivity fuel in the outer row of the rack.

4.2 METHODOLOGY

The principal method for the criticality analysis of the high-density storage racks is the three-dimensional Monte Carlo code MCNP4a [4.3]. MCNP4a is a continuous energy three-dimensional Monte Carlo code developed at the Los Alamos National Laboratory. MCNP4a was selected because it has been used previously and verified for criticality analyses and has all of the necessary features for this analysis. MCNP4a calculations used continuous energy cross-section data based on ENDF/B-V and ENDF/B-VI. Exceptions are two lumped fission products calculated by the CASMO-4 depletion code that do not have corresponding cross sections in MCNP4a. For these isotopes, the CASMO-4 cross sections are used in MCNP4a. This approach has been validated [4.4] by showing that the cross sections result in the same reactivity effect in both CASMO-4 and MCNP4a.

Benchmark calculations, presented in Appendix 4A, indicate a bias of 0.0009 with an uncertainty of $\pm$ 0.0011 for MCNP4a, evaluated with a 95% probability at the 95% confidence level [4.1]. The

calculations for this analysis utilize the same computer platform and cross-section libraries used for the benchmark calculations discussed in Appendix 4A.

The convergence of a Monte Carlo criticality problem is sensitive to the following parameters: (1) number of histories per cycle, (2) the number of cycles skipped before averaging, (3) the total number of cycles and (4) the initial source distribution. The MCNP4a criticality output contains a great deal of useful information that may be used to determine the acceptability of the problem convergence. This information has been used in parametric studies to develop appropriate values for the aforementioned criticality parameters to be used in storage rack criticality calculations. Based on these studies, a minimum of 10,000 histories were simulated per cycle, a minimum of 100 cycles were skipped before averaging, a minimum of 150 cycles were accumulated, and the initial source was specified as uniform over the fueled regions (assemblies). Further, the output was reviewed to ensure that each calculation achieved acceptable convergence. These parameters represent an acceptable compromise between calculational precision and computational time.

Fuel depletion analyses during core operation were performed with CASMO-4 (using the 70-group cross-section library), a two-dimensional multigroup transport theory code based on capture probabilities [4.7-4.9]. CASMO-4 is used to determine the isotopic composition of the spent fuel. In addition, the CASMO-4 calculations are restarted in the storage rack geometry, yielding the two-dimensional infinite multiplication factor (k_{inf}) for the storage rack to determine the reactivity effect of fuel and rack tolerances, temperature variation, depletion uncertainty, and to perform various studies. For all calculations in the spent fuel pool racks, the Xe-135 concentration in the fuel is conservatively set to zero.

The evaluation performed to establish the burnup versus enrichment curve (loading curve) for the Region 1 and Region 2 racks, consists of MCNP4a calculations performed at selected enrichments between 2.0 wt% and 5.0 wt%, and for burnup values slightly above and below the expected loading curve. Points on the proposed loading curve are then calculated by linear interpolation for each enrichment, based on an appropriate target value (max k_{eff} = 0.9950) for the reactivity. Burnup versus enrichment values are calculated for cooling times of 0, 5, 10, 15 and 20 years. For the Region 3 racks the minimum required burnup for the single spent fuel assembly was determined with MCNP4a calculations, performed at an enrichment of 5.0 wt% ^{235}U and at burnup values slightly above and below the expected required burnup. The minimum burnup was then calculated by linear interpolation, based on an appropriate target value (max k_{eff} = 0.9958) for the reactivity.

The maximum k_{eff} is determined from the MCNP4a calculated k_{eff}, the calculational bias, the temperature bias, and the applicable uncertainties and tolerances (bias uncertainty, calculational uncertainty, rack tolerances, fuel tolerances, depletion uncertainty) using the following formula:

$$\text{Max } k_{eff}^{[1]} = \text{Calculated } k_{eff} + \text{biases} + [\Sigma_i (\text{Uncertainty}_i)^2]^{1/2}$$

In the geometric models used for the calculations, each fuel rod and its cladding were described explicitly and reflecting or periodic boundary conditions were used in the radial direction which has the effect of creating an infinite radial array of storage cells, except for the assessment of certain abnormal/accident conditions in which neutron leakage is inherent.

4.3 ACCEPTANCE CRITERIA

The high-density spent fuel PWR storage racks for ANO are analyzed in accordance with the applicable codes and standards listed below. The objective of this analysis is to ensure that the effective neutron multiplication factor (k_{eff}) is less than or equal to 0.95 with the storage racks fully loaded with fuel of the highest permissible reactivity and the pool flooded with borated water at a temperature corresponding to the highest reactivity. In addition, it is demonstrated that k_{eff} is less than 1.0 under the assumed loss of soluble boron in the pool water, i.e. assuming unborated water in the spent fuel pool. The maximum calculated reactivities include a margin for uncertainty in reactivity calculations, including manufacturing tolerances, and are calculated with a 95% probability at a 95% confidence level [4.1].

Applicable codes, standard, and regulations or pertinent sections thereof, include the following:

- *Code of Federal Regulations*, Title 10, Part 50, Appendix A, General Design Criterion 62, "Prevention of Criticality in Fuel Storage and Handling."

- USNRC Standard Review Plan, NUREG-0800, Section 9.1.2, Spent Fuel Storage, Rev. 3 - July 1981.

- USNRC letter of April 14, 1978, to all Power Reactor Licensees - OT Position for Review and Acceptance of Spent Fuel Storage and Handling Applications, including modification letter dated January 18, 1979.

- L. Kopp, "Guidance on the Regulatory Requirements for Criticality Analysis of Fuel Storage at Light-Water Reactor Power Plants," NRC Memorandum from L. Kopp to T. Collins, August 19, 1998.

- USNRC Regulatory Guide 1.13, Spent Fuel Storage Facility Design Basis, Rev. 2 (proposed), December 1981.

---

[1] The maximum k_{eff} value listed in Table 4.7.1 through Table 4.7.12 may differ from the calculated value based on this formula ($\Delta k = 0.0001$) due to rounding.

- ANSI ANS-8.17-1984, Criticality Safety Criteria for the Handling, Storage and Transportation of LWR Fuel Outside Reactors.

- Code of Federal Regulation 10CFR50.68, Criticality Accident Requirements (for soluble boron).

4.4 ASSUMPTIONS

To assure the true reactivity will always be less than the calculated reactivity, the following conservative design criteria and assumptions were employed:

1) Moderator is borated or unborated water at a temperature in the operating range that results in the highest reactivity, as determined by the analysis.

2) Neutron absorption in minor structural members is neglected, i.e., spacer grids are replaced by water.

3) The effective multiplication factor of an infinite radial array of fuel assemblies was used in the analyses, except for the assessment of certain abnormal/accident conditions in which neutron leakage is inherent.

4) The B_4C loading in the neutron absorber panels is nominally 25 wt%, with an uncertainty of $\pm$ 0.5 wt%

5) Axial Power Shaping Rods (APSRs) and Burnable Poison Rod Assemblies (BPRAs) are assumed to cover the entire active fuel length of the assembly during depletion. No credit is taken in the rack criticality calculations for the APSRs and BPRAs.

4.5 INPUT DATA

4.5.1 Fuel Assembly Specification

The spent fuel storage racks are designed to accommodate B&W 15x15 fuel assemblies (HTP[2] and NON-HTP). The design specifications for these fuel assemblies, which were used for this analysis, are given in Table 4.5.1.

---

[2] HTP - High Thermal Performance

4.5.2 Core Operating Parameters

Core operating parameters are necessary for fuel depletion calculations performed with CASMO-4. The core parameters necessary for the depletion calculations are presented in Table 4.5.2. Temperature and soluble boron values are taken as the upper bound (most conservative) of the core operating parameters of ANO Unit 1. The neutron spectrum is hardened by each of these parameters, leading to a greater production of plutonium during depletion, which results in conservative reactivity values.

4.5.3 Axial Burnup Distribution

Axial burnup profiles were provided by Entergy and are documented in Table 4.5.3 for low burnup assemblies (<25 GWD/MTU). For assemblies with burnup greater than or equal to 25 GWD/MTU, the axial burnup distribution from [4.12] was specified and is also provided in Table 4.5.3 under the Holtec column. This distribution has been used and approved in previous wet storage rack submittals to the NRC (Docket #'s: 50-368, ANO Unit 2; 50-395, V.C. Summer; 50-275/50-323, Diablo Canyon).

4.5.4 Core Inserts

There is the potential for an insert (BPRA or APSR or both, but not simultaneously) to be located in the assembly during different exposure intervals in the assembly's core lifetime. The design specifications for the BPRAs and APSRs are given in Tables 4.5.4 through 4.5.6. The core inserts are conservatively considered only in the depletion calculations; no credit is taken for core inserts in the rack criticality calculations.

4.5.5 ANO Unit 1 Storage Rack Specification

The storage cell characteristics for the Region 1, 2 & 3 storage racks which are used in the criticality evaluations are summarized in Table 4.5.7 through Table 4.5.9.

4.5.5.1 Region 1 Style Storage Racks

The Region 1 storage cells are composed of stainless steel boxes separated by a gap with Boraflex neutron absorber panels, (attached by stainless steel sheathing) centered on each side of the storage cell. The steel walls define the storage cells and the stainless steel sheathing supports the Boraflex neutron absorber panel and defines the boundary of the flux-trap water-gap used to augment reactivity control. The Boraflex is conservatively assumed to be completely degraded

and replaced with water. Stainless steel channels connect the storage cells in a rigid structure and define the flux-trap between the sheathing of the neutron absorber panels. Figure 4.5.9 provides a sketch of the Region 1 racks along with the critical dimensions. Additionally, the Region 1 racks contain sheathing on the side of the racks that faces another rack, however there is no sheathing on the side of the racks that faces the spent fuel pool wall.

The calculational models consist of either a single storage cell or a group of 25 storage cells (5x5) with reflecting boundary conditions or a group of four storage cells (2x2) with periodic boundary conditions through the centerline of the water gap on the outer boundary of the four cells, thus simulating an infinite array of Region 1 storage cells. Figure 4.5.1 and Figure 4.5.2 show the actual MCNP4a calculational model of the nominal Region 1 spent fuel storage cell, as drawn by the two-dimensional plotter in MCNP4a for the individual cell model and the 2x2 model, respectively.

4.5.5.2 Region 2 Style Storage Racks

The Region 2 storage cells are composed of stainless steel walls with no neutron absorber panels. The stainless steel walls are formed in such a way as to create a water gap between adjacent cells. Figure 4.5.10 provides a sketch of the Region 2 racks along with the critical dimensions.

The calculational models consist of either a single storage cell or a group of 25 storage cells (5x5) with reflecting boundary conditions or a group of four storage cells (2x2) with periodic boundary conditions through the centerline of the water gap on the outer boundary of the four cells, thus simulating an infinite array of Region 2 storage cells. Figure 4.5.3 and Figure 4.5.4 shows the actual MCNP4a calculational model of the nominal Region 2 spent fuel storage cell, as drawn by the two-dimensional plotter in MCNP4a for the individual cell model and the 2x2 model, respectively.

4.5.5.3 Region 3 Style Storage Racks

The Region 3 storage cells are identical to the Region 2 storage cells, with the single exception of a metamic insert centrally located in the water gap between storage cells. Figure 4.5.11 provides a sketch of the Region 3 racks along with the critical dimensions.

The calculational models consist of either a single storage cell or a group of 25 storage cells (5x5) with reflecting boundary conditions or a group of four storage cells (2x2) with periodic boundary conditions through the centerline of the water gap on the outer boundary of the four cells, thus simulating an infinite array of Region 3 storage cells. Figure 4.5.5 and Figure 4.5.6 shows the actual MCNP4a calculational model of the nominal Region 3 spent fuel storage cell, as drawn by the two-dimensional plotter in MCNP4a for the individual cell model and the 2x2 model, respectively.

4.5.5.4 Gaps Between Adjacent Racks

In addition to the calculations for each style of rack in the ANO Unit 1 spent fuel pool, the reactivity effect of potential interaction between adjacent racks and between different loading patterns is addressed. Figure 4.5.7 shows a diagram of the spent fuel pool layout, including location of the different styles of racks, with respect to each other, and the distances of the gaps between adjacent racks. The values taken from this figure are the minimum distances from the center of one storage cell to the center of the storage cell in the adjacent rack, denoted by a "C" and followed by the dimension in inches. Table 4.5.10 identifies the possible rack-to-rack interactions, the centerline-to-centerline distance, and the calculated gap between the adjacent racks. Figure 4.5.8 presents a diagram as to how the distance between racks listed in Table 4.5.10 is measured.

4.6 COMPUTER CODES

The following computer codes were used during this analysis.

- MCNP4a [4.3] is a three-dimensional continuous energy Monte Carlo code developed at Los Alamos National Laboratory. This code offers the capability of performing full three-dimensional calculations for the loaded storage racks. MCNP4a was run on the PCs at Holtec.

- CASMO-4, Version 2.05.14 [4.7-4.9] is a two-dimensional multigroup transport theory code developed by Studsvik of Sweden. CASMO-4 performs cell criticality calculations and burnup. CASMO-4 has the capability of analytically restarting burned fuel assemblies in the rack configuration. This code was used to determine the reactivity effects of tolerances and fuel depletion. The CASMO-4 code was run on a PC at Holtec.

4.7 ANALYSIS

This section describes the calculations that were used to determine the acceptable storage criteria for the Region 1, Region 2 and Region 3 style racks. In addition, this section discusses the possible abnormal and accident conditions.

Unless otherwise stated, all calculations assumed nominal characteristics for the fuel and the fuel storage cells. The effect of the manufacturing tolerances is accounted for with a reactivity adjustment as discussed below.

As discussed in Section 4.2, MCNP4a was the primary code used in the PWR calculations. CASMO-4 was used to determine the reactivity effect of tolerances and for depletion calculations. MCNP4a was used for reference cases and to perform calculations which are not possible with CASMO-4 (e.g. eccentric fuel positioning, axial burnup distributions, and fuel misloading).

Figures 4.5.1 through 4.5.6 are pictures of the basic calculational models used in MCNP4a. These pictures were created with the two-dimensional plotter in MCNP4a and clearly indicate the explicit modeling of fuel rods in each fuel assembly. In CASMO-4, a single cell is modeled, and since CASMO-4 is a two-dimensional code, the fuel assembly hardware above and below the active fuel length is not represented. The three-dimensional MCNP4a models that included axial leakage assumed approximately 30 cm of water above and below the active fuel length. Additional models with more than four cells were generated with MCNP4a to investigate the effect of accident conditions. These models are discussed in the appropriate section.

4.7.1 Calculational Methodologies Applicable to Region 1, Region 2 & Region 3

4.7.1.1 Moderator Temperature Effect

For the depletion calculations, the temperature at the top of the active region is used as the moderator temperature (see Table 4.5.2). However, the reactivity in the rack is dominated by the area slightly below the top of the active region, where the moderator temperature in the core is lower. Since the reactivity increases significantly with increasing moderator temperature, the assumption used in the depletion calculations is conservative.

4.7.1.2 Reactivity Effect of Inserts During Depletion

Due to variations in plant operation, it is impossible to predict the exact exposure intervals that BPRAs and APSRs will be in the assemblies during core operation. Therefore, for conservatism, BPRAs are assumed to be present early in the assembly's life, when the BPRA has a stronger reactivity effect than the APSR. APSRs are then assumed to be inserted into the assembly once the BPRA has received a high enough burnup for their reactivity effect to be less than that of the APSRs, typically around 15 GWD/MTU.

To determine the burnup at which to change from a BPRA to an APSR, termed here as the "crossover burnup", depletion calculations are performed in CASMO-4 with the HTP assembly containing an APSR, a BPRA or no insert. The assembly and the insert, if the assembly has one, is then transferred into the Region 1 rack. The calculated reactivities as a function of burnup are compared between the three assemblies (with APSR, with BPRA and with no insert) and the burnup at which the reactivity of the assembly with the BPRA is equal to the reactivity of the assembly with the APSR is calculated. Calculations to determine the reactivity of the assembly with an APSR or BPRA were performed for enrichments between 2.0 and 5.0 wt% ^{235}U in 0.5 wt% increments and for cooling times between 0 and 20 years. Table 4.7.16 presents an example of the reactivity effect of the presence of fuel inserts (BPRA, APSR and no insert) for an enrichment of 5.0 wt% ^{235}U and a cooling time of 0 years. From the calculations it was determined that the crossover burnup is dependent upon enrichment, but shows only little variation with cooling time. Therefore, the crossover burnup for each enrichment is calculated

by averaging the crossover burnup for each enrichment at cooling times of 0, 5, 10, 15 and 20 years. The enrichment dependency of the crossover burnup is shown in Table 4.7.13. These values are used in all subsequent depletion calculations.

4.7.1.3 Reactivity Effect of Axial Burnup Distribution

Initially, fuel loaded into the reactor will burn with a slightly skewed cosine power distribution. As burnup progresses, the burnup distribution will tend to flatten, becoming more highly burned in the central regions than in the upper and lower ends. At high burnup, the more reactive fuel near the ends of the fuel assembly (less than average burnup) occurs in regions of lower reactivity worth due to neutron leakage. Consequently, it would be expected that over most of the burnup history, distributed burnup fuel assemblies would exhibit a slightly lower reactivity than that calculated for the average burnup. As burnup progresses, the distribution, to some extent, tends to be self-regulating as controlled by the axial power distribution, precluding the existence of large regions of significantly reduced burnup.

Generic analytic results of the axial burnup effect for assemblies without axial blankets have been provided by Turner [4.12] based upon calculated and measured axial burnup distributions. These analyses confirm the minor and generally negative reactivity effect of the axially distributed burnup compared to a flat distribution, becoming positive at burnups greater than about 30 GWD/MTU. The trends observed in [4.12] suggest the possibility of a small positive reactivity effect above 30 GWD/MTU increasing to slightly over 1% Δk at 40 GWD/MTU. The required burnup for the maximum enrichment is slightly higher than 30 GWD/MTU. Therefore, a positive reactivity effect of the axially distributed burnup is possible. Calculations are performed with the HTP axial burnup distribution from Table 4.5.3 for burnups at or below 25 GWD/MTU and with the Holtec axial burnup distribution for burnups above 25 GWD/MTU. As Section 4.5.3 discusses, the Holtec axial burnup distribution is specified to be used for burnups at 25 GWD/MTU. However, use of the HTP axial burnup distribution specified in Table 4.5.3 at 25 GWD/MTU is conservative, due to the significantly lower relative burnups near the ends of the active fuel region.

4.7.1.4 Isotopic Compositions

To perform the criticality evaluation for spent fuel in MCNP4a, the isotopic composition of the fuel is calculated with the depletion code CASMO-4 and then specified as input data in the MCNP4a run. The CASMO-4 calculations to obtain the isotopic compositions for MCNP4a were performed generically, with one calculation for each enrichment, and burnups in increments of 2.5 GWD/MTU or less. The isotopic composition for any given burnup is then determined by linear interpolation.

4.7.1.5 Uncertainty in Depletion Calculations

Since critical experiment data with spent fuel is not available for determining the uncertainty in burnup-dependent reactivity calculations, an allowance for uncertainty in reactivity was assigned based upon other considerations. Assuming the uncertainty in depletion calculations is less than 5% of the total reactivity decrement, a burnup dependent uncertainty in reactivity for burnup calculations may be assigned [4.10]. This allowance is statistically combined with the other reactivity allowances in the determination of the maximum k_{eff} for normal conditions where assembly burnup is credited.

4.7.2 Region 1

The purpose of the criticality calculations for the Region 1 style racks is to qualify the racks for storage of spent fuel assemblies with design specifications as shown in Table 4.5.1 and a maximum nominal initial enrichment of 5.0 wt% ^{235}U that have accumulated a minimum burnup with credit for cooling times between 0 and 20 years. The purpose of the criticality calculations is to determine the initial enrichment and burnup combinations required for the storage of spent fuel assemblies with nominal initial enrichments up to 5.0 wt% ^{235}U and for cooling times up to 20 years. Additionally, the Region 1 racks are qualified for storage of fresh fuel assemblies, in a checkerboard pattern with empty storage cells, at a maximum nominal enrichment of 5.0 wt% ^{235}U.

4.7.2.1 Identification of Reference Fuel Assembly

CASMO-4 calculations were performed to determine which of the two assemblies in Table 4.5.1 is bounding in the Region 1 racks. In the calculations, the fuel assembly is burned in the core configuration and restarted in the rack configuration. Three different scenarios were analyzed: empty guide tubes in the core, BPRAs in the guide tubes in the core, and APSRs in the guide tubes in the core. In all scenarios, the insert was removed when the assembly was modeled in the rack. The HTP assembly was determined to have the highest reactivity for all burnup and enrichment combinations. This assembly type is therefore used in all subsequent calculations.

4.7.2.2 Eccentric Fuel Assembly Positioning

The fuel assembly is assumed to be normally located in the center of the storage rack cell. In the absence of a fixed neutron absorber, the eccentric location of fuel assemblies in the storage cells may produce a positive reactivity effect. Therefore, MCNP4a calculations for a uniform loading of spent fuel assemblies and a checkerboard of fresh fuel assemblies and empty storage locations were performed with the fuel assemblies assumed to be in the corner of the storage rack cell (four-assembly cluster at closest approach). Three different enrichment and burnup combinations were analyzed for the spent fuel configuration. These calculations indicate that eccentric fuel positioning results in an increase in reactivity.

The eccentric positioning is performed in a very conservative manner, assuming 4 assemblies in the corners of the storage cell, at closest approach to each other, and that these clusters of four assemblies are repeated throughout the rack. However, since eccentric positioning is highly unlikely to occur in this manner and recognizing that placement of fuel assemblies in the storage cells is random, the maximum reactivity effect of eccentric positioning for both spent and fresh fuel is applied as an uncertainty, and combined statistically with other uncertainties as shown in Table 4.7.1 through Table 4.7.4.

4.7.2.3 Uncertainties Due to Manufacturing Tolerances

In the calculation of the final k_{eff}, the effect of manufacturing tolerances on reactivity must be included. CASMO-4 was used to perform these calculations. As allowed in [4.10], the methodology employed to calculate the tolerance effects combine both the worst-case bounding value and sensitivity study approaches. The evaluations include tolerances of the rack dimensions (see Table 4.5.7) and tolerances of the fuel dimensions (see Table 4.5.1). As for the bounding assembly, calculations are performed for different enrichments and burnups. The reference condition is the condition with nominal dimensions and properties. To determine the Δk associated with a specific manufacturing tolerance, the k_{inf} calculated for the reference condition is compared to the k_{inf} from a calculation with the tolerance included. Note that for the individual parameters associated with a tolerance, no statistical approach is utilized. Instead, the full tolerance value is utilized to determine the maximum reactivity effect. All of the Δk values from the various tolerances are statistically combined (square root of the sum of the squares) to determine the final reactivity allowance for manufacturing tolerances. Only the Δk values in the positive direction (increasing reactivity) were used in the statistical combination. The fuel and rack tolerances included in this analysis are described below:

Fuel Tolerances	
• Increased Fuel Density	0.20g/cm^3
• Increased Fuel Enrichment	0.05 wt% ^{235}U
• Fuel Rod Pitch	+0.00258 in./-0.00387 in.
• Fuel Rod Cladding Outside Diameter	± 0.002 in.
• Fuel Rod Cladding Inner Diameter	± 0.002 in.
• Fuel Pellet Outside Diameter	± 0.0005 in.
• Guide Tube Outside Diameter	± 0.002 in.
• Guide Tube Inside Diameter	± 0.0052 in.
Rack Tolerances	
• Variable Cell Inner Dimension & Constant Water Gap	+0.025 in./-0.05 in.

- Variable Water Gap & Constant Pitch +0.05 in./-0.025 in.[3]
- Box Wall Thickness ± 0.004 in.
- Sheathing Thickness ± 0.004 in.
- Poison Gap Thickness ± 0.010 in.

The reactivity effects of the fuel and rack tolerances shown above were calculated for enrichments between 2.0 and 5.0 wt% ^{235}U and for 0 cooling time. For longer cooling times the fuel and rack tolerances from 0 cooling time are used. Table 4.7.17 provides representative examples of the reactivity effect of the fuel and rack tolerances for the Region 1 racks.

4.7.2.4 Temperature and Water Density Effects

Pool water temperature effects on reactivity in the Region 1 racks have been calculated with CASMO-4 for enrichments from 2.0 to 5.0 wt% ^{235}U and cooling times from 0 years to 20 years. The results in Table 4.7.18 for 5.0 wt% ^{235}U show that the spent fuel pool temperature coefficient of reactivity is positive, i.e. a higher temperature results in a higher reactivity. Consequently, all CASMO-4 calculations are evaluated at 150 °F. Temperatures higher than 150 °F are treated as accidents and discussed in Section 4.7.5.

In MCNP4a, the Doppler treatment and cross-sections are valid only at 300K (27 °C). Therefore, a Δk is determined in CASMO-4 from 27 °C (80.33 °F) to 150 °F, and is included in the final k_{eff} calculation as a bias. The temperature bias is shown on Table 4.7.1 through Table 4.7.4.

4.7.2.5 Calculation of Maximum k_{eff}

Using the calculational model shown in Figure 4.5.1 and 4.5.2 and the reference HTP 15x15 fuel assembly, the k_{eff} in the Region 1 storage racks has been calculated with MCNP4a. A summary of the calculation of the maximum k_{eff}, which is based on the formula in Section 4.2, for spent fuel of maximum nominal initial enrichment of 5 wt% ^{235}U and for the fresh fuel checkerboard is shown in Table 4.7.1 and Table 4.7.3 without soluble boron. Uncertainties associated with depletion are not applicable to the Region 1 checkerboard of fresh fuel assemblies and empty storage cells. Results show that the maximum k_{eff} of the Region 1 racks is less than 1.0 at a 95% probability at a 95% confidence level with no credit for soluble boron.

---

[3] No tolerance was given for the water gap, therefore it was assumed that the water gap tolerance is consistent with the tolerance for the storage cell inner dimension.

4.7.2.6 Determination of Burnup Versus Enrichment Values

To establish a burnup versus enrichment curve (loading curve), calculations were performed at selected enrichments between 2.0 wt% and 5.0 wt%, and for burnup values slightly above and below the expected loading curve. Points on the proposed loading curve are then calculated by linear interpolation for each enrichment, based on an appropriate target value (max k_{eff} = 0.9950) for the reactivity. Burnup versus enrichment values are calculated for cooling times of 0, 5, 10, 15 and 20 years and presented in Table 4.7.14.

4.7.2.7 Soluble Boron Concentration for Maximum k_{eff} of 0.95

Calculations crediting soluble boron in the spent fuel pool to ensure that the reactivity does not exceed 0.95 are also performed. Calculations for a uniform loading of spent fuel are performed for enrichment and cooling time combinations of 2.0 wt% ^{235}U at 0 years cooling, 5.0 wt% ^{235}U at 0 years cooling and 5.0 wt% ^{235}U at 20 years cooling at a soluble boron level of 0 ppm and 400 ppm. For a checkerboard of fresh fuel and empty cells, calculations are performed at 5.0 wt% ^{235}U and with a soluble boron level of 0 ppm and 400 ppm. The minimum soluble boron requirement is determined by linear interpolation between soluble boron levels to achieve a target maximum k_{eff} of 0.9450. In all cases, the maximum k_{eff} including all applicable biases and uncertainties is below the regulatory limit of 0.95. The results for 5.0 wt% initial enrichment are also listed in Table 4.7.2 and Table 4.7.4 for uniform loading of spent fuel and a checkerboard of fresh fuel assemblies and empty storage cells, respectively.

4.7.3 Region 2

The purpose of the criticality calculations for the PWR Region 2 style racks is to qualify the racks for storage of fuel assemblies with design specifications as shown in Table 4.5.1 and a maximum nominal initial enrichment of 5.0 wt% ^{235}U that have accumulated a minimum burnup with credit for cooling times between 0 and 20 years. The purpose of the criticality calculations is to determine the initial enrichment and burnup combinations required for the storage of fuel assemblies with nominal initial enrichments up to 5.0 wt% ^{235}U and for cooling times up to 20 years. Additionally, the Region 2 racks are qualified for storage of fresh fuel assemblies, in a checkerboard pattern with empty storage cells, at a maximum nominal enrichment of 5.0 wt% ^{235}U.

4.7.3.1 Identification of Reference Fuel Assembly

CASMO-4 calculations were performed to determine which of the two assemblies in Table 4.5.1 is bounding in the Region 2 racks. In the calculations, the fuel assembly is burned in the core configuration and restarted in the rack configuration. Three different scenarios were analyzed: empty guide tubes in the core, BPRAs in the guide tubes in the core, and APSRs in the guide

tubes in the core. In all scenarios, the insert was removed when the assembly was modeled in the rack. The HTP assembly was determined to have the highest reactivity for all burnup and enrichment combinations. This assembly type is therefore used in all subsequent calculations.

4.7.3.2 Eccentric Fuel Assembly Positioning

The fuel assembly is assumed to be normally located in the center of the storage rack cell. In the absence of a fixed neutron absorber, the eccentric location of fuel assemblies in the storage cells may produce a positive reactivity effect. Therefore, MCNP4a calculations for a uniform loading of spent fuel assemblies and a checkerboard of fresh fuel assemblies and empty storage locations were performed with the fuel assemblies assumed to be in the corner of the storage rack cell (four-assembly cluster at closest approach). Three different enrichment and burnup combinations were analyzed for the spent fuel configuration. These calculations indicate that eccentric fuel positioning results in an increase in reactivity.

The eccentric positioning is performed in a very conservative manner, assuming 4 assemblies in the corners of the storage cell, at closest approach to each other, and that these clusters of four assemblies are repeated throughout the rack. However, since eccentric positioning is highly unlikely to occur in this manner and recognizing that placement of fuel assemblies in the storage cells is random, the maximum reactivity effect of eccentric positioning for both spent and fresh fuel is applied as an uncertainty, and combined statistically with other uncertainties as shown in Table 4.7.5 through Table 4.7.8.

4.7.3.3 Uncertainties Due to Manufacturing Tolerances

In the calculation of the final k_{eff}, the effect of manufacturing tolerances on reactivity must be included. CASMO-4 was used to perform these calculations. As allowed in [4.10], the methodology employed to calculate the tolerance effects combine both the worst-case bounding value and sensitivity study approaches. The evaluations include tolerances of the rack dimensions (see Table 4.5.8) and tolerances of the fuel dimensions (see Table 4.5.1). As for the bounding assembly, calculations are performed for different enrichments and burnups. The reference condition is the condition with nominal dimensions and properties. To determine the Δk associated with a specific manufacturing tolerance, the k_{inf} calculated for the reference condition is compared to the k_{inf} from a calculation with the tolerance included. Note that for the individual parameters associated with a tolerance, no statistical approach is utilized. Instead, the full tolerance value is utilized to determine the maximum reactivity effect. All of the Δk values from the various tolerances are statistically combined (square root of the sum of the squares) to determine the final reactivity allowance for manufacturing tolerances. Only the Δk values in the positive direction (increasing reactivity) were used in the statistical combination. The fuel and rack tolerances included in this analysis are described below:

Fuel Tolerances

• Increased Fuel Density	0.20g/cm^3
• Increased Fuel Enrichment	0.05 wt% ^{235}U
• Fuel Rod Pitch	+0.00258 in./-0.00387 in.
• Fuel Rod Cladding Outside Diameter	± 0.002 in.
• Fuel Rod Cladding Inner Diameter	± 0.002 in.
• Fuel Pellet Outside Diameter	± 0.0005 in.
• Guide Tube Outside Diameter	± 0.002 in.
• Guide Tube Inside Diameter	± 0.0052 in.

Rack Tolerances

• Variable Cell Inner Dimension & Constant Water Gap	+0.05 in./-0.025 in.
• Variable Water Gap & Constant Pitch	+0.166 in./-0.221 in.
• Box Wall Thickness	± 0.004 in.

The reactivity effect of the fuel and rack tolerances shown above were calculated for enrichments between 2.0 and 5.0 wt% ^{235}U and for 0 cooling time. For longer cooling times the fuel and rack tolerances from 0 cooling time are used. Table 4.7.19 provides representative examples of the reactivity effect of the fuel and rack tolerances for the Region 2 racks.

4.7.3.4 Temperature and Water Density Effects

Pool water temperature effects on reactivity in the Region 2 racks have been calculated with CASMO-4 for enrichments from 2.0 to 5.0 wt% ^{235}U and cooling times from 0 to 20 years. The results in Table 4.7.20 for 5.0 wt% ^{235}U show that the spent fuel pool temperature coefficient of reactivity is positive, i.e. a higher temperature results in a higher reactivity. Consequently, all CASMO-4 calculations are evaluated at 150 °F. Temperatures higher than 150 °F are treated as accidents and discussed in Section 4.7.5.

In MCNP4a, the Doppler treatment and cross-sections are valid only at 300K (27 °C). Therefore, a Δk is determined in CASMO-4 from 27 °C (80.33 °F) to 150 °F, and is included in the final k_{eff} calculation as a bias. The temperature bias is shown on Table 4.7.5 through Table 4.7.8.

4.7.3.5 Calculation of Maximum k_{eff}

Using the calculational model shown in Figure 4.5.3 and 4.5.4 and the reference HTP 15x15 fuel assembly, the k_{eff} in the Region 2 storage racks has been calculated with MCNP4a. Summary of the calculation of the maximum k_{eff}, which is based on the formula in Section 4.2, for spent fuel of maximum nominal enrichment of 5.0 wt% ^{235}U and for the fresh fuel checkerboard are shown in Table 4.7.5 and Table 4.7.7 without soluble boron. Uncertainties associated with depletion are not applicable to the Region 2 checkerboard of fresh fuel assemblies and empty storage cells. Results show that the maximum k_{eff} of the Region 2 racks is less than 1.0 at a 95% probability at a 95% confidence level with no credit for soluble boron.

4.7.3.6 Determination of Burnup Versus Enrichment Values

To establish a burnup versus enrichment curve (loading curve), calculations were performed at selected enrichments between 2.0 wt% and 5.0 wt%, and for burnup values slightly above and below the expected loading curve. Points on the proposed loading curve are then calculated by linear interpolation for each enrichment, based on an appropriate target value (max k_{eff} = 0.9950) for the reactivity. Burnup versus enrichment values are calculated for cooling times of 0, 5, 10, 15 and 20 years and presented in Table 4.7.15.

4.7.3.7 Soluble Boron Concentration for Maximum k_{eff} of 0.95

The calculations crediting soluble boron in the spent fuel pool to ensure that the reactivity does not exceed 0.95 are also performed. Calculations for a uniform loading of spent fuel are performed for enrichment and cooling time combinations of 2.0 wt% ^{235}U at 0 years cooling, 5.0 wt% ^{235}U at 0 years cooling and 5.0 wt% ^{235}U at 20 years cooling at a soluble boron level of 0 ppm and 400 ppm. For a checkerboard of fresh fuel and empty storage cells, calculations are performed at 5.0 wt% ^{235}U and with a soluble boron concentration of 0 ppm and 400 ppm. The minimum soluble boron requirement is determined by linear interpolation between soluble boron levels to achieve a target maximum k_{eff} of 0.9450. In all cases, the maximum k_{eff} including all applicable biases and uncertainties is below the regulatory limit of 0.95. The results for 5.0 wt% initial enrichment is also listed in Table 4.7.6 and Table 4.7.8 for uniform loading of spent fuel and a checkerboard of fresh fuel assemblies and empty storage cells, respectively.

4.7.4 Region 3

The purpose of the criticality calculations for the PWR Region 3 style racks is to qualify the racks for storage of new unburned fuel assemblies with design specifications as shown in Table 4.5.1 and a maximum nominal enrichment of 4.35 wt% ^{235}U. Additionally, the Region 3 style racks are qualified for storage of a "3 of 4" configuration of 3 fresh fuel assemblies with a maximum nominal enrichment of 5.0 wt% ^{235}U and 1 spent fuel assembly with a maximum nominal initial enrichment of 5.0 wt% ^{235}U that have accumulated a minimum burnup of 20.1 GWD/MTU with 0 years cooling time. No credit was taken in the "3 of 4" configuration for longer cooling times, as this would provide only a small reduction in the required burnup for the single spent fuel assembly in this configuration.

4.7.4.1 Identification of Reference Fuel Assembly

CASMO-4 calculations were performed to determine which of the two assemblies in Table 4.5.1 is bounding in the Region 3 racks. In the calculations, the fuel assembly is burned in the core configuration and restarted in the rack configuration. Three different scenarios were analyzed: empty guide tubes in the core, BPRAs in the guide tubes in the core, and APSRs in the guide

tubes in the core. In all scenarios, the insert was removed when the assembly was modeled in the rack. The HTP assembly was determined to have the highest reactivity for all burnup and enrichment combinations. This assembly type is therefore used in all subsequent calculations.

4.7.4.2 Eccentric Fuel Assembly Positioning

The fuel assembly is assumed to be normally located in the center of the storage rack cell. Nevertheless, MCNP4a calculations were made with the fuel assemblies assumed to be in the corner of the storage rack cell (four-assembly cluster at closest approach). These calculations indicate that eccentric fuel positioning results in a decrease in reactivity. The highest reactivity, therefore, corresponds to the reference design with the fuel assemblies positioned in the center of the storage cells.

4.7.4.3 Uncertainties Due to Manufacturing Tolerances

In the calculation of the final k_{eff}, the effect of manufacturing tolerances on reactivity must be included. CASMO-4 was used to perform these calculations. As allowed in [4.10], the methodology employed to calculate the tolerance effects combine both the worst-case bounding value and sensitivity study approaches. The evaluations include tolerances of the rack dimensions (see Table 4.5.9) and tolerances of the fuel dimensions (see Table 4.5.1).

The reference fuel assembly with an initial nominal enrichment of 4.35 wt% ^{235}U and 5.0 wt% ^{235}U was used for these studies in the fresh fuel configuration and the "3 of 4" configuration, respectively. The reference condition is the condition with nominal dimensions and properties. To determine the Δk associated with a specific manufacturing tolerance, the reference k_{inf} was compared to the k_{inf} from a calculation with the tolerance included. Note that for the individual parameters associated with a tolerance, no statistical approach is utilized. Instead, the full tolerance value is utilized to determine the maximum reactivity effect. All of the Δk values from the various tolerances are statistically combined (square root of the sum of the squares) to determine the final reactivity allowance for manufacturing tolerances. Only the Δk values in the positive direction (increasing reactivity) were used in the statistical combination. The fuel and rack tolerances included in this analysis are described below:

Fuel Tolerances

- Increased Fuel Density — $0.20 g/cm^3$
- Increased Fuel Enrichment — 0.05 wt% ^{235}U
- Fuel Rod Pitch — +0.00258 in./-0.00387 in.
- Fuel Rod Cladding Outside Diameter — ± 0.002 in.
- Fuel Rod Cladding Inner Diameter — ± 0.002 in.
- Fuel Pellet Outside Diameter — ± 0.0005 in.
- Guide Tube Outside Diameter — ± 0.002 in.
- Guide Tube Inside Diameter — ± 0.0052 in.

Rack Tolerances

• Cell Inner Dimension & Pitch	+0.05 in./-0.025 in.
• Cell Inner Dimension & Water Gap	+0.166 in./-0.221 in.[4]
• Box Wall Thickness	± 0.004 in.
• Insert Sheathing Thickness	± 0.003 in.
• Insert Water Gap	± 0.05 in.
• Metamic Thickness	± 0.003 in.
• Metamic Width	± 0.062 in.
• Metamic B_4C Weight Percent	0.5 wt%

The reactivity effect of the fuel and rack tolerances shown above were calculated for enrichments of 4.35 wt% ^{235}U and 5.0 wt% ^{235}U and for 0 cooling time. Table 4.7.21 provides representative examples of the reactivity effect of the fuel and rack tolerances for the Region 3 racks.

4.7.4.4 Temperature and Water Density Effects

Pool water temperature effects on reactivity in the Region 3 racks have been calculated with CASMO-4 for enrichments of 4.35 and 5.0 wt% ^{235}U. The results in Table 4.7.22 for 4.35 wt% ^{235}U and 5.0 wt% ^{235}U show that the spent fuel pool temperature coefficient of reactivity is negative, i.e. a lower temperature results in a higher reactivity. Consequently, all CASMO-4 calculations are evaluated at 4 °C, which corresponds to the highest density of water.

In MCNP4a, the Doppler treatment and cross-sections are valid only at 300K (27 °C). Therefore, a Δk is determined in CASMO-4 from 27 °C to 4 °C, and is included in the final k_{eff} calculation as a bias. The temperature bias is shown on Table 4.7.9 though Table 4.7.12.

4.7.4.5 Calculation of Maximum k_{eff}

Using the calculational model shown in Figure 4.5.5 and Figure 4.5.6 and the reference HTP 15x15 fuel assembly, the k_{eff} in the Region 3 storage racks has been calculated with MCNP4a. Calculation of the maximum k_{eff}, which is based on the formula in Section 4.2, for the 3 of 4 loading configuration and uniform loading of fresh fuel at 4.35 wt% ^{235}U, is summarized in Table 4.7.9 and Table 4.7.11 without soluble boron. Uncertainties associated with depletion

---

[4] The tolerances listed are for the water gap between storage cells. A reduction in the rack water gap causes an equal increase in the storage cell inner dimension. The maximum reduction possible in the rack water gap is -0.21", as this would make the rack water gap just large enough to fit the metamic insert.

(e.g., depletion uncertainty and axial burnup distribution penalty) are not applicable to the Region 3 loading pattern with all fresh fuel of 4.35 wt% ^{235}U. Results show that the maximum k_{eff} of the Region 3 racks is less than 1.0 at a 95% probability at a 95% confidence level with no credit for soluble boron.

4.7.4.6 Determination of the Minimum Burnup for a Single Spent Assembly in the 3 of 4 Loading Pattern

To establish a minimum required burnup for the loading pattern with 3 fresh fuel assemblies and one spent fuel assembly, calculations were performed with all assemblies having a maximum nominal initial enrichment of 5.0 wt% ^{235}U and the single spent fuel assembly having burnup values slightly above and below the expected burnup value. The acceptable burnup for the single spent fuel assembly is then calculated by linear interpolation, based on an appropriate target value (max k_{eff} = 0.9958) for the reactivity. All calculations were performed at 0 cooling time; no credit was taken for additional cooling time for the single spent assembly as the reduction in burnup would be minimal. The minimum burnup is shown for 3 of 4 loading in Table 4.7.9.

4.7.4.7 Soluble Boron Concentration for Maximum k_{eff} of 0.95

Calculations crediting soluble boron in the spent fuel pool to ensure that the reactivity does not exceed 0.95 are also performed. Calculations are performed at enrichments of 4.35 wt% ^{235}U and 5.0 wt% ^{235}U for uniform loading of fresh fuel and a 3 of 4 configuration, respectively, at a soluble boron level of 400 ppm and 800 ppm. The minimum soluble boron requirement is determined by linear interpolation between soluble boron levels to achieve a target maximum k_{eff} of 0.9450. In all cases, the maximum k_{eff} including all applicable biases and uncertainties is below the regulatory limit of 0.95. The results for each loading pattern in Region 3 is also listed in Table 4.7.10 and Table 4.7.12 for a 3 of 4 configuration and uniform loading of fresh fuel, respectively.

4.7.5 Abnormal and Accident Conditions for Region 1, 2 & 3 Racks

The effects on reactivity of credible abnormal and accident conditions are examined in this section. This section identifies which of the credible abnormal or accident conditions will result in exceeding the limiting reactivity ($k_{eff} \leq 0.95$). For those accidents or abnormal conditions that result in exceeding the limiting reactivity, a minimum soluble boron concentration is determined to ensure that $k_{eff} \leq 0.95$. The double contingency principal of ANS-8.1/N16.1-1975 [4.2] (and the USNRC letter of April 1978) specifies that it shall require at least two unlikely independent and concurrent events to produce a criticality accident. This principle precludes the necessity of considering the simultaneous occurrence of multiple accident conditions.

4.7.5.1 Abnormal Temperature

All calculations for Region 1 & 2 are performed at the maximum temperature of 150°F. As shown in Section 4.7.2.4 and 4.7.3.4 above, the temperature coefficient of reactivity is positive, and temperatures above the maximum would cause an increase in the reactivity, and therefore are treated as accidents. Additional calculations for both spent fuel loading and checkerboard loading of fresh fuel at higher temperatures and with a soluble boron content of 400 ppm were performed to determine the minimum soluble boron concentration necessary to ensure that the maximum k_{eff} is below 0.95. The soluble boron content necessary to offset the reactivity effect due to an increase in temperature is shown on Table 4.7.23 and Table 4.7.24 for Region 1 and Region 2, respectively.

All calculations for Region 3 are performed at a pool temperature of 4°C. As shown in Section 4.7.4.4 above, the temperature coefficient of reactivity is negative, therefore any increase in temperature above the minimum would cause a reduction in the reactivity. Table 4.7.22 shows the reactivity effects of increasing the temperature and boiling in the spent fuel pool.

4.7.5.2 Dropped Assembly - Horizontal

For the case in which a fuel assembly is assumed to be dropped on top of a rack, the fuel assembly will come to rest horizontally on top of the rack with a minimum separation distance from the active fuel region of more than 12 inches, which is sufficient to preclude neutron coupling (i.e., an effectively infinite separation). Consequently, the horizontal fuel assembly drop accident will not result in a significant increase in reactivity. Furthermore, the soluble boron in the spent fuel pool water assures that the true reactivity is always less than the limiting value for this dropped fuel accident.

4.7.5.3 Dropped Assembly - Vertical

It is also possible to vertically drop an assembly into a location that might be occupied by another assembly or that might be empty. Such a vertical impact would at most cause a small compression of the stored assembly, if present, or result in a small deformation of the baseplate for an empty cell. These deformations could potentially increase reactivity. However, the reactivity increase would be small compared to the reactivity increase created by the abnormal location of a fresh assembly discussed in the following section. The vertical drop is therefore bounded by this abnormal location accident and no separate calculation is performed for the drop accident.

4.7.5.4 Abnormal Location of a Fuel Assembly

4.7.5.4.1 Misloaded Fresh Fuel Assembly

The misloading of a fresh unburned fuel assembly could, in the absence of soluble poison, result in exceeding the regulatory limit (k_{eff} of 0.95). This could possibly occur if a fresh fuel assembly of the highest permissible enrichment (5.0 wt%) were to be inadvertently misloaded into a storage cell intended to be used for spent fuel or misloaded into a storage cell intended to be empty in the checkerboard patterns in Region 1 or Region 2. For the misloading accident in the Region 1 or Region 2 racks filled with spent fuel, enrichment and burnup combinations of 2.0 wt% ^{235}U at 0 years cooling time, 5.0 wt% ^{235}U at 0 years cooling time and 5.0 wt% ^{235}U at 20 years cooling time were analyzed at the appropriate burnup. The calculations for the misloading accident in the Region 3 racks conservatively assume that all spent fuel assemblies are replaced with fresh fuel assemblies. This configuration will also conservatively bound the misloading accident in the Region 3 rack filled with fresh fuel at 4.35 wt% ^{235}U.

The corresponding calculational model for the Region 1 and Region 2 style storage racks consists of a 5x5 array storage cells with a single, fresh unburned assembly in the center cell. The model is surrounded by periodic boundary conditions, which generates an infinite arrangement of 5x5 arrays with a misloaded assembly. Calculations are performed with 400 ppm, 800 ppm and 1200 ppm (if necessary) soluble boron, and the final soluble boron concentration is determined by linear interpolation.

The corresponding calculational model for the Region 3 style storage racks consists of a 2x2 array of storage cells with a fresh assembly of 5.0 wt% ^{235}U in all cells. The model is surrounded by reflecting boundary conditions, which generates an infinite arrangement of Region 3 cells, all filled with the maximum reactivity assembly. Calculations are performed with 400 ppm and 800 ppm soluble boron, and the final soluble boron concentration is determined by linear interpolation.

4.7.5.4.2 Mislocated Fresh Fuel Assembly

The mislocation of a fresh unburned fuel assembly could, in the absence of soluble poison, result in exceeding the regulatory limit (k_{eff} of 0.95). This could possibly occur if a fresh fuel assembly of the highest permissible enrichment (5.0 wt%) were to be accidentally mislocated outside of a storage rack adjacent to other fuel assemblies.

For the checkerboard pattern in the Region 1 and Region 2 style storage racks it is assumed that the mislocated assembly is placed adjacent to a storage cell containing another fresh fuel assembly. For the mislocated assembly accident outside the Region 1 and Region 2 racks filled with spent fuel, enrichment and burnup combinations of 5.0 wt% ^{235}U at 0 years cooling time and 5.0 wt% ^{235}U at 20 years cooling time were analyzed at the appropriate burnups.

For the Region 3 racks it is assumed that no metamic panel is located between the mislocated assembly and the assemblies in the rack. For the loading pattern with 3 fresh fuel assemblies and 1 spent fuel assembly, it was assumed that all fresh fuel assemblies are facing the mislocated assembly. This configuration would bound the case of a misplaced assembly with the Region 3 rack filled with fresh fuel of maximum nominal enrichment of 4.35 wt% ^{235}U.

The MCNP4a model consists of a 5x5 array of fuel storage cells with a single fresh, unburned assembly placed adjacent to the rack and a 30cm water reflector. The other three sides of the model consist of reflecting boundary conditions. The mislocated assembly is placed as close to the rack face as possible to maximize the possible reactivity effect. Calculations are performed with 400pm, 800 ppm and 1200 ppm (if necessary) soluble boron, and the final soluble boron concentration is determined by linear interpolation.

4.7.5.5 Loss of All Metamic

An additional calculation was performed to determine the reactivity of the Region 3 rack in the unlikely event that the neutron absorber was to be completely absent. Credit was taken for 1600 ppm soluble boron (actual pool soluble boron concentration is higher) and the metamic material was replaced with water. The Region 3 racks without any neutron absorber are analyzed for both the 3 of 4 loading pattern and uniform loading of fresh fuel assemblies having a maximum enrichment of 4.35wt% ^{235}U (identified in Section 4.7.4). The results of this postulated accident condition show that the maximum k_{eff} is 0.9388 including bias and uncertainties.

4.7.6 Interfaces Within and Between Racks

4.7.6.1 Normal Conditions

In addition to the calculations performed for each individual rack detailed in the preceding sections, the possibility of an increased reactivity effect due to the rack interfaces within and between the racks was determined. Figure 4.5.7 is a layout of the entire ANO Unit 1 spent fuel pool, with the gaps between racks detailed for each interface. The gaps provided in Figure 4.5.7, denoted by a "C" at the rack corners, are measured from the centerline of the adjacent storage cells. Table 4.5.10 summarizes the potential rack interfaces and the gaps between these racks. The gap distances provided in the last column of Table 4.5.10 are determined from the centerline distances between racks from Figure 4.5.7 and the geometric characteristics of each type of rack. Figure 4.5.8 illustrates the measurement of the distances between the outside surfaces of the racks.

Table 4.7.26 provides a summary of the various interface calculations performed for the ANO Unit 1 spent fuel pool. Interfaces within the rack include spent and fresh fuel loading patterns within the same rack to determine acceptability. Interface calculations between racks include

Region 1-Region 1, Region 2-Region 2, Region 3-Region 3, Region 1-Region 3 and Region 2-Region 3. Figures 4.7.1 through 4.7.14 are referenced in Table 4.7.26 and provide a visual representation of the interface calculation performed. The figures show the loading pattern assumed in each rack and the value for the water gap between the racks. The calculated reactivity from the interface calculation is then compared to the calculated reactivity from the reference infinite array calculations.

4.7.6.2 Rack Lateral Motion – Seismic Event

A seismic event, could, in the absence of soluble boron, result in exceeding the regulatory limit (maximum k_{eff} of 0.95). This could possibly occur if the seismic event caused sufficient movement of the rack to a closer proximity. The seismic analysis identifies a maximum differential displacement between racks during a seismic event of 0.635 inches. Selected cases from the interface calculations described in the previous section were chosen to address this potential accident condition. The MCNP4a models described above were modified to reduce the gap between racks by an additional 0.635 inches. Calculations were performed with 800 ppm of soluble boron. The calculated reactivities from MCNP4a show that all calculated reactivities for this accident condition are below 0.90. Even with the addition of the applicable biases and uncertainties, the maximum k_{eff} would be below 0.95.

4.7.7 Boron Dilution Evaluation

The soluble boron in the spent fuel pool water is conservatively analyzed to contain a minimum of 1600 ppm under operating conditions. Significant loss or dilution of the soluble boron concentration is extremely unlikely, if not incredible. Nonetheless, an evaluation was performed based on the ANO spent fuel pool data.

The required minimum soluble boron concentration is 457 ppm under normal conditions. The volume of water in the pool is approximately 268,000 gallons. Large amounts of unborated water would be necessary to reduce the boron concentration from 1600 ppm to 457 ppm. Abnormal or accident conditions are discussed below for either low dilution rates (abnormal conditions) or high dilution rates (accident conditions). The general equation for boron dilution is,

$$C_t = C_o e^{-\frac{F}{V}t},$$

where

C_t the boron concentration at time t,
C_o the initial boron concentration,
V is the volume of water in the pool, and
F is the flow rate of unborated water into the pool

This equation conservatively assumes the unborated water flowing into the pool mixes instantaneously with the water in the pool.

For convenience, the above equation may be re-arranged to permit calculating the time required to dilute the soluble boron from its initial concentration to a specified minimum concentration, which is given below.

$$t = \frac{V}{F}\ln(C_o / C_t)$$

If V is expressed in gallons and F in gallons per minute (gpm), the time, t, will be in minutes.

4.7.7.1 Low Flow Rate Dilution

Small dilution flow around pump seals and valve stems or mis-aligned valves could possibly occur in the normal soluble boron control system or related systems. Such failures might not be immediately detected. These flow rates would be of the order of 2 gpm maximum and the increased frequency of makeup flow might not be observed. However, an assumed loss flow-rate of 2 gpm dilution flow rate would require some 118 days to reduce the boron concentration to the minimum required 457 ppm under normal conditions. Routine surveillance measurements of the soluble boron concentration would readily detect the reduction in soluble boron concentration with ample time for corrective action.

Administrative controls require a measurement of the soluble boron concentration in the pool water at least weekly. Thus, the longest time period that a potential boron dilution might exist without a direct measurement of the boron concentration is 7 days. In this time period, an undetected dilution flow rate of 33.7 gpm would be required to reduce the boron concentration to 457 ppm. No known dilution flow rate of this magnitude has been identified. Further, a total of more than 300,000 gallons of unborated water would be associated with the dilution event and such a large flow of unborated water would be readily evident by high-level alarms and by visual inspection on daily walk-downs of the storage pool area.

4.7.7.2 High Flow Rate Dilution

Under certain accident conditions, it is conceivable that a high flow rate of unborated water could flow onto the top of the pool. Such an accident scenario could result from rupture of a unborated water supply line or possibly the rupture of a fire protection system header, both events potentially allowing unborated water to spray onto the pool. A flow rate of up to 2500 gpm could possibly spray onto the spent fuel pool as a result of a rupture of the fire protection line. This would be the most serious condition and bounds all other accident scenarios.

Conservatively assuming that all the unborated water from the break poured onto the top of the pool and further assuming instantaneous mixing of the unborated water with the pool water, it would take approximately 136 minutes to dilute the soluble boron concentration to 457 ppm, which is the minimum required concentration to maintain k_{eff} below 0.95 under normally operating conditions. In this dilution accident, some 340,000 gallons of water would spill on the auxiliary building floor and into the air-conditioning duct system. Well before the spilling of such a large volume of water, multiple alarms would have alerted the control room of the accident consequences (including the fuel pool high-level alarm, the fire protection system pump operation alarm, and the floor drain receiving tank high level alarm).

Instantaneous mixing of pool water with the water from the rupture of the unborated water supply line is an extremely conservative assumption. Water falling on to the pool surface would mix with the top layer of pool water and the portions of the mixed volumes would continuously spill out of the pool. The density difference between water at 150 °F (maximum permissible pool bulk water temperature) and at the temperature of the unborated water supply is small. This density difference will not cause the water falling on to the pool surface to instantaneously sink down into the racks overcoming the principal driving force for the flow in the pool, which is the buoyancy force generated in the spent fuel pool racks region due to the heat generation from the spent fuel in the racks. This would further enhance the mixing process between the pool water and spilled water above the racks.

For the fire protection system line break, upon the initial break, the fire protection system header pressure would drop to the auto start set point of the fire protection pumps. The start is accompanied with an alarm in the main control room. The annunciator response is to dispatch an operator to find the source of the pump start. Approximately 3 minutes into the event, a spent fuel pool high level alarm would be received in the main control room, assuming that the spent fuel pool level started at the low alarm. The annunciator response for high spent fuel pool level is to investigate the cause. The coincidence of the 2 alarms would quickly lead to the discovery of the failure of the fire protection system and sufficient time to isolate the failure.

The maximum flow rate from demineralized water supply would provide approximately 900 gpm into the spent fuel pool. Failure of the demineralized water header is not accompanied with an alarm; however, the time to dilute the spent fuel pool from 1600 to 457 ppm is greater than the bounding case described above. An alarm on high spent fuel pool level would be received approximately 9 minutes into the event in the main control room, assuming that the spent fuel pool level started at the low alarm. In this scenario, there is sufficient time to isolate the failure and to prevent the spilling of some 340,000 gallons of water.
The analysis assumes that for a double-ended break in the a fire protection system piping, the stream of water will arch through the air some 40 feet falling on top of the pool. This is virtually an incredible event. Should the stream of water fall upon the pool deck, a 3 inch high curb would channel some of the water to the pool drain and prevent all of the water from reaching the pool. Furthermore, the evaluation also assumes at least 3 independent and concurrent accidents occur simultaneously:

- Large amount of water flowing from the double-ended pipe break would remain undetected and is ignored.

- Pool water high level alarms either fail or are ignored.
- Alarms indicating large amounts of water flowing into the floor drain have failed or are ignored.

Considering all related facts, a significant dilution of the pool soluble boron concentration in a short period of time without corrective action is not considered a credible event.

It is not considered credible that multiple alarms would fail or be ignored or that the spilling of large volumes of water would not be observed. Therefore, such a major failure would be detected in sufficient time for corrective action to avoid violation of an administrative guideline and to assure that the health and safety of the public is protected.

4.8 New Fuel Storage Racks Criticality Analysis

The New Fuel Storage Vault is intended for the receipt and storage of fresh fuel under normally dry conditions where the reactivity is very low. To assure the criticality safety under accident conditions and to conform to the requirements of General Design Criterion 62, "Prevention of Criticality in Fuel Storage and Handling," two separate criteria must be satisfied as defined in NUREG-0800, Standard Review Plan 9.1.1, "New Fuel Storage." These criteria are as follows:

- When fully loaded with fuel of the highest anticipated reactivity and flooded with clean, unborated water, the maximum reactivity, including uncertainties, shall not exceed a k_{eff} of 0.95.
- With fuel of the highest anticipated reactivity in place and assuming optimum hypothetical low density moderation (i.e., fog or foam), the maximum reactivity shall not exceed a k_{eff} of 0.98.

The New Fuel Storage Vault provides two 4 x 9 storage rack modules with cell array storage location arranged on a 21 inch lattice spacing. Calculations were made with 238-group NITAWL/KENO5a code package (SCALE 4.3), a three-dimensional Monte Carlo analytical technique, with fresh fuel assemblies with 4.95 wt% nominal intitial enrichment. These calculations were made for various moderator densities and the results are shown in Figure 4.8.1; the peak reactivity (optimum moderation) occurs at 9% moderator density. The calculations for the configuration illustrated in Figure 4.8.2 confirms that five locations in each of the storage racks are required to remain empty in order to meet the regulatory limits. Results of the criticality safety analysis are summarized in Table 4.8.1 for the two accident conditions for fuel assemblies of 4.95 ± 0.05 wt% initial enrichment. The maximum reactivity at 9% moderator density is 0.9726, including uncertainties, which is within the regulatory limit of 0.98, thus confirming the acceptability of the New Fuel Vault for 4.95 ± 0.05 wt% fuel.

Additional calculations at 9% moderator density, performed for the storage pattern depicted in Figure 4.8.3, show that this storage configuration is acceptable for storage of fresh fuel assemblies of up to 4.20 wt% enrichment with four locations in each rack array required to remain empty.

For the fully flooded accident condition, calculations are performed as infinite array calculations (i.e., no blocked cells). Under these conditions and with fuel of 4.95 ± 0.05 wt% enrichment, the maximum reactivity, including all uncertainties is less than the regulatory limit of 0.95 for k_{eff}, thus confirming the acceptability of the NFV for 4.95 wt% fuel in the fully flooded accident condition. At 4.2 wt% enrichment in the flooded condition, the reactivity will be substantially lower than that for 4.95 ± 0.05 wt% enrichment and would therefore be acceptable for storage.

4.9 Fuel Handling Equipment

Criticality safety evaluations were also performed for handling of fresh fuel assemblies during transfer from the new fuel vault to the reactor core, including the new-fuel elevator, the upender and fuel carriage, and the temporary storage rack within the transfer canal. The new fuel elevator is located on the south wall of the pool facing the Region 1 spent fuel storage racks. This device can position a fresh fuel assembly 16 inches (assembly center line) from the wall. The distance from the wall to the edge of the rack is 24.5 inches. A distance of 7.845 inches exists between the centerline of the assembly in the elevator and the edge of the closest fuel storage cell in the rack. The maximum reactivity with fuel in the new fuel elevator (with Region 1 containing a checkerboard of fresh fuel) is 0.9359 with credit for 100 ppm soluble boron. Additional calculations were performed to evaluate the effect of accidentally dropping or misplacing an assembly adjacent to the new fuel elevator while it is loaded. A most reactive location for the dropped assembly was determined. A credit of 700 ppm boron will ensure k-effective remains below 0.95 should such an event occur. The new fuel elevator therefore meets the criticality acceptance criteria defined in 10 CFR 50.68. The upender/fuel carriage device handles a single assembly. The maximum reactivity of a single fresh assembly containing 4.95 w/o ± 0.05 enriched fuel in water is bounded by the fresh fuel, fully moderated case in Table 4.8.1, which has a maximum k_{eff} of 0.9431. Furthermore for a postulated accident in which a second fresh assembly was positioned near the upender/fuel carriage, the presence of soluble boron (1600 ppm minimum) excludes the possibility of any criticality concern.

The transfer canal incorporates a 7-cell temporary storage rack on a linear array at a 21-1/8 inch spacing (6 locations for fuel assemblies and 1 location for damaged fuel). The maximum k-effective for normal operation of this rack was determined to be 0.9412. Evaluations of a potential mis-placement of a fresh fuel assembly at a position of closest approach to another assembly in the spent fuel rack, separated only by the structure of the temporary rack, shows that the maximum k_{eff} (in the absence of any soluble boron) would be 0.9702. The presence of 200 ppm soluble boron would be sufficient to maintain the maximum k-effective below 0.95. However, the transfer canal, during refueling operations, would always contain the minimum Technical Specification boron concentration (> 2000 ppm), significantly reducing reactivity and further eliminating any criticality concern.

4.10 REFERENCES

[4.1] M.G. Natrella, Experimental Statistics, National Bureau of Standards, Handbook 91, August 1963.

[4.2] ANS-8.1/N16.1-1975, "American National Standard for Nuclear Criticality Safety in Operations with Fissionable Materials Outside Reactors," April 14, 1975.

[4.3] J.F. Briesmeister, Editor, "MCNP - A General Monte Carlo N-Particle Transport Code, Version 4A," LA-12625, Los Alamos National Laboratory (1993).

[4.4] "Lumped Fission Product and Pm148m Cross Sections for MCNP," Holtec Report HI-2033031, Rev 0, September 2003.

[4.5] Deleted

[4.6] Deleted

[4.7] M. Edenius, K. Ekberg, B.H. Forssén, and D. Knott, "CASMO-4 A Fuel Assembly Burnup Program User's Manual," Studsvik/SOA-95/1, Studsvik of America, Inc. and Studsvik Core Analysis AB (proprietary).

[4.8] D. Knott, "CASMO-4 Benchmark Against Critical Experiments," SOA-94/13, Studsvik of America, Inc., (proprietary).

[4.9] D. Knott, "CASMO-4 Benchmark Against MCNP," SOA-94/12, Studsvik of America, Inc., (proprietary).

[4.10] L.I. Kopp, "Guidance on the Regulatory Requirements for Criticality Analysis of Fuel Storage at Light-Water Reactor Power Plants," NRC Memorandum from L. Kopp to T. Collins, August 19, 1998.

[4.11] Deleted

[4.12] S.E. Turner, "Uncertainty Analysis - Burnup Distributions," presented at the DOE/SANDIA Technical Meeting on Fuel Burnup Credit, Special Session, ANS/ENS Conference, Washington, D.C., November 2, 1988.

Table 4.5.1
PWR Fuel Assembly Specifications[5]

Fuel Rod Data		
Assembly type	**15x15 Non-HTP**	**15x15 HTP**
Fuel pellet outside diameter, in.	0.370 ± 0.0005	0.3735 ± 0.0005
Cladding inside diameter, in.	0.377 ± 0.002	0.380 ± 0.002
Cladding outside diameter, in.	0.430 ± 0.002	0.430 ± 0.002
Cladding material	Zr-4	M5
Stack density, g/cc	10.412 ± 0.2	10.522 ± 0.2
Maximum enrichment, wt% ^{235}U	5.0 ± 0.05	5.0 ± 0.05
Fuel Assembly Data		
Fuel rod array	15x15	15x15
Number of fuel rods	208	208
Fuel rod pitch, in.	0.568 ± 0.0058	0.568 +0.010/-0.015[6]
Number of guide tubes	16	16
Guide Tube outside diameter, in.	0.530 ± 0.002	0.530 ± 0.002
Guide Tube inside diameter, in.	0.498 ± 0.0026	0.498 ± 0.0052
Number of instrument tubes	1	1
Instrument Tube outside diameter, in.	0.493 ± 0.002	0.493 ± 0.002[7]
Instrument Tube inside diameter, in.	0.441 ± 0.002	0.400 ± 0.002[7]
Active fuel Length, in.[8]	140.6-144	142.75 ± 0.290

[5] Tolerances for fuel enrichment and fuel density are assumed values based on industry standards.
[6] Tolerance stated is the tolerance of the total assembly width. The tolerance for each individual fuel rod is determined by dividing this value by the square root of the number of rods of one side of the assembly.
[7] This is the stated value and tolerance for the bottom of the instrument tube. The different instrument tube ID and tolerance for the top half of the assembly has a negligible effect on reactivity.
[8] The active fuel length is conservatively modeled as 144 inches.

Table 4.5.2
Core Operating Parameters for Depletion Analyses

Parameter	Non-HTP	HTP
Soluble Boron Concentration (cycle average), ppm	1000	1000
Reactor Specific Power, MW/MTU	31.4	31.4
Core Average Fuel Temperature, °F	1010	970
Core Average Moderator Temperature at the Top of the Active Region, °F	603	603
In-Core Assembly Pitch, Inches	8.587	8.587

Table 4.5.3
Axial Burnup Profile

Axial Segment (cm)	Relative Burnup		
	Non-HTP	HTP	Holtec [4.12]
0 to 15.24	0.5000	0.500	0.5485
15.24 to 30.48	0.8477	0.848	0.8477
30.48 to 60.96	1.0500	1.070	1.077
60.96 to 121.92	1.1161	1.130	1.105
121.92 to 182.88	1.1090	1.109	1.098
182.88 to 243.84	1.0909	1.100	1.079
243.84 to 304.80	1.0583	1.080	1.050
304.80 to 335.28	0.9606	0.883	0.9604
335.28 to 350.52	0.7338	0.670	0.7338
350.52 to 365.76	0.4000	0.400	0.467

Table 4.5.4
BPRA Data

Parameter	Value
Number of BPRs per assembly	0 or 16
Outer Radius of BPRA Clad (cm)	0.54610
Inner Radius of BPRA Clad (cm)	0.45720
Cladding Material	Zr-4
Poison Material	B_4C in Al_2O_3 (3.5 wt%)
Pellet Density (g/cm^3)	3.38420 (3.5 wt% B_4C)
Pellet Radius (cm)	0.45720

Table 4.5.5
Weight Percents of BPRA Material (3.5 wt% B_4C)

Material	Wt %
Boron-10	0.50063
Boron-11	2.23809
Carbon	0.76128
Aluminum	51.07266
Oxygen	45.42734

Table 4.5.6
APSR Data

Parameter	Value
Number of APSR rodlets per assembly	16
Clad Outer Radius (cm)	0.55880
Clad Inner Radius (cm)	0.49022
Poison Radius (cm)	0.49022
Poison Density (g/cm^3)	7.9564
Cladding Material	SS-304
Poison Material	Inconel-600 (76% nickel, 8% iron, 16% chromium)

Table 4.5.7

Fuel Rack Specifications – Region 1 Racks

Parameter	Value
Cell ID, Inches	8.970 +0.025/-0.05
Box Wall Thickness, Inches	0.075 ± 0.004
Sheathing Thickness, Inches	0.020 ± 0.004
Poison Pocket Thickness, Inches	0.090 ± 0.010
Sheathing Width, Inches	7.25
Cell Pitch, Inches	10.650
Water Gap, Inches	1.31

Table 4.5.8

Fuel Rack Specifications – Region 2 Racks

Parameter	Value
Cell ID, Inches	9.116 +0.05/-0.025
Box Wall Thickness, Inches	0.062 ± 0.004
Cell Pitch, Inches	10.650
Water Gap	1.41 +0.166/-0.221

Table 4.5.9

Fuel Rack Specifications – Region 3 Racks

Parameter	Value
Cell ID, Inches	9.116 +0.05/-0.025
Box Wall Thickness, Inches	0.062 ± 0.004
Cell Pitch, Inches	10.650
Water Gap	1.41 +0.166/-0.221
Metamic Insert Width	1.20 ± 0.05
Metamic Insert Sheathing Thickness	0.02 ± 0.003
Metamic Poison Thickness	0.100 ± 0.003
Metamic Poison Width	7.00 ± 0.062
Metamic Poison B_4C Weight Percent	25 ± 0.5

Table 4.5.10
Identification of Possible Rack Interaction and Minimum Distances between Racks

Rack-to-Rack Interaction	Center to Center Cell Spacing from Figure 4.5.7 [inches]	Minimum Distance Between Racks [inches]
Region 1 to Region 1	13	3.66
Region 1 to Region 3	15.75	5.755
Region 2 to Region 3	12.875	2.225
Region 2 to Region 2	13	2.35
Region 3 to Region 3	13.1875	2.5375

Table 4.7.1
Summary of the Criticality Safety Analyses for Region 1 without Soluble Boron at 0 Years Cooling Time

Design Basis Burnup at 5.0 wt% ^{235}U		38.4 GWD/MTU
Soluble Boron		0 ppm
Uncertainties		
Bias Uncertainty (95%/95%)	± 0.0011	
Calculational Statistics (95%/95%, 2.0×σ)	± 0.0010	
Fuel Eccentricity	+ 0.0132	
Rack Tolerances	± 0.0066	
Fuel Tolerances	± 0.0074	
Depletion Uncertainty	± 0.0125	
Statistical Combination of Uncertainties[9]	± 0.0208	
Reference k_{eff} (MCNP4a)		0.9648
Total Uncertainty (above)		0.0208
Temperature Bias		0.0085
Calculational Bias (see Appendix 4A)		0.0009
Maximum k_{eff}		**0.9950**
Regulatory Limiting k_{eff}		**1.0000**

[9] Square root of the sum of the squares.

Table 4.7.2
Summary of the Criticality Safety Analyses for Region 1 with Soluble Boron at 0 Years Cooling Time

Design Basis Burnup at 5.0 wt% ^{235}U		38.4 GWD/MTU
Soluble Boron		242 ppm
Uncertainties		
Bias Uncertainty (95%/95%)	± 0.0011	
Calculational Statistics (95%/95%, 2.0×σ)	± 0.0011	
Fuel Eccentricity	+ 0.0132	
Rack Tolerances	± 0.0066	
Fuel Tolerances	± 0.0074	
Depletion Uncertainty	± 0.0125	
Statistical Combination of Uncertainties[10]	± 0.0208	
Reference k_{eff} (MCNP4a)		0.9148
Total Uncertainty (above)		0.0208
Temperature Bias		0.0085
Calculational Bias (see Appendix 4A)		0.0009
Maximum k_{eff}		**0.9450**
Regulatory Limiting k_{eff}		**0.9500**

[10] Square root of the sum of the squares.

Table 4.7.3
Summary of the Criticality Safety Analyses for Region 1 without Soluble Boron for a 2x2 Checkerboard of Fresh Fuel and Empty Cells

Design Basis Burnup at 5.0 wt% ^{235}U		0 GWD/MTU
Soluble Boron		0 ppm
Uncertainties		
Bias Uncertainty (95%/95%)	± 0.0011	
Calculational Statistics (95%/95%, 2.0×σ)	± 0.0012	
Fuel Eccentricity	+ 0.0046	
Rack Tolerances	± 0.0081	
Fuel Tolerances	± 0.0074	
Depletion Uncertainty	N/A	
Statistical Combination of Uncertainties[11]	± 0.0120	
Reference k_{eff} (MCNP4a)		0.9329
Total Uncertainty (above)		0.0120
Temperature Bias		0.0101
Calculational Bias (see Appendix 4A)		0.0009
Maximum k_{eff}		**0.9559**
Regulatory Limiting k_{eff}		**1.0000**

[11] Square root of the sum of the squares.

Table 4.7.4
Summary of the Criticality Safety Analyses for Region 1 with Soluble Boron for a 2x2 Checkerboard of Fresh Fuel and Empty Cells

Design Basis Burnup at 5.0 wt% ^{235}U		0 GWD/MTU
Soluble Boron		70 ppm
Uncertainties		
Bias Uncertainty (95%/95%)	± 0.0011	
Calculational Statistics (95%/95%, 2.0×σ)	± 0.0012	
Fuel Eccentricity	+ 0.0046	
Rack Tolerances	± 0.0081	
Fuel Tolerances	± 0.0074	
Depletion Uncertainty	N/A	
Statistical Combination of Uncertainties[12]	± 0.0120	
Reference k_{eff} (MCNP4a)		0.9220
Total Uncertainty (above)		0.0120
Temperature Bias		0.0101
Calculational Bias (see Appendix 4A)		0.0009
Maximum k_{eff}		**0.9450**
Regulatory Limiting k_{eff}		**0.9500**

[12] Square root of the sum of the squares.

Table 4.7.5
Summary of the Criticality Safety Analyses for Region 2 without Soluble Boron at 0 Years Cooling Time

Design Basis Burnup at 5.0 wt% ^{235}U	42.7 GWD/MTU
Soluble Boron	0 ppm
Uncertainties	
Bias Uncertainty (95%/95%)	± 0.0011
Calculational Statistics (95%/95%, 2.0×σ)	± 0.0011
Fuel Eccentricity	+ 0.0165
Rack Tolerances	± 0.0039
Fuel Tolerances	± 0.0073
Depletion Uncertainty	± 0.0139
Statistical Combination of Uncertainties[13]	± 0.0232
Reference k_{eff} (MCNP4a)	0.9614
Total Uncertainty (above)	0.0232
Temperature Bias	0.0093
Calculational Bias (see Appendix 4A)	0.0009
Maximum k_{eff}	**0.9948**
Regulatory Limiting k_{eff}	**1.0000**

[13] Square root of the sum of the squares.

Table 4.7.6
Summary of the Criticality Safety Analyses for Region 2 with Soluble Boron at 0 Years Cooling Time

Design Basis Burnup at 5.0 wt% ^{235}U		42.7 GWD/MTU
Soluble Boron		232 ppm[14]
Uncertainties		
Bias Uncertainty (95%/95%)	± 0.0011	
Calculational Statistics (95%/95%, 2.0×σ)	± 0.0012	
Fuel Eccentricity	+ 0.0165	
Rack Tolerances	± 0.0039	
Fuel Tolerances	± 0.0073	
Depletion Uncertainty	± 0.0139	
Statistical Combination of Uncertainties[15]	± 0.0232	
Reference k_{eff} (MCNP4a)		0.9116
Total Uncertainty (above)		0.0232
Temperature Bias		0.0093
Calculational Bias (see Appendix 4A)		0.0009
Maximum k_{eff}		**0.9450**
Regulatory Limiting k_{eff}		**0.9500**

[14] Calculations performed for 5.0 wt% fuel with a burnup of 36.2 GWD/MTU at 20 years cooling time, resulted in a slightly higher soluble boron requirement of 233ppm
[15] Square root of the sum of the squares.

Table 4.7.7
Summary of the Criticality Safety Analyses for Region 2 without Soluble Boron for a 2x2 Checkerboard of Fresh Fuel and Empty Cells

Design Basis Burnup at 5.0 wt% ^{235}U	0 GWD/MTU
Soluble Boron	0 ppm
Uncertainties	
Bias Uncertainty (95%/95%)	± 0.0011
Calculational Statistics (95%/95%, 2.0×σ)	± 0.0014
Fuel Eccentricity	+ 0.0053
Rack Tolerances	± 0.0049
Fuel Tolerances	± 0.0071
Depletion Uncertainty	N/A
Statistical Combination of Uncertainties[16]	± 0.0103
Reference k_{eff} (MCNP4a)	0.9431
Total Uncertainty (above)	0.0103
Temperature Bias	0.0110
Calculational Bias (see Appendix 4A)	0.0009
Maximum k_{eff}	**0.9653**
Regulatory Limiting k_{eff}	**1.0000**

[16] Square root of the sum of the squares.

Table 4.7.8
Summary of the Criticality Safety Analyses for Region 2 with Soluble Boron for a 2x2 Checkerboard of Fresh Fuel and Empty Cells

Design Basis Burnup at 5.0 wt% ^{235}U		0 GWD/MTU
Soluble Boron		117 ppm
Uncertainties		
Bias Uncertainty (95%/95%)	± 0.0011	
Calculational Statistics (95%/95%, 2.0×σ)	± 0.0014	
Fuel Eccentricity	+ 0.0053	
Rack Tolerances	± 0.0049	
Fuel Tolerances	± 0.0071	
Depletion Uncertainty	N/A	
Statistical Combination of Uncertainties[17]	± 0.0103	
Reference k_{eff} (MCNP4a)		0.9228
Total Uncertainty (above)		0.0103
Temperature Bias		0.0110
Calculational Bias (see Appendix 4A)		0.0009
Maximum k_{eff}		**0.9450**
Regulatory Limiting k_{eff}		**0.9500**

[17] Square root of the sum of the squares.

Table 4.7.9
Summary of the Criticality Safety Analyses for Region 3 without Soluble Boron for a 2x2 Checkerboard of 3 Fresh Fuel Assemblies and 1 Spent Fuel Assembly at 0 Years Cooling Time

Design Basis Burnup for Single (5.0 wt%) Spent Assembly	20.1 GWD/MTU
Soluble Boron	0 ppm
Uncertainties	
Bias Uncertainty (95%/95%)	± 0.0011
Calculational Statistics (95%/95%, 2.0×σ)	± 0.0014
Fuel Eccentricity	Negative
Rack Tolerances	± 0.0060
Fuel Tolerances	± 0.0053
Depletion Uncertainty	± 0.0012
Statistical Combination of Uncertainties[18]	± 0.0082
Reference k_{eff} (MCNP4a)	0.9850
Total Uncertainty (above)	0.0082
Temperature Bias	0.0017
Calculational Bias (see Appendix 4A)	0.0009
Maximum k_{eff}	**0.9958**
Regulatory Limiting k_{eff}	**1.0000**

[18] Square root of the sum of the squares.

Table 4.7.10
Summary of the Criticality Safety Analyses for Region 3 with Soluble Boron for a 2x2 Checkerboard of 3 Fresh Fuel Assemblies and 1 Spent Fuel Assembly at 0 Years Cooling Time

Design Basis Burnup for Single (5.0 wt%) Spent Assembly	20.1 GWD/MTU
Soluble Boron	457 ppm
Uncertainties	
Bias Uncertainty (95%/95%)	± 0.0011
Calculational Statistics (95%/95%, 2.0×σ)	± 0.0012
Fuel Eccentricity	Negative
Rack Tolerances	± 0.0060
Fuel Tolerances	± 0.0053
Depletion Uncertainty	± 0.0012
Statistical Combination of Uncertainties[19]	± 0.0082
Reference k_{eff} (MCNP4a)	0.9342
Total Uncertainty (above)	0.0082
Temperature Bias	0.0017
Calculational Bias (see Appendix 4A)	0.0009
Maximum k_{eff}	**0.9450**
Regulatory Limiting k_{eff}	**0.9500**

[19] Square root of the sum of the squares.

Table 4.7.11
Summary of the Criticality Safety Analyses for Region 3 without Soluble Boron

Design Basis Burnup at 4.35 wt% ^{235}U	0 GWD/MTU
Soluble Boron	0 ppm
Uncertainties	
Bias Uncertainty (95%/95%)	± 0.0011
Calculational Statistics (95%/95%, 2.0×σ)	± 0.0014
Fuel Eccentricity	Negative
Rack Tolerances	± 0.0059
Fuel Tolerances	± 0.0052
Depletion Uncertainty	N/A
Statistical Combination of Uncertainties[20]	± 0.0081
Reference k_{eff} (MCNP4a)	0.9860
Total Uncertainty (above)	0.0081
Temperature Bias	0.0019
Calculational Bias (see Appendix 4A)	0.0009
Maximum k_{eff}	**0.9969**
Regulatory Limiting k_{eff}	**1.0000**

[20] Square root of the sum of the squares.

Table 4.7.12
Summary of the Criticality Safety Analyses for Region 3 with Soluble Boron

Design Basis Burnup at 4.35 wt% ^{235}U	0 GWD/MTU
Soluble Boron	409 ppm
Uncertainties	
Bias Uncertainty (95%/95%)	± 0.0011
Calculational Statistics (95%/95%, 2.0×σ)	± 0.0012
Fuel Eccentricity	Negative
Rack Tolerances	± 0.0059
Fuel Tolerances	± 0.0052
Depletion Uncertainty	N/A
Statistical Combination of Uncertainties[21]	± 0.0081
Reference k_{eff} (MCNP4a)	0.9342
Total Uncertainty (above)	0.0081
Temperature Bias	0.0019
Calculational Bias (see Appendix 4A)	0.0009
Maximum k_{eff}	**0.9450**
Regulatory Limiting k_{eff}	**0.9500**

[21] Square root of the sum of the squares.

Table 4.7.13
Burnup Value at which APSRs and BPRAs have Equivalent Reactivity Effect

Enrichment	Burnup
2.0	9.68
2.5	11.38
3.0	13.06
3.5	14.64
4.0	16.17
4.5	17.58
5.0	19.01

Table 4.7.14[22]
Minimum Burnup versus Enrichment Values for Region 1 Racks with Spent Fuel

Enrichment	2.0	2.5	3.0	3.5	4.0	4.5	5.0
Cooling Time	Minimum Burnup (GWD/MTU)						
0	2.1	8.6	15.0	21.8	27.2	32.7	38.4
5	2.0	8.2	14.1	20.7	26.2	30.8	36.4
10	1.9	7.9	13.7	19.5	25.5	29.5	34.6
15	1.8	7.7	13.2	18.8	24.7	28.8	33.8
20	1.8	7.5	13.0	18.4	24.2	28.2	33.0

[22] Linear interpolation between burnups for a given cooling time is allowed. However, linear interpolation between cooling times is not allowed, therefore the cooling time of a given assembly must be rounded down to the nearest cooling time.

Table 4.7.15[23]
Minimum Burnup versus Enrichment Values for Region 2 Racks with Spent Fuel

Enrichment	2.0	2.5	3.0	3.5	4.0	4.5	5.0
Cooling Time	Minimum Burnup (GWD/MTU)						
0	4.0	11.2	18.2	25.0	30.1	36.6	42.7
5	3.8	10.6	17.1	23.9	28.8	34.4	40.3
10	3.6	10.1	16.2	22.7	27.8	32.7	38.3
15	3.5	9.8	15.8	21.9	27.1	31.7	37.1
20	3.3	9.6	15.2	21.4	26.6	30.7	36.2

[23] Linear interpolation between burnups for a given cooling time is allowed. However, linear interpolation between cooling times is not allowed, therefore the cooling time of a given assembly must be rounded down to the nearest cooling time.

Table 4.7.16
Reactivity Effect of Insert Type
Enrichment 5.0 wt% ^{235}U, 0 Cooling Time

Burnup (GWD/MTU)	Insert Type		
	Empty	APSR	BPRA
0.0	1.20377	1.149	1.07214
1.0	1.18851	1.13469	1.06223
3.0	1.17333	1.12036	1.05558
5.0	1.15866	1.10645	1.04952
7.0	1.14412	1.09265	1.04376
9.0	1.12993	1.0792	1.03855
10.0	1.12298	1.07263	1.03616
12.5	1.10601	1.05661	1.03062
15.0	1.08962	1.04119	1.0255
17.5	1.07355	1.02611	1.02063
20.0	1.0578	1.01138	1.01532
22.5	1.04225	0.9969	1.00902
25.0	1.02684	0.98262	1.00133
27.5	1.01153	0.96848	0.99212
30.0	0.99628	0.95449	0.98152
32.5	0.9811	0.94062	0.96981
35.0	0.96599	0.92689	0.9573
37.5	0.95094	0.91331	0.94426
40.0	0.93597	0.89986	0.93092
42.5	0.92109	0.88659	0.91746
45.0	0.90633	0.8735	0.90398
47.5	0.89171	0.86061	0.89057
50.0	0.87729	0.84796	0.87731

Table 4.7.17
Reactivity Effect of Fuel and Rack Tolerances for Region 1 Racks

Tolerance	**5.0 wt%, 40 GWD/MTU 0 CT**	**5.0 wt%, 0 GWD/MTU 0 CT**
Fuel Tolerance	**Δk**	**Δk**
Fuel Density	0.0018	0.0011
Fuel Enrichment	0.0027	0.0019
Fuel Rod Pitch	0.0066	0.0069
Fuel Rod Clad OD	0.0003	0.0011
Fuel Rod Clad ID	0.0002	0.0003
Fuel Pellet OD	0.0003	0.0002
Guide Tube OD	0.0001	0.0002
Guide Tube ID	0.0002	0.0004
Statistical Combination	**0.0074**	**0.0074**
Rack Tolerance	**Δk**	**Δk**
Cell ID, Constant Water Gap	0.0057	0.0072
Water Gap, Constant Cell Pitch	0.0006	0.0006
Box Wall Thickness	0.0023	0.0028
Sheathing Thickness	0.0020	0.0023
Poison Gap Thickness	0.0001	0.0002
Statistical Combination	**0.0065**	**0.0081**

Table 4.7.18
Reactivity Effect of Temperature Variation in Region 1 Racks

Temperature (°F)	5.0 wt%, 40 GWD/MTU 0 CT	5.0 wt%, 0 GWD/MTU 0CT
	Δk	Δk
32 (0 °C)	-0.0150	-0.0178
68 (20 °C)	-0.0101	-0.0120
80.33 (300K)	-0.0085	-0.0101
150 (max normal temp)	Reference	Reference
254 (120 °C)	0.0127	0.0146
254 + 10% Void	0.0156	0.0216

Table 4.7.19
Reactivity Effect of Fuel and Rack Tolerances for Region 2 Racks

Tolerance	**5.0 wt%, 42.5 GWD/MTU 0 CT**	**5.0 wt%, 0 GWD/MTU 0CT**
Fuel Tolerance	**Δk**	**Δk**
Fuel Density	0.0019	0.0010
Fuel Enrichment	0.0027	0.0019
Fuel Rod Pitch	0.0065	0.0066
Fuel Rod Clad OD	0.0002	0.0011
Fuel Rod Clad ID	0.0002	0.0003
Fuel Pellet OD	0.0003	0.0001
Guide Tube OD	0.0001	0.0002
Guide Tube ID	0.0002	0.0004
Statistical Combination	**0.0073**	**0.0071**
Rack Tolerance	**Δk**	**Δk**
Cell ID, Constant Water Gap	0.0027	0.0035
Water Gap, Constant Cell Pitch	0.0005	0.0007
Box Wall Thickness	0.0028	0.0034
Statistical Combination	**0.0039**	**0.0049**

Table 4.7.20
Reactivity Effect of Temperature Variation in Region 2 Racks

Temperature (°F)	5.0 wt%, 42.5 GWD/MTU 0 CT	5.0 wt%, 0 GWD/MTU 0CT
	Δk	Δk
32 (0 °C)	-0.0162	-0.0192
68 (20 °C)	-0.0110	-0.0131
80.33 (300K)	-0.0093	-0.0110
150 (max normal temp)	Reference	Reference
254 (120 °C)	0.0141	0.0161
254 + 10% Void	0.0205	0.0277

Table 4.7.21
Reactivity Effect of Fuel and Rack Tolerances for Region 3 Racks

Tolerance	**4.35 wt%, 0 GWD/MTU 0 CT**	**5.0 wt%, 0 GWD/MTU 0CT**
Fuel Tolerance	**Δk**	**Δk**
Fuel Density	0.0017	0.0016
Fuel Enrichment	0.0020	0.0016
Fuel Rod Pitch	0.0040	0.0042
Fuel Rod Clad OD	0.0021.	0.0021
Fuel Rod Clad ID	0.0000	0.0000
Fuel Pellet OD	0.0002	0.0002
Guide Tube OD	0.0002	0.0002
Guide Tube ID	0.0006	0.0006
Statistical Combination	**0.0052**	**0.0053**
Rack Tolerance	**Δk**	**Δk**
Cell ID, Constant Water Gap	0.0001	0.0002
Water Gap, Constant Cell Pitch	0.0039	0.0039
Box Wall Thickness	0.0000	0.0000
Insert Sheathing Thickness	0.0015	0.0015
Insert Water Gap	0.0041	0.0041
Metamic Thickness	0.0003	0.0003
Metamic Width	0.0009	0.0010
Metamic B_4C wt%	0.0005	0.0005
Statistical Combination	**0.0059**	**0.0060**

Table 4.7.22
Reactivity Effect of Temperature Variation in Region 3 Racks

Temperature (°F)	4.35 wt%, 0 GWD/MTU 0 CT	5.0 wt%, 0 GWD/MTU 0 CT
	Δk	Δk
32 (0 °C)	0.0001	0.0001
39.2 (4 °C)	Reference	Reference
68 (20 °C)	-0.0011	-0.0010
80.33 (300K)	-0.0018	-0.0016
150 (max normal temp)	-0.0076	-0.0071
254 (120 °C)	-0.0202	-0.0194
254 + 10% Void	-0.0443	-0.0436

Table 4.7.23
Region 1 Accident Conditions

Abnormal/Accident Condition	Soluble Boron Requirement
Abnormal Temperature – Spent Fuel	317 ppm
Abnormal Temperature – Fresh Fuel	209 ppm
Dropped Assembly – Horizontal	Negligible
Dropped Assembly – Vertical	Negligible
Misloaded Assembly – Spent Fuel	514 ppm
Misloaded Assembly – Fresh Fuel	804 ppm
Mislocated Assembly – Spent Fuel	485 ppm
Mislocated Assembly – Fresh Fuel	889 ppm
Maximum	**889 ppm**

Table 4.7.24
Region 2 Accident Conditions

Abnormal/Accident Condition	Soluble Boron Requirement
Abnormal Temperature – Spent Fuel	327 ppm
Abnormal Temperature – Fresh Fuel	278 ppm
Dropped Assembly – Horizontal	Negligible
Dropped Assembly – Vertical	Negligible
Misloaded Assembly – Spent Fuel	544 ppm
Misloaded Assembly – Fresh Fuel	867 ppm
Mislocated Assembly – Spent Fuel	484 ppm
Mislocated Assembly – Fresh Fuel	875 ppm
Maximum	**875 ppm**

Table 4.7.25
Region 3 Accident Conditions

Abnormal/Accident Condition	Soluble Boron Requirement
Abnormal Temperature	Negative
Dropped Assembly – Horizontal	Negligible
Dropped Assembly – Vertical	Negligible
Misloaded Assembly – 3 of 4 Pattern	672 ppm
Mislocated Assembly – 3 of 4 Pattern	852 ppm
Maximum	**852 ppm**

Table 4.7.26 Interface Calculations

Interface Calculation	Figure #	Reactivity (k_{calc})	Reference Reactivity (k_{calc})	Delta k	Acceptable?
Region 1 to Region 1 with fresh fuel checkerboard in each rack. Fresh fuel assemblies facing in adjacent racks.	4.7.1	0.9352	0.9329	+0.0023	N
Region 1 – Checkerboard and Spent Fuel in same rack.	4.7.2	0.9605	0.9648	-0.0043	Y
Region 2 to Region 2 with fresh fuel checkerboard in each rack. Fresh fuel assemblies facing in adjacent racks.	4.7.3	0.9454	0.9431	+0.0023	N
Region 2 – Checkerboard and Spent Fuel in same rack.	4.7.4	0.9665	0.9670	-0.0005	Y
Region 3 to Region 3 with no Metamic Panel in the gap. 3 of 4 pattern with fresh fuel at 5.0 wt% ^{235}U facing each other in both racks.	4.7.5	0.9903	0.9850	+0.0053	N
Region 3 to Region 3 with no Metamic Panel in the gap. 3 of 4 pattern with fresh fuel at 5.0 wt% ^{235}U in one rack facing fresh and spent fuel in other rack across gap.	4.7.6	0.9867	0.9850	+0.0017	Y
Region 3 to Region 3 with no Metamic Panel in the gap. All fresh fuel at 4.35 wt% ^{235}U in one rack, 3 of 4 pattern with fresh fuel facing gap in other rack.	4.7.7	0.9881	0.9860	+0.0021	N
Region 3 to Region 3 with no Metamic Panel in the gap. All fresh fuel at 4.35 wt% ^{235}U in one rack, 3 of 4 pattern with fresh and spent fuel facing gap in other rack.	4.7.8	0.9832	0.9860	-0.0028	Y
Region 1 to Region 3, Fresh Fuel Checkerboard in Region 1 rack, 3 of 4 pattern in Region 3 rack.	4.7.9	0.9822	0.9850	-0.0028	Y
Region 1 to Region 3, Spent Fuel in Region 1 rack, 3 of 4 pattern in Region 3 rack.	4.7.10	0.9832	0.9850	-0.0018	Y
Region 2 to Region 3, Fresh Fuel Checkerboard in Region 2 rack, 3 of 4 pattern in Region 3 rack.	4.7.11	0.9837	0.9850	-0.0013	Y
Region 2 to Region 3, Spent Fuel in Region 2 rack, 3 of 4 pattern in Region 3 rack.	4.7.12	0.9831	0.9850	-0.0019	Y
Region 3 – 3 of 4 and Fresh Fuel 4.35 wt% ^{235}U in same rack. All fresh 5.0 wt% facing all fresh 4.35 wt%	4.7.13	0.9889	0.9860	+0.0029	N
Region 3 – 3 of 4 and Fresh Fuel 4.35 wt% ^{235}U in same rack. Fresh and spent 5.0 wt% facing all fresh 4.35 wt%	4.7.14	0.9826	0.9860	-0.0034	Y

Table 4.8.1
Summary of New Fuel Vault Criticality Safety Analysis

	OPTIMUM MODERATION	FLOODED MODERATION [24]	OPTIMUM MODERATION
Initial Enrichment, wt%	4.95 ± 0.05	4.95 ± 0.05	4.20 ± 0.05
Temperature for analysis	20°C (68°F)	20°C (68°F)	20°C (68°F)
Reference k_{eff}	0.9652	0.9368	0.9655
Calculational bias, Δk	0.0030	0.0030	0.0030
Uncertainties			
KENO Bias	±0.0012	±0.0012	±0.0012
KENO Statistics	±0.0006	±0.0007	±0.0006
Lattice Spacing	±0.0025	±0.0007	±0.0016
Fuel Density	±0.0021	±0.0025	±0.0021
Fuel Enrichment	±0.0025	±0.0016	±0.0019
Statistical Combination	±0.0044	±0.0033	±0.0036
Total k_{eff}	0.9682 ± 0.0044	0.9398 ± 0.0033	0.9685 ± 0.0036
Maximum k-eff	0.9726	0.9431	0.9721
Regulatory Limit	0.98	0.95	0.98

[24] These calculations were conservatively performed as infinite array calculations. At 4.2 wt% enrichment, the flooded condition reactivity would be much lower than the 4.95% case.

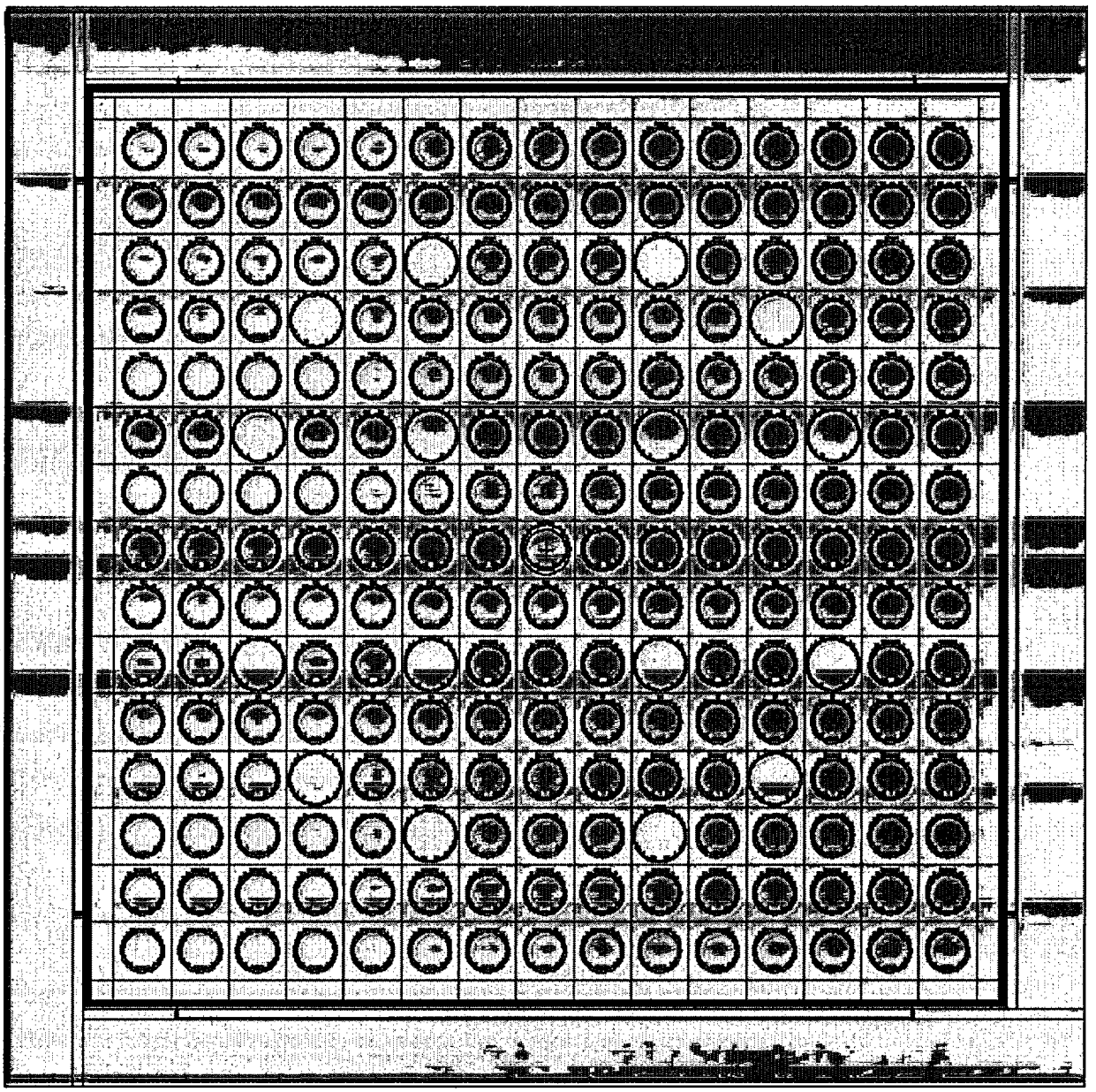

Figure 4.5.1: A Two-Dimensional Representation of the Actual Calculational Model Used for the Region 1 Rack Analysis for Uniform Loading of Spent Fuel. This Figure was Drawn (To Scale) with the Two-Dimensional Plotter in MCNP4a.

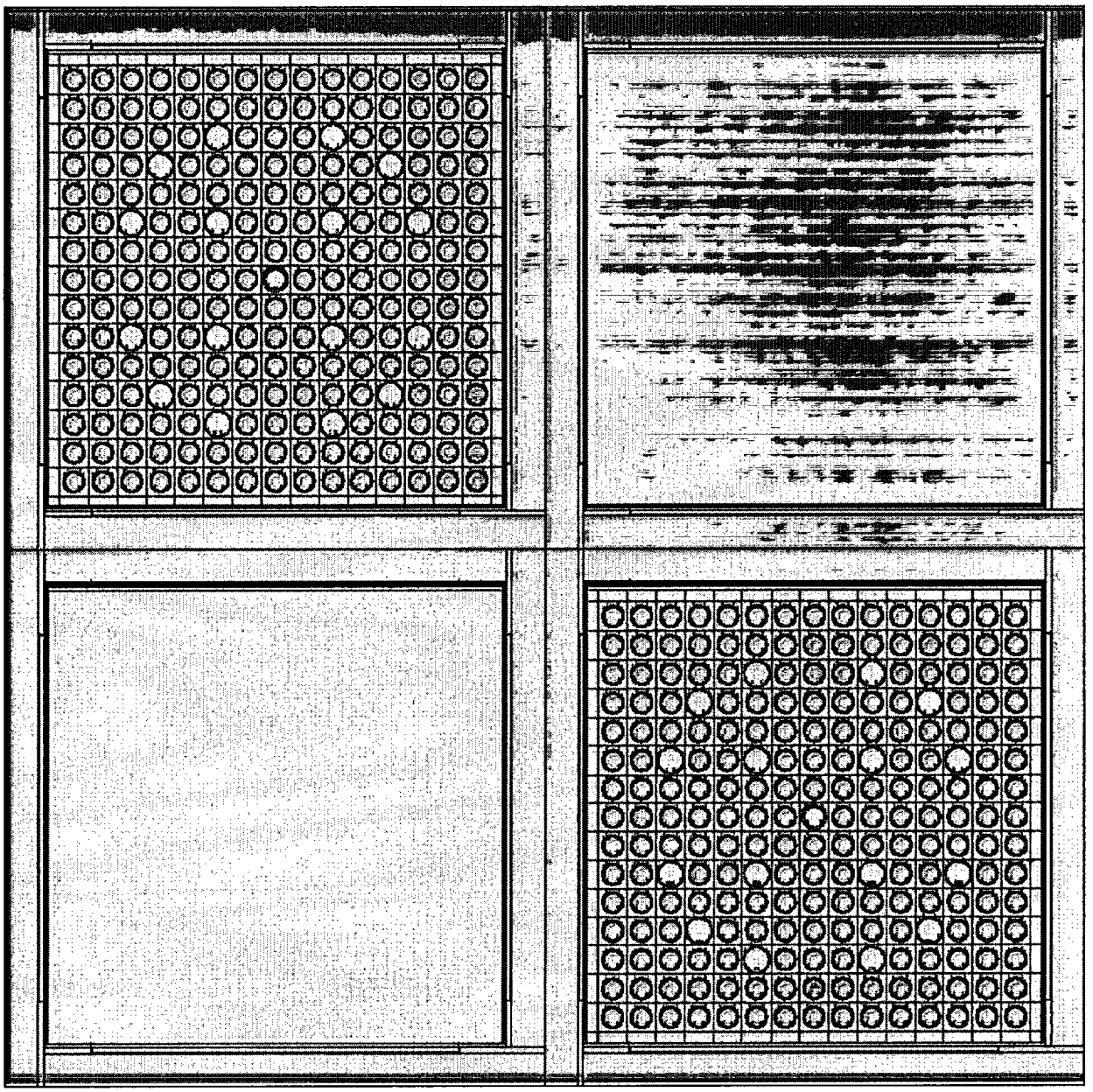

Figure 4.5.2: A Two-Dimensional Representation of the Actual Calculational Model Used for the Region 1 Rack Analysis for Checkerboard Loading of Fresh Fuel. This Figure was Drawn (To Scale) with the Two-Dimensional Plotter in MCNP4a.

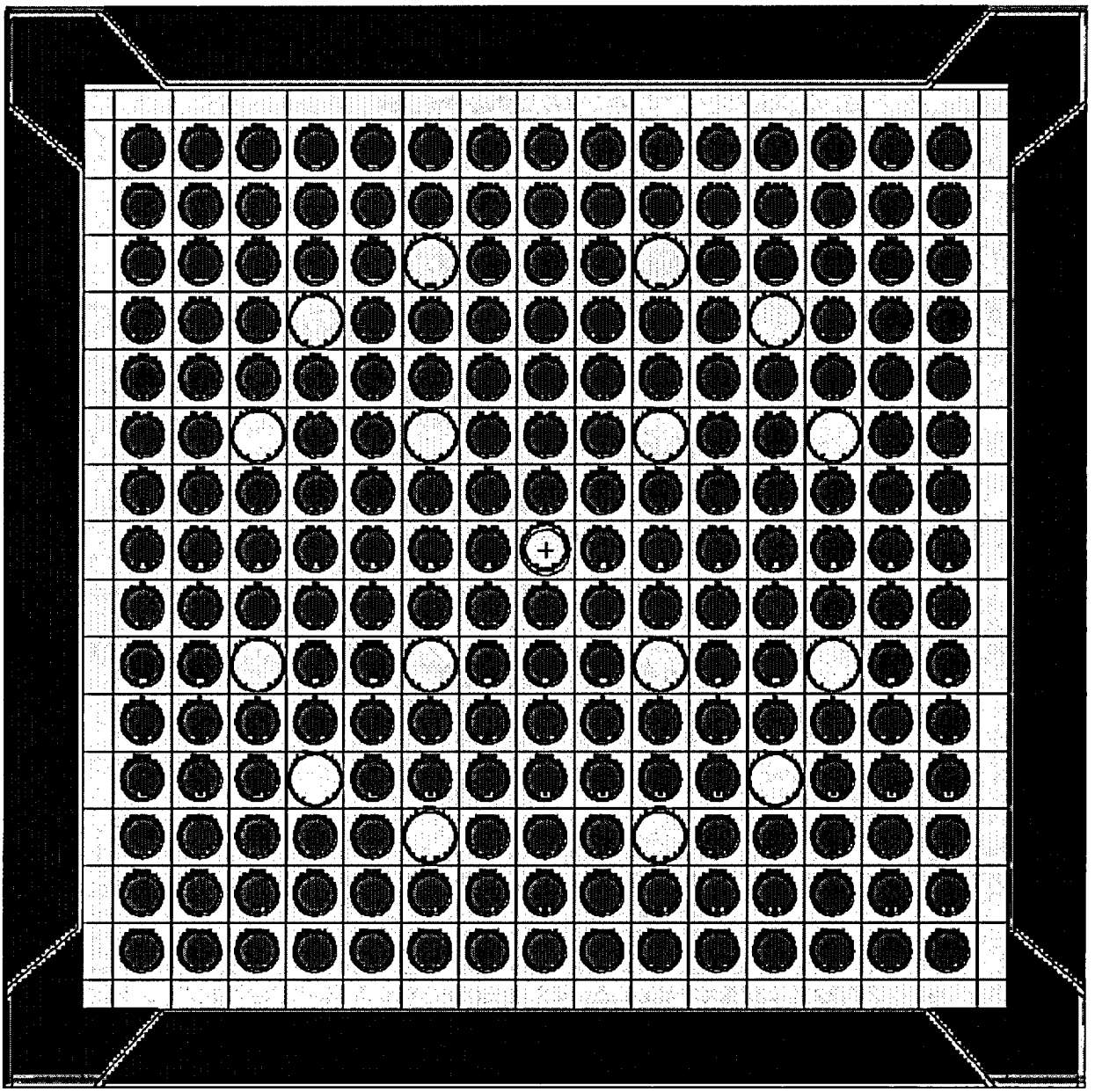

Figure 4.5.3: A Two-Dimensional Representation of the Actual Calculational Model Used for the Region 2 Rack Analysis for Uniform Loading of Spent Fuel. This Figure was drawn (To Scale) with the Two-Dimensional Plotter in MCNP4a.

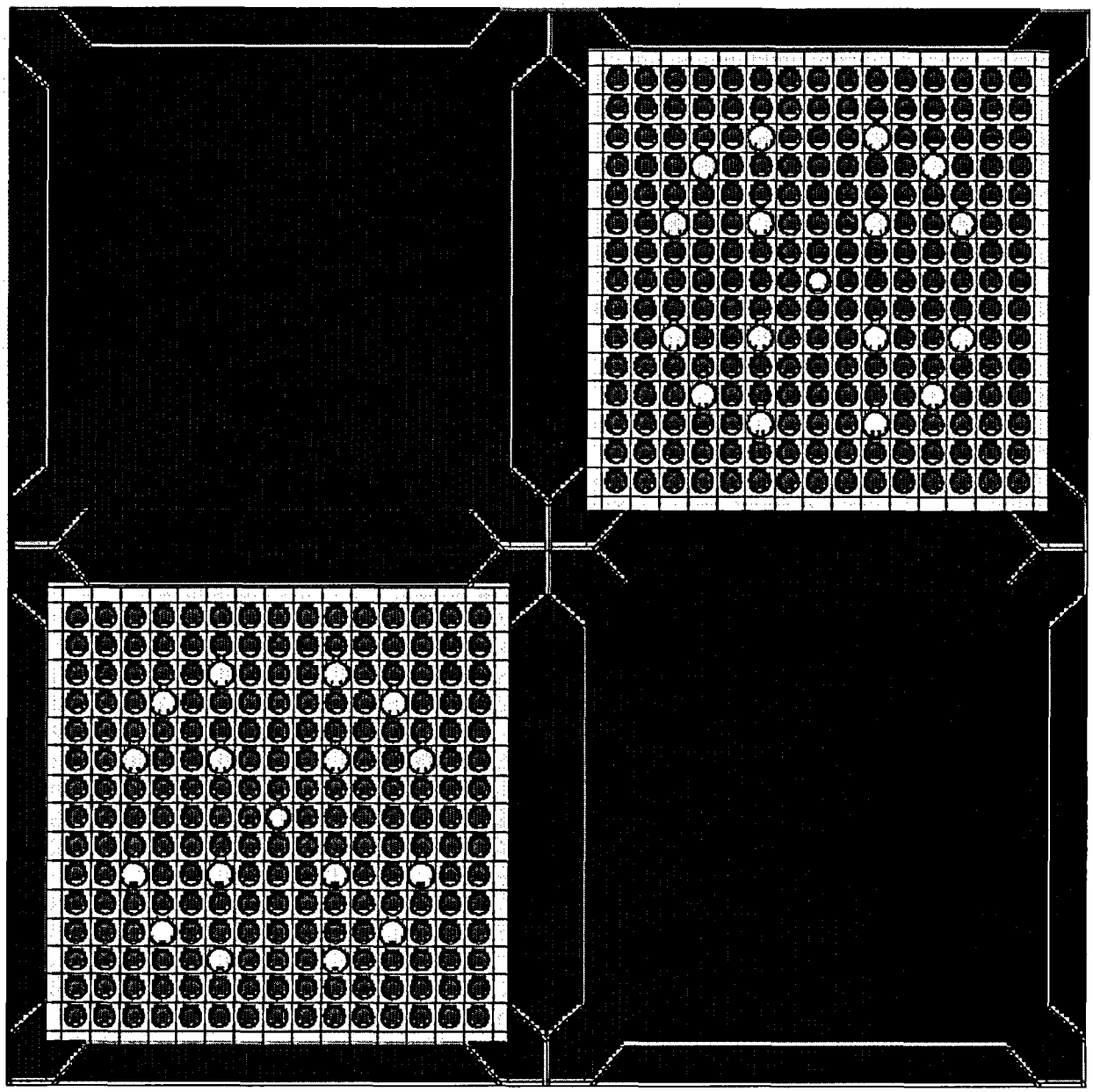

Figure 4.5.4: A Two-Dimensional Representation of the Actual Calculational Model Used for the Region 2 Rack Analysis for Checkerboard Loading of Fresh Fuel. This Figure was Drawn (To Scale) with the Two-Dimensional Plotter in MCNP4a.

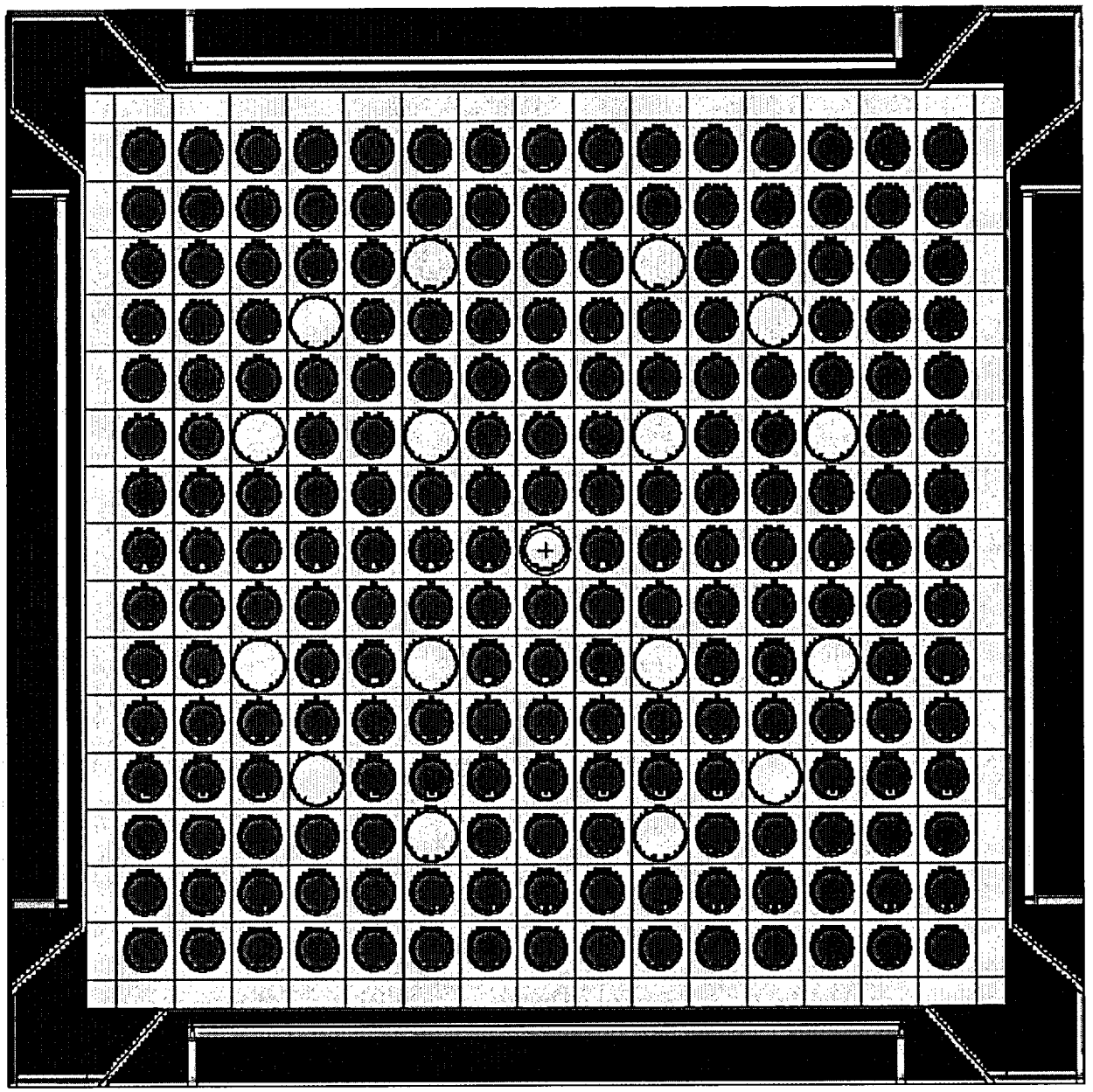

Figure 4.5.5: A Two-Dimensional Representation of the Actual Calculational Model Used for the Region 3 Rack Analysis for Uniform Loading of Fresh Fuel. This Figure was drawn (To Scale) with the Two-Dimensional Plotter in MCNP4a.

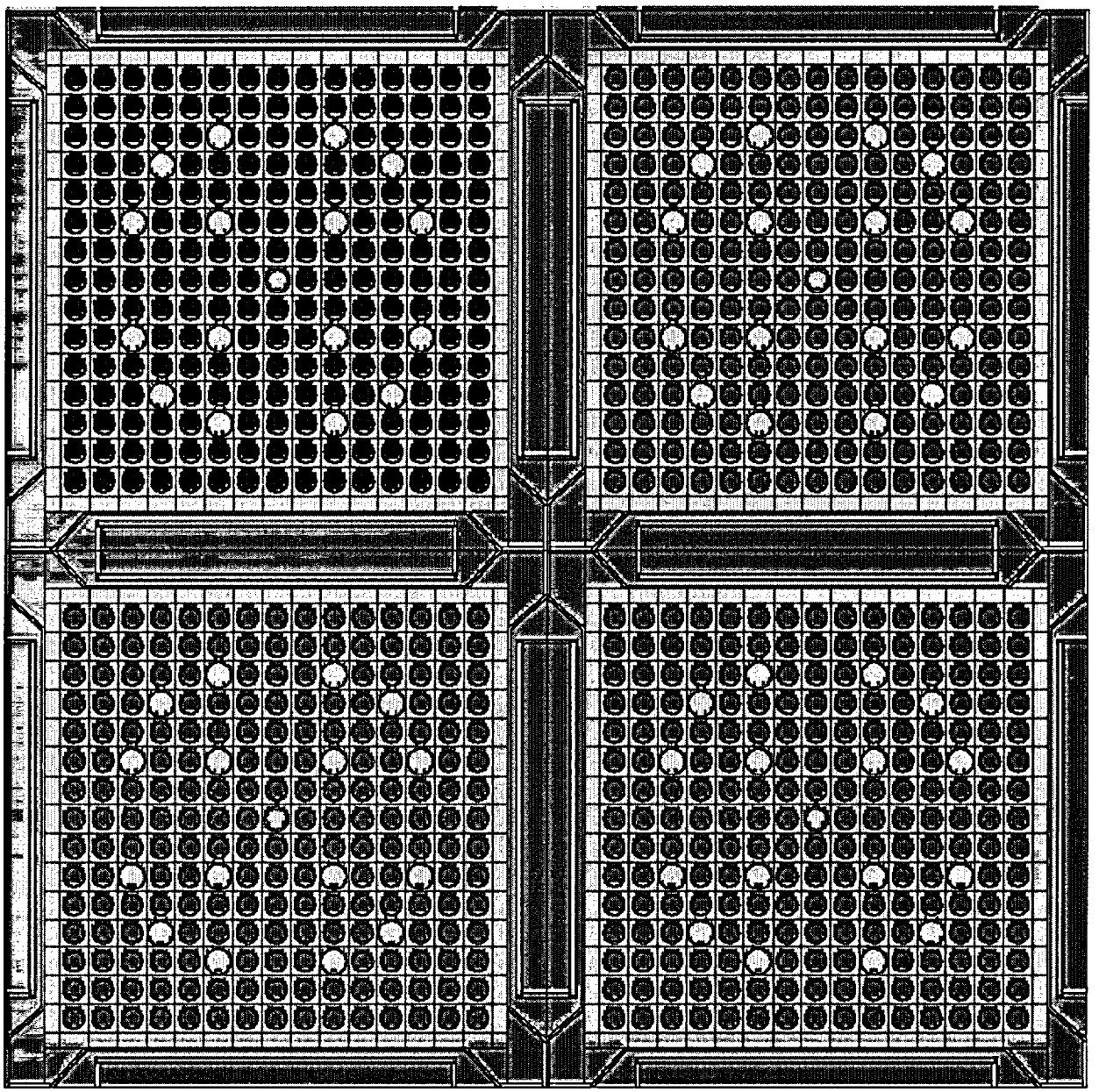

Figure 4.5.6: A Two-Dimensional Representation of the Actual Calculational Model Used for the Region 3 Rack Analysis for "3 of 4" Loading of Spent and Fresh Fuel. This Figure was drawn (To Scale) with the Two-Dimensional Plotter in MCNP4a.

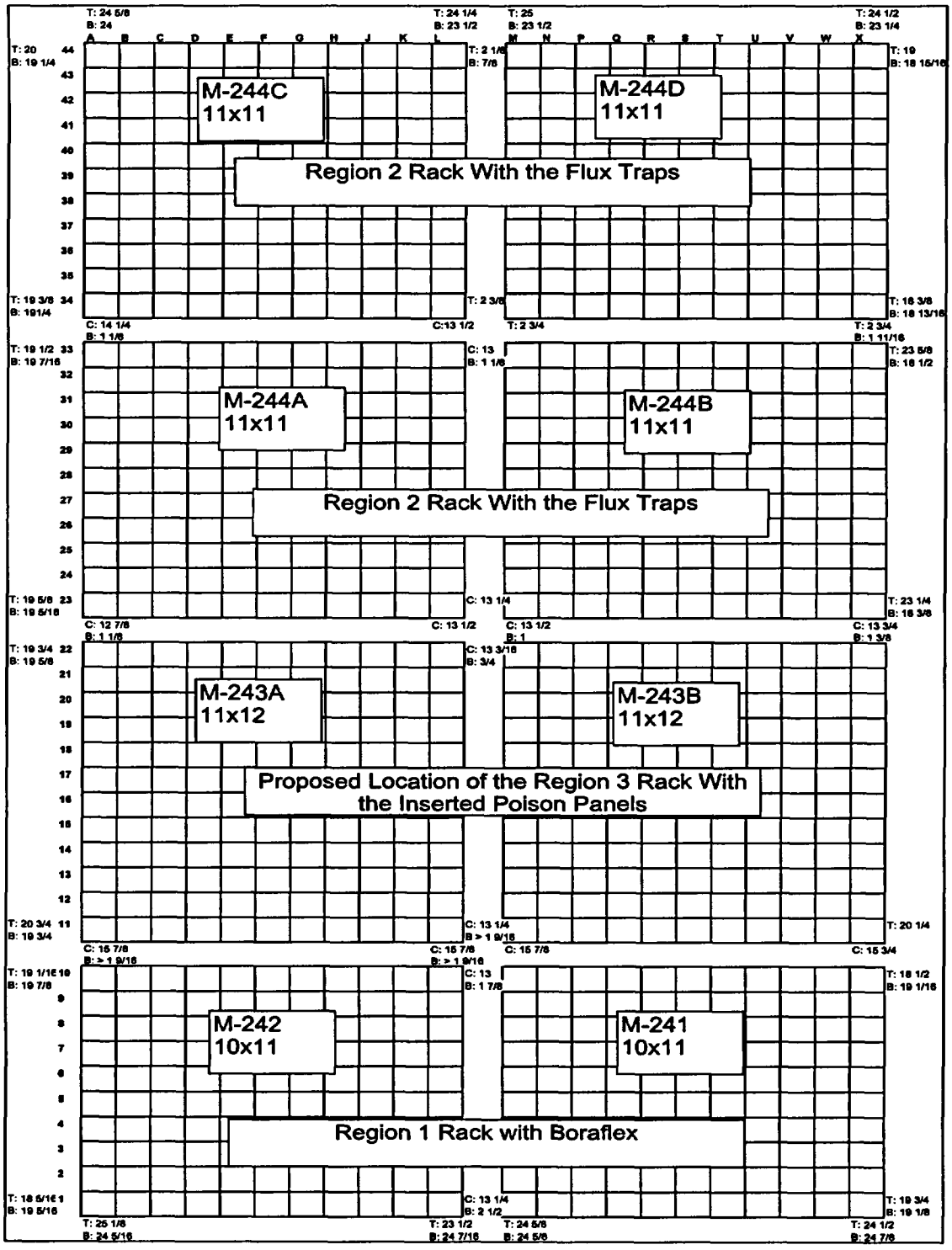

T: The distance between the outer most top portion of the racks.
B: The distance between the bottom of the racks at the base plate.
C: The distance between the top cell centerlines

Figure 4.5.7: A Two-Dimensional Representation of the ANO Unit 1 Spent Fuel Pool Layout with Rack Region Layout and Gaps between Adjacent Racks

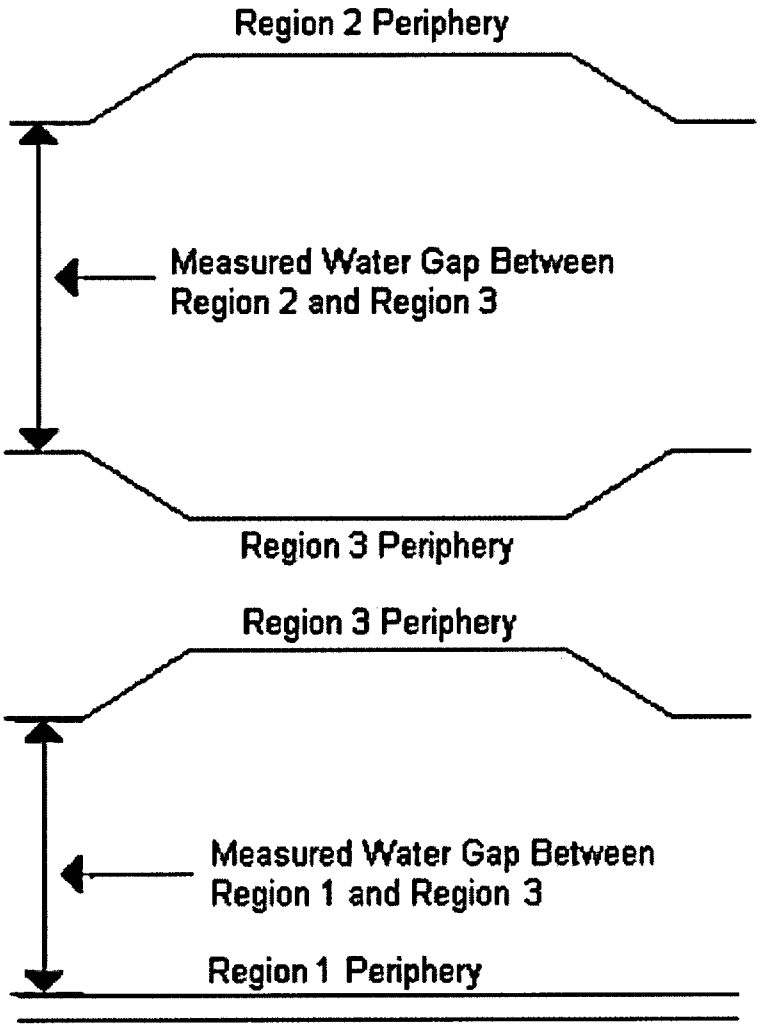

Figure 4.5.8: Sketch Illustrating Locations of Measurements of Water Gaps Between Adjacent Racks.[25]

[25] In measuring the gap between Region 1 and Region 3 the outside of the region 1 racks is the stainless steel sheathing surrounding the Boraflex.

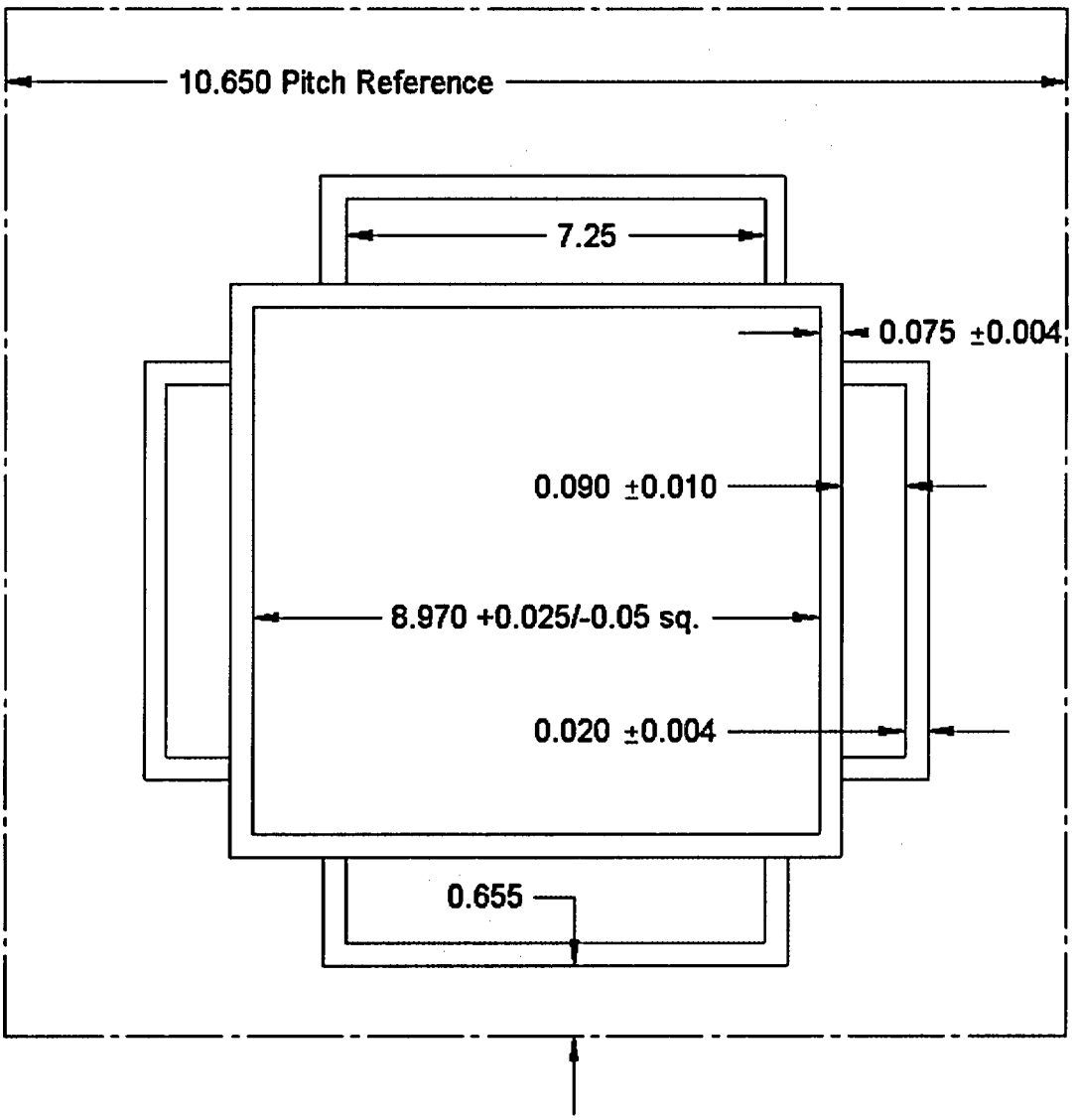

Figure 4.5.9: Sketch of Region 1 Racks, Detailing Important Dimensions and Tolerances (NOT TO SCALE, all dimensions in inches)

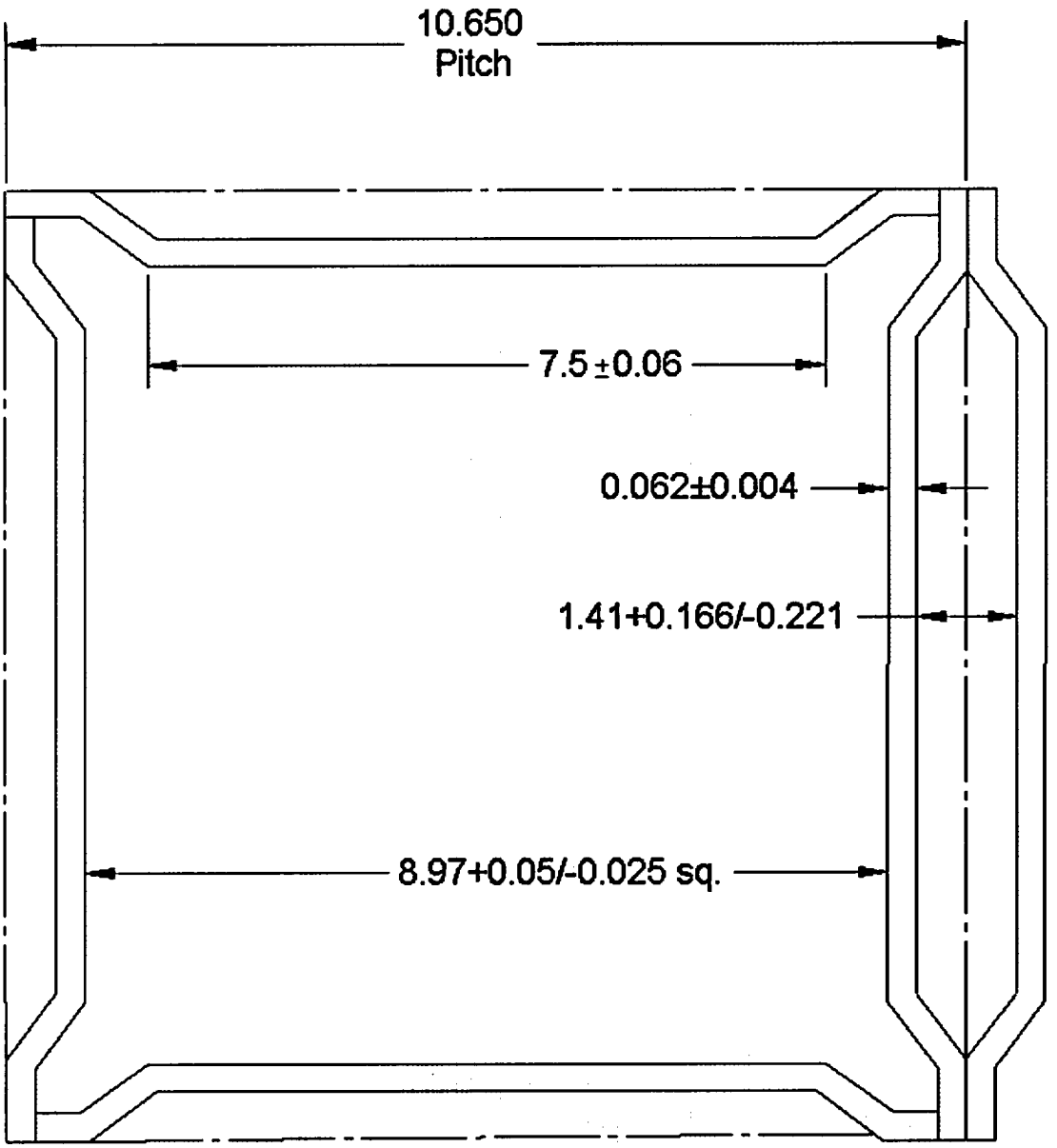

Figure 4.5.10: Sketch of Region 2 Racks, Detailing Important Dimensions and Tolerances. (NOT TO SCALE, all dimensions in inches)[26]

[26] In order to preserve the pitch due to a conservative reduction of the flux trap gap width from a design reference value of 1.556 inches to 1.41 inches (based on measurements), the nominal cell ID was modeled as 9.116 +0.50/-0.025 inches.

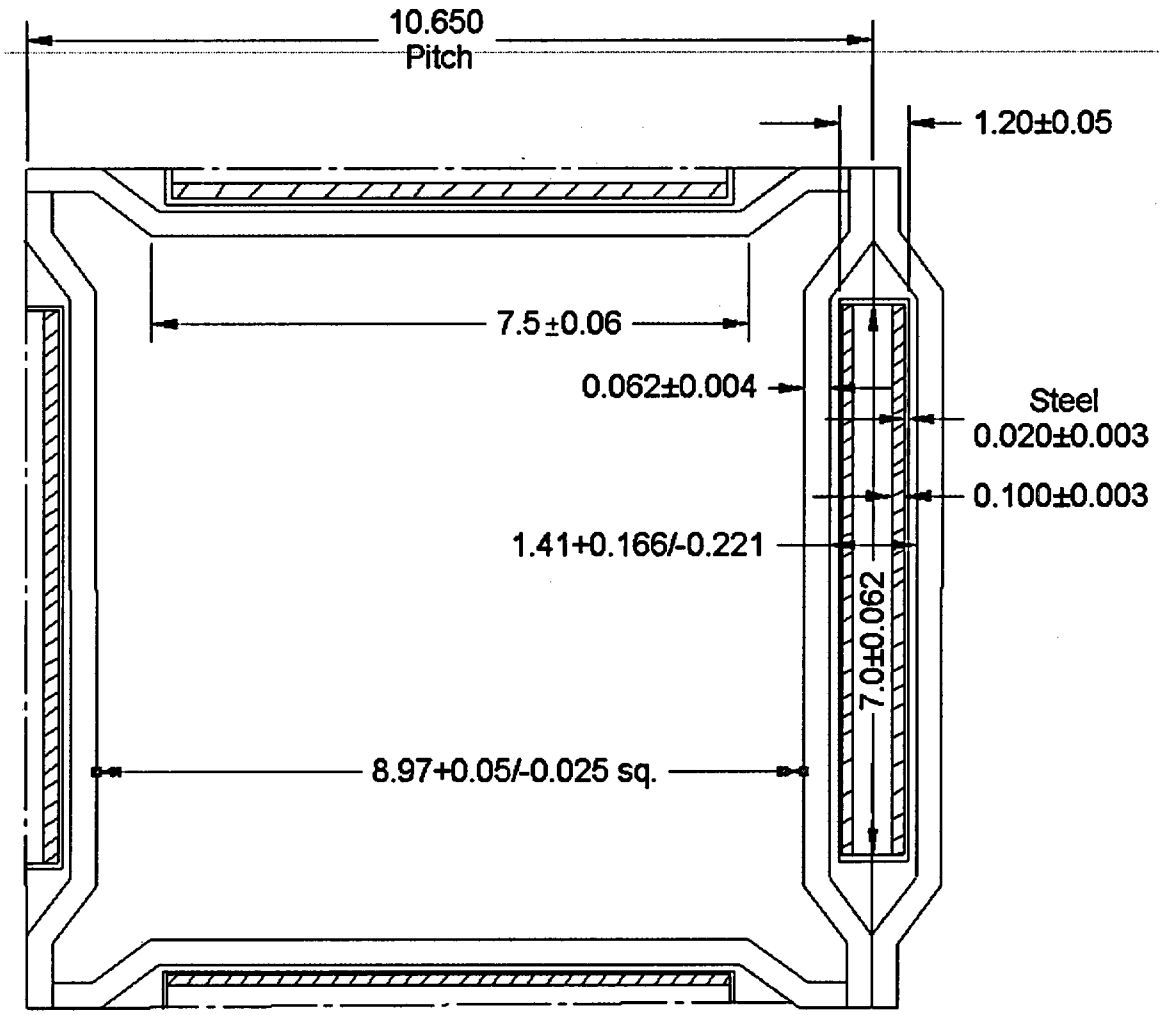

Figure 4.5.11: Sketch of Region 3 Racks, Detailing Important Dimensions and Tolerances. (NOT TO SCALE, all dimensions in inches)[27]

[27] In order to preserve the pitch due to a conservative reduction of the flux trap gap width from a design reference value of 1.556 inches to 1.41 inches (based on measurements), the nominal cell ID was modeled as 9.116 +0.50/-0.025 inches.

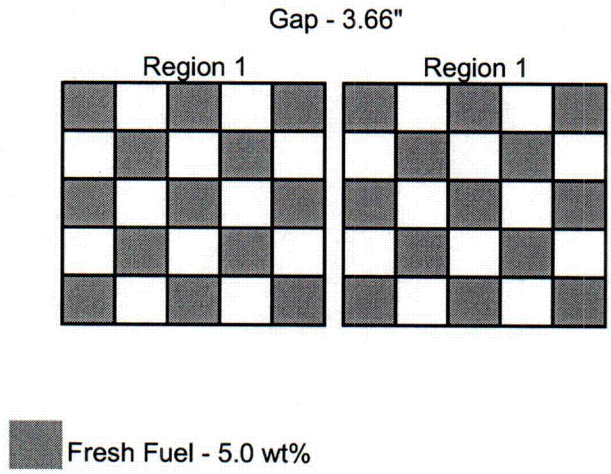

Figure 4.7.1: Interface Calculation for Adjacent Region 1 Racks Containing Fresh Fuel Checkerboards with Fresh Fuel Assemblies Facing Across the Gap – NOT ALLOWED

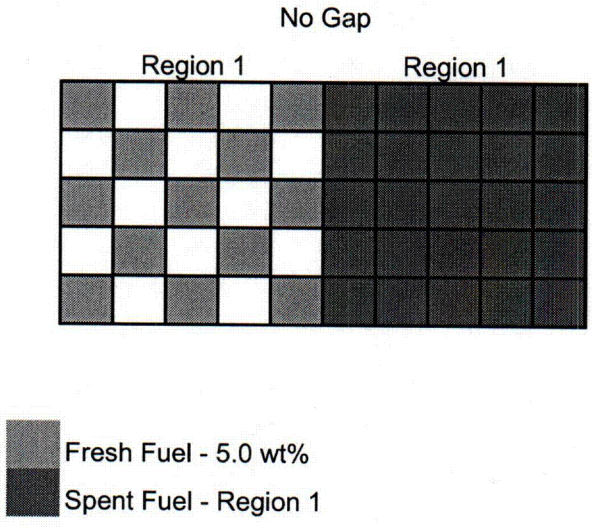

Figure 4.7.2: Fresh Fuel Checkerboard and Spent Fuel in same Region 1 Rack - ALLOWED

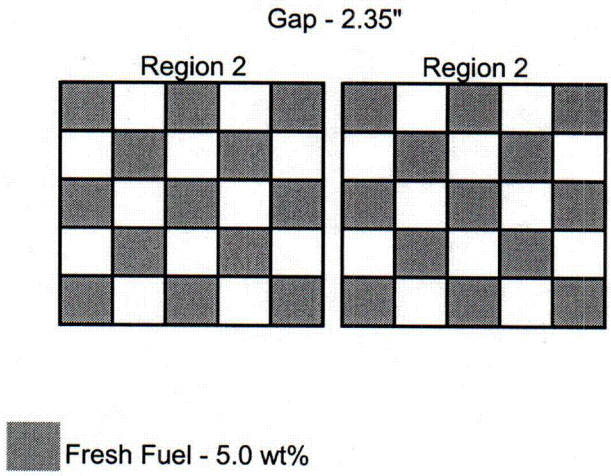

Figure 4.7.3: Interface Calculation for Adjacent Region 2 Racks Containing Fresh Fuel Checkerboards with Fresh Fuel Assemblies Facing Across the Gap – NOT ALLOWED

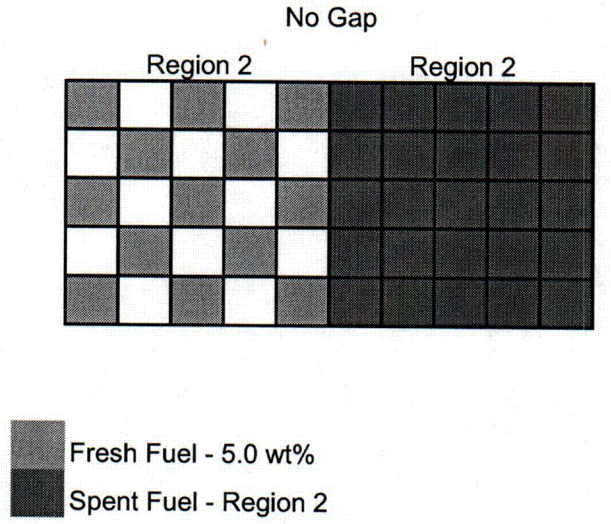

Figure 4.7.4: Fresh Fuel Checkerboard and Spent Fuel in same Region 2 Rack - ALLOWED

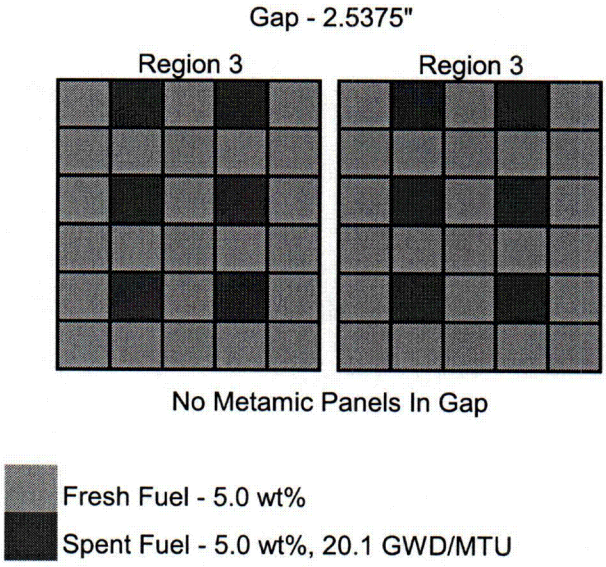

Figure 4.7.5: Interface Calculation for Adjacent Region 3 Racks with 3 of 4 Pattern and Fresh Fuel Facing Across the Gap – NOT ALLOWED

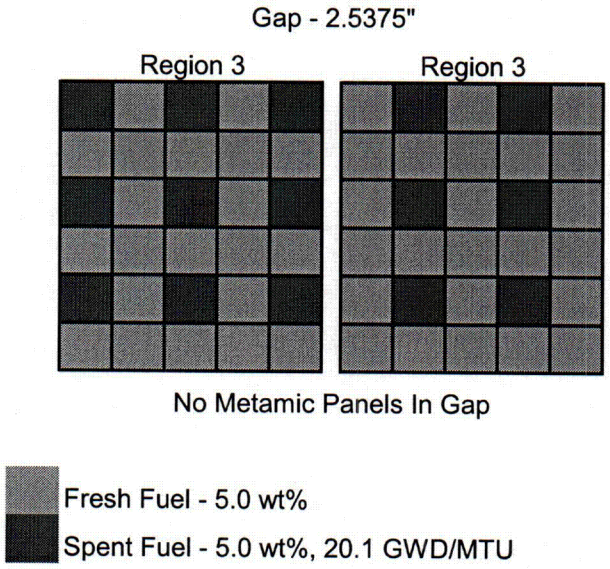

Figure 4.7.6: Interface Calculation for Region 3 Racks. Fresh Fuel in one Region 3 Rack Facing Fresh and Spent Fuel in the Adjacent Rack - ALLOWED

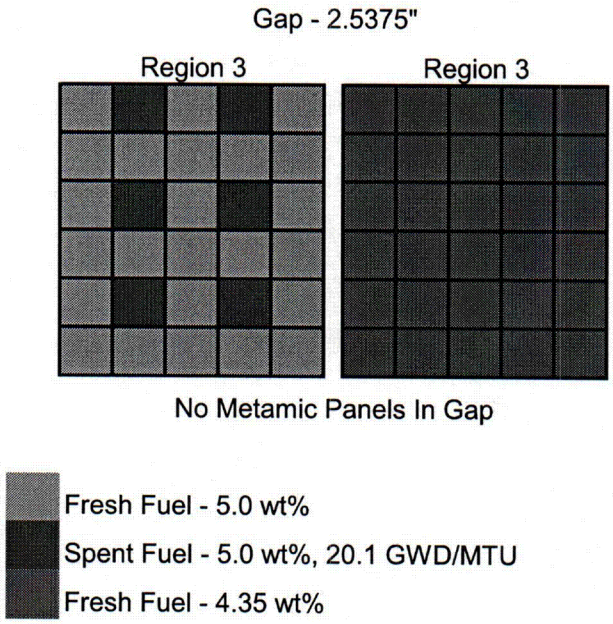

Figure 4.7.7: Interface Calculation for Region 3 Racks. All Fresh Fuel (4.35 wt%) in one Rack, 3 of 4 Pattern with Fresh Fuel Facing Gap in Adjacent Rack. – NOT ALLOWED

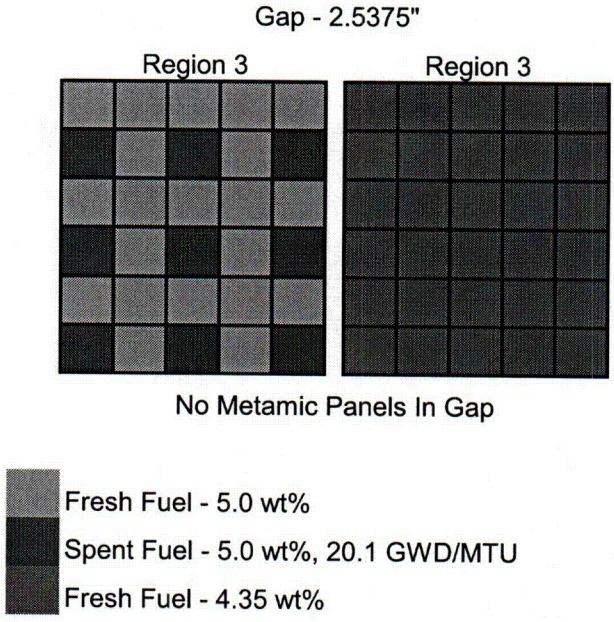

Figure 4.7.8: Interface Calculation for Region 3 Racks. All Fresh Fuel (4.35 wt%) in one Rack, 3 of 4 Pattern with Fresh and Spent Fuel Facing Gap in Adjacent Rack. - ALLOWED

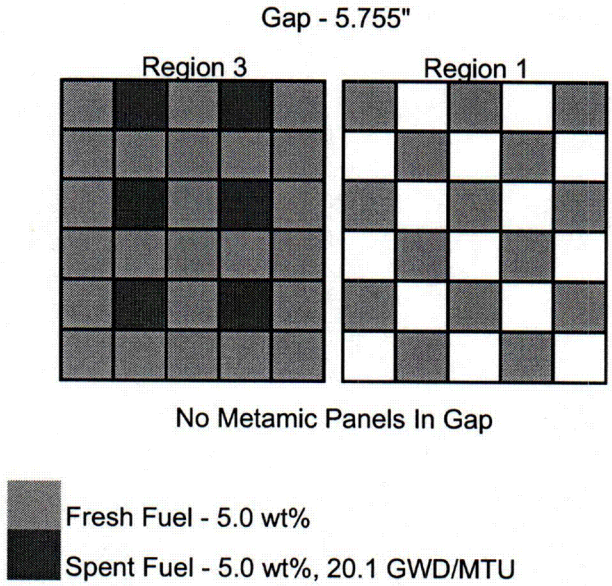

Figure 4.7.9: Interface Calculation for Region 1 and Region 3 Racks. Fresh Fuel Checkerboard in Region 1 Rack, 3 of 4 pattern in Region 3 Rack with Fresh Fuel Facing Gap. - ALLOWED

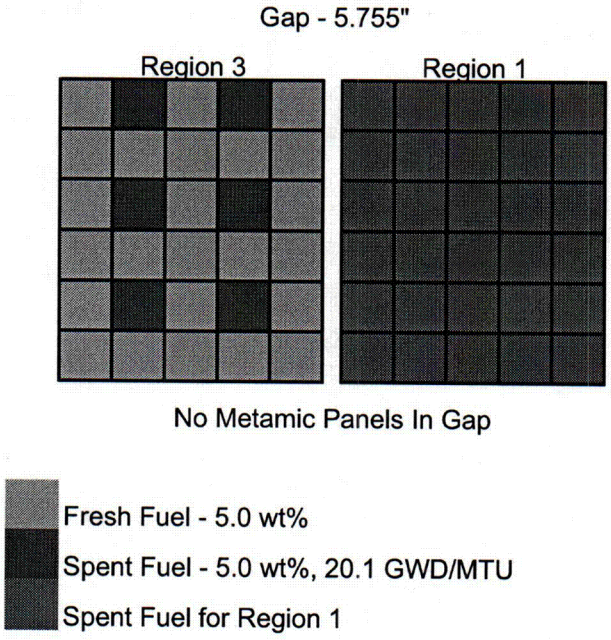

Figure 4.7.10: Interface Calculation for Region 1 and Region 3 Racks. Spent Fuel in Region 1 Rack, 3 of 4 Pattern in Region 3 Rack with Fresh Fuel Facing Gap. - ALLOWED

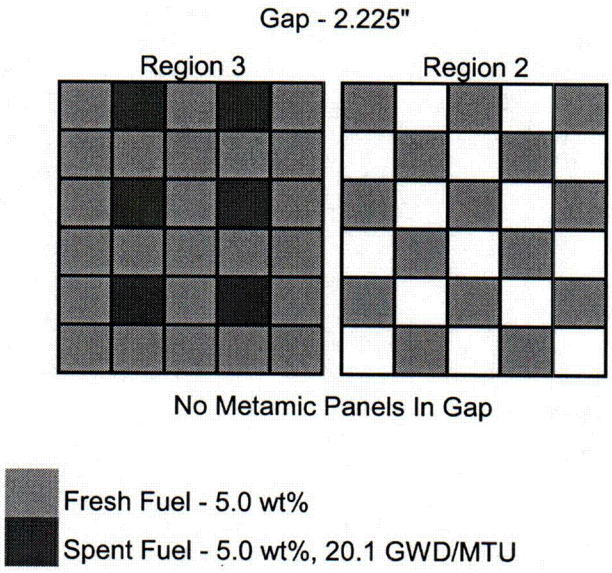

Figure 4.7.11: Interface Calculation for Region 2 and Region 3 Racks. Fresh Fuel Checkerboard in Region 2 Rack, 3 of 4 pattern in Region 3 Rack with Fresh Fuel Facing Gap. - ALLOWED

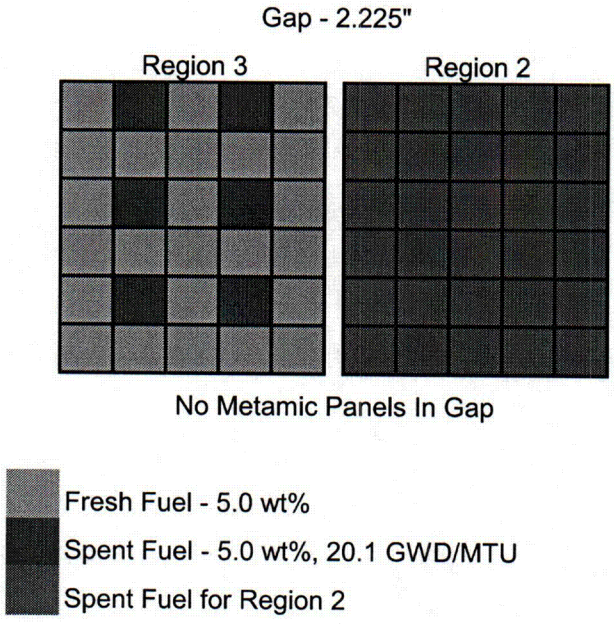

Figure 4.7.12: Interface Calculation for Region 2 and Region 3 Racks. Spent Fuel in Region 2 Rack, 3 of 4 Pattern in Region 3 Rack with Fresh Fuel Facing Gap. – ALLOWED

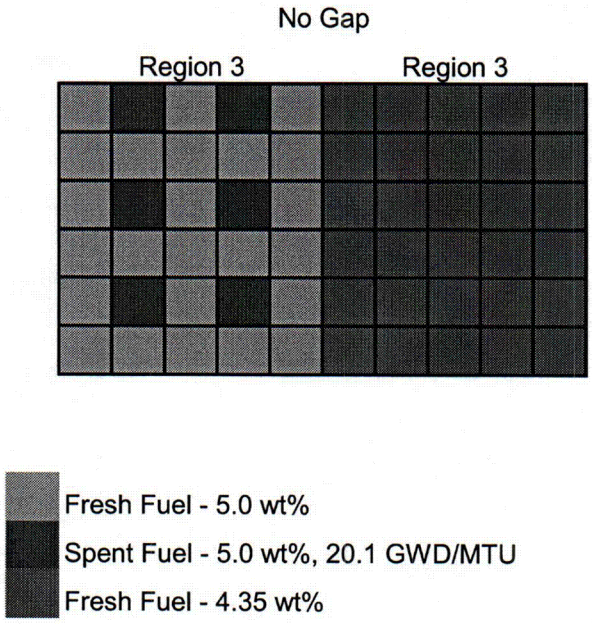

Figure 4.7.13: 3 of 4 Loading Pattern and Fresh Fuel (4.35 wt% ^{235}U) in same Region 3 Rack, All fresh 5.0 wt% facing all fresh 4.35 wt% - NOT ALLOWED

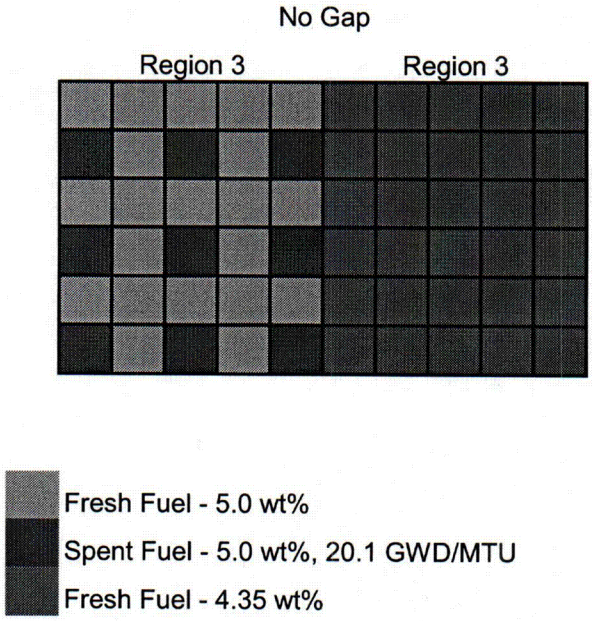

Figure 4.7.14: 3 of 4 Loading Pattern and Fresh Fuel (4.35 wt% ^{235}U) in same Region 3 Rack, Fresh and spent 5.0 wt% facing all fresh 4.35 wt% - ALLOWED

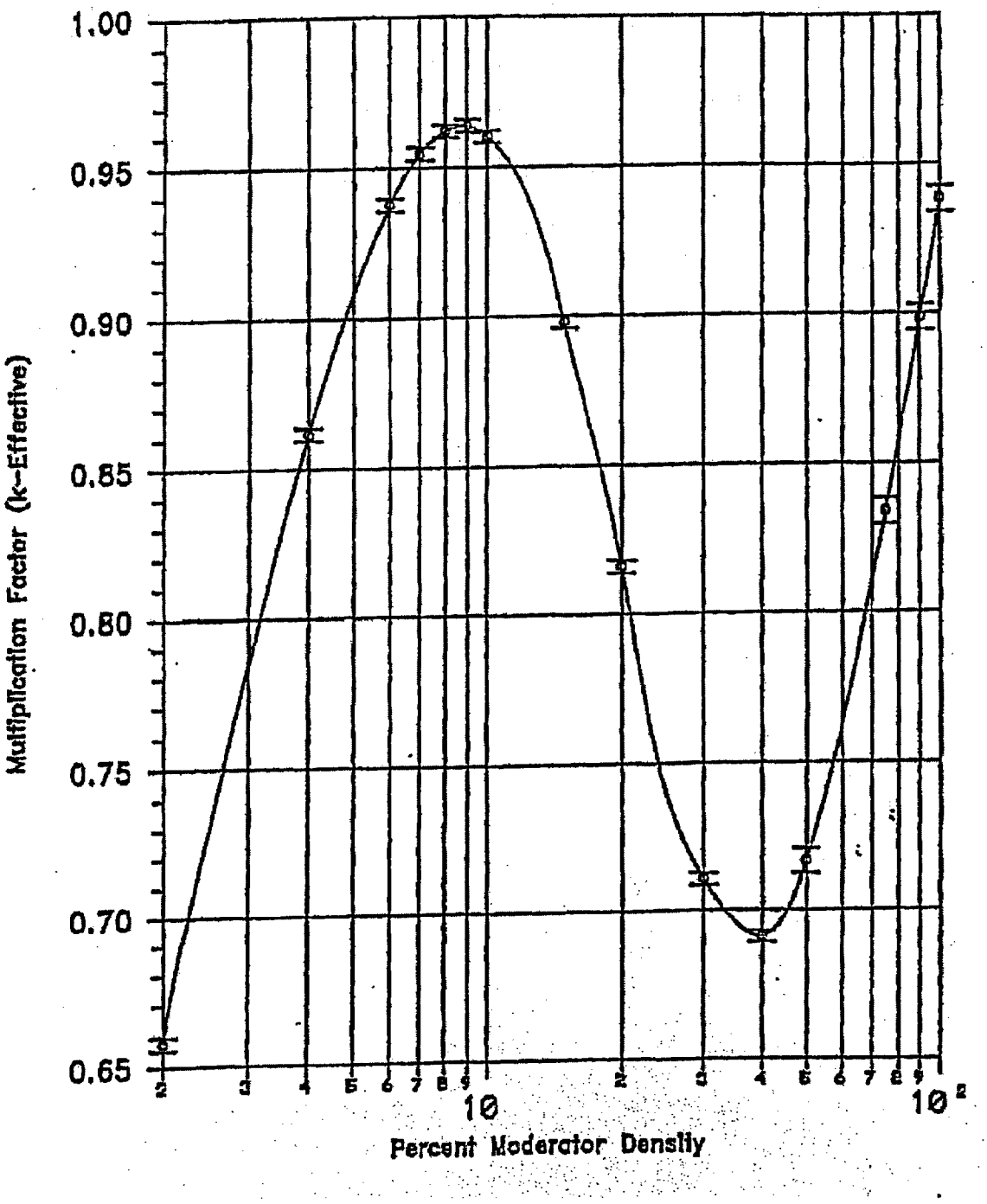

Figure 4.8.1: Reactivity of the New Fuel Vault as a Function of Moderator Density for 4.95 wt% Fuel.

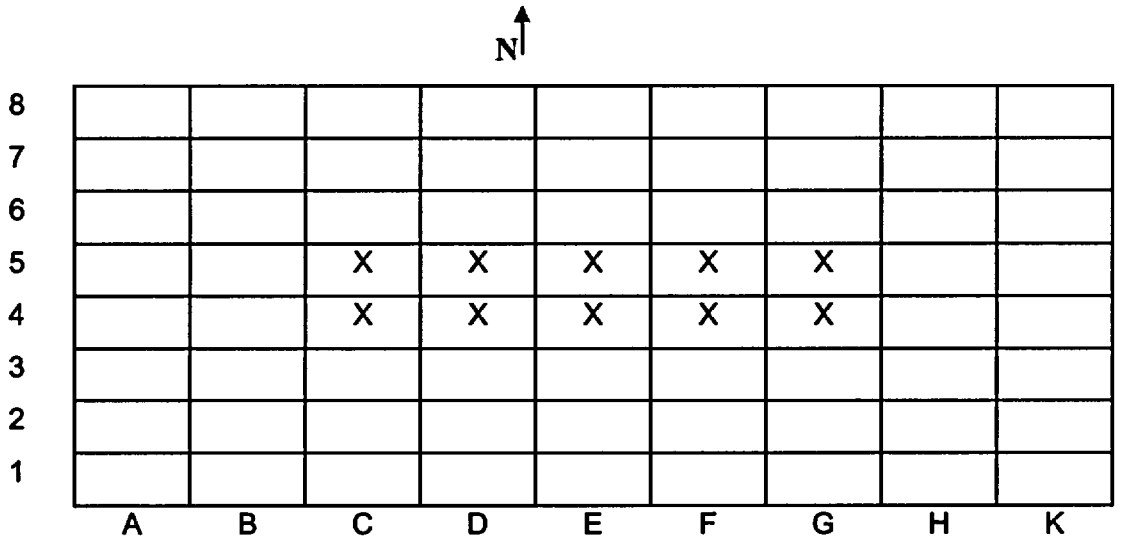

Figure 4.8.2: Acceptable New Fuel Storage Vault Configuration for up to 4.95 wt% Enrichment Fresh Fuel.

Note: X's show the locations where fuel assemblies will not be stored.

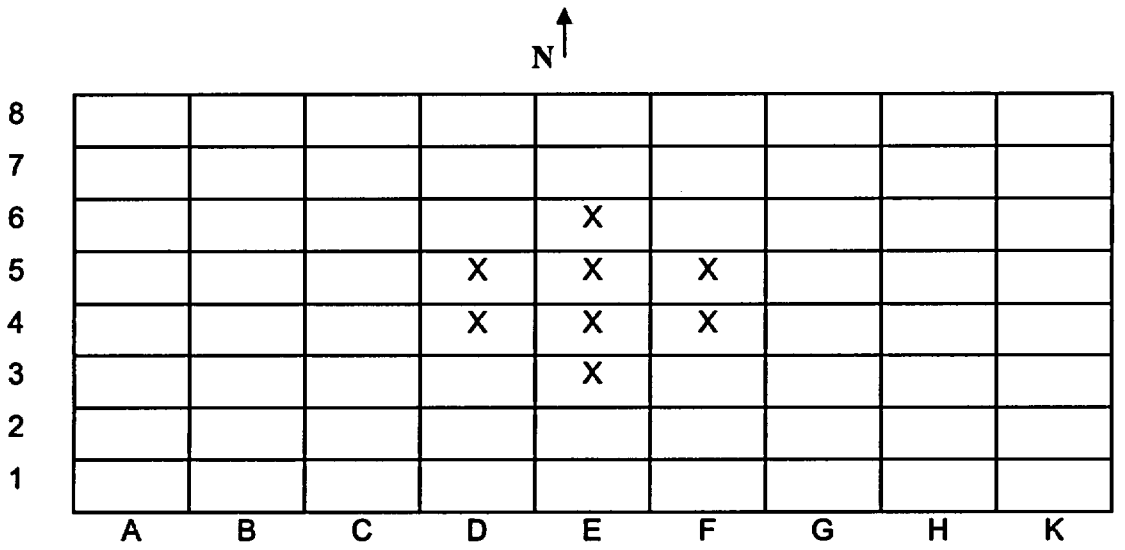

Figure 4.8.3: Acceptable New Fuel Storage Vault Configuration for up to 4.2 wt% Enrichment Fresh Fuel.

Note: X's show the locations where fuel assemblies will not be stored.

APPENDIX 4A: BENCHMARK CALCULATIONS

4A.1 INTRODUCTION AND SUMMARY

Benchmark calculations have been made on selected critical experiments, chosen, in so far as possible, to bound the range of variables in the rack designs. Two independent methods of analysis were used, differing in cross section libraries and in the treatment of the cross sections. MCNP4a [4A.1] is a continuous energy Monte Carlo code and KENO5a [4A.2] uses group-dependent cross sections. For the KENO5a analyses reported here, the 238-group library was chosen, processed through the NITAWL-II [4A.2] program to create a working library and to account for resonance self-shielding in uranium-238 (Nordheim integral treatment). The 238 group library was chosen to avoid or minimize the errors† (trends) that have been reported (e.g., [4A.3 through 4A.5]) for calculations with collapsed cross section sets.

In rack designs, the three most significant parameters affecting criticality are (1) the fuel enrichment, (2) the ^{10}B loading in the neutron absorber, and (3) the lattice spacing (or water-gap thickness if a flux-trap design is used). Other parameters, within the normal range of rack and fuel designs, have a smaller effect, but are also included in the analyses.

Table 4A.1 summarizes results of the benchmark calculations for all cases selected and analyzed, as referenced in the table. The effect of the major variables are discussed in subsequent sections below. It is important to note that there is obviously considerable overlap in parameters since it is not possible to vary a single parameter and maintain criticality; some other parameter or parameters must be concurrently varied to maintain criticality.

One possible way of representing the data is through a spectrum index that incorporates all of the variations in parameters. KENO5a computes and prints the "energy of the average lethargy causing fission" (EALF). In MCNP4a, by utilizing the tally option with the identical 238-group energy structure as in KENO5a, the number of fissions in each group may be collected and the EALF determined (post-processing).

---

† Small but observable trends (errors) have been reported for calculations with the 27-group and 44-group collapsed libraries. These errors are probably due to the use of a single collapsing spectrum when the spectrum should be different for the various cases analyzed, as evidenced by the spectrum indices.

Figures 4A.1 and 4A.2 show the calculated k_{eff} for the benchmark critical experiments as a function of the EALF for MCNP4a and KENO5a, respectively (UO_2 fuel only). The scatter in the data (even for comparatively minor variation in critical parameters) represents experimental error† in performing the critical experiments within each laboratory, as well as between the various testing laboratories. The B&W critical experiments show a larger experimental error than the PNL criticals. This would be expected since the B&W criticals encompass a greater range of critical parameters than the PNL criticals.

Linear regression analysis of the data in Figures 4A.1 and 4A.2 show that there are no trends, as evidenced by very low values of the correlation coefficient (0.13 for MCNP4a and 0.21 for KENO5a). The total bias (systematic error, or mean of the deviation from a k_{eff} of exactly 1.000) for the two methods of analysis are shown in the table below.

Calculational Bias of MCNP4a and KENO5a	
MCNP4a	0.0009 ± 0.0011
KENO5a	0.0030 ± 0.0012

The bias and standard error of the bias were derived directly from the calculated k_{eff} values in Table 4A.1 using the following equations††, with the standard error multiplied by the one-sided K-factor for 95% probability at the 95% confidence level from NBS Handbook 91 [4A.18] (for the number of cases analyzed, the K-factor is ~2.05 or slightly more than 2).

$$\bar{k} = \frac{1}{n} \sum_{i}^{n} k_i \qquad (4A.1)$$

---

† A classical example of experimental error is the corrected enrichment in the PNL experiments, first as an addendum to the initial report and, secondly, by revised values in subsequent reports for the same fuel rods.

†† These equations may be found in any standard text on statistics, for example, reference [4A.6] (or the MCNP4a manual) and is the same methodology used in MCNP4a and in KENO5a.

$$\sigma_{\bar{k}}^2 = \frac{\sum_{i=1}^{n} k_i^2 - (\sum_{i=1}^{n} k_i)^2 / n}{n\,(n-1)} \qquad (4A.2)$$

$$Bias = (1 - \bar{k}) \pm K\,\sigma_{\bar{k}} \qquad (4A.3)$$

where k_i are the calculated reactivities of n critical experiments; $\sigma_{\bar{k}}$ is the unbiased estimator of the standard deviation of the mean (also called the standard error of the bias (mean)); K is the one-sided multiplier for 95% probability at the 95% confidence level (NBS Handbook 91 [4A.18]).

Formula 4.A.3 is based on the methodology of the National Bureau of Standards (now NIST) and is used to calculate the values presented on page 4.A-2. The first portion of the equation, (1- $\bar{k}$), is the actual bias which is added to the MCNP4a and KENO5a results. The second term, $K\sigma_{\bar{k}}$, is the uncertainty or standard error associated with the bias. The K values used were obtained from the National Bureau of Standards Handbook 91 and are for one-sided statistical tolerance limits for 95% probability at the 95% confidence level. The actual K values for the 56 critical experiments evaluated with MCNP4a and the 53 critical experiments evaluated with KENO5a are 2.04 and 2.05, respectively.

The bias values are used to evaluate the maximum k_{eff} values for the rack designs. KENO5a has a slightly larger systematic error than MCNP4a, but both result in greater precision than published data [4A.3 through 4A.5] would indicate for collapsed cross section sets in KENO5a (SCALE) calculations.

4A.2 Effect of Enrichment

The benchmark critical experiments include those with enrichments ranging from 2.46 w/o to 5.74 w/o and therefore span the enrichment range for rack designs. Figures 4A.3 and 4A.4 show the calculated k_{eff} values (Table 4A.1) as a function of the fuel enrichment reported for the critical experiments. Linear regression analyses for these data confirms that there are no trends, as indicated by low values of the correlation coefficients (0.03 for MCNP4a and 0.38 for KENO5a). Thus, there are no corrections to the bias for the various enrichments.

As further confirmation of the absence of any trends with enrichment, a typical configuration was calculated with both MCNP4a and KENO5a for various enrichments. The cross-comparison of calculations with codes of comparable sophistication is suggested in Reg. Guide 3.41. Results of this comparison, shown in Table 4A.2 and Figure 4A.5, confirm no significant difference in the calculated values of k_{eff} for the two independent codes as evidenced by the 45° slope of the curve. Since it is very unlikely that two independent methods of analysis would be subject to the same error, this comparison is considered confirmation of the absence of an enrichment effect (trend) in the bias.

4A.3 Effect of ^{10}B Loading

Several laboratories have performed critical experiments with a variety of thin absorber panels similar to the Boral panels in the rack designs. Of these critical experiments, those performed by B&W are the most representative of the rack designs. PNL has also made some measurements with absorber plates, but, with one exception (a flux-trap experiment), the reactivity worth of the absorbers in the PNL tests is very low and any significant errors that might exist in the treatment of strong thin absorbers could not be revealed.

Table 4A.3 lists the subset of experiments using thin neutron absorbers (from Table 4A.1) and shows the reactivity worth (Δk) of the absorber.†

No trends with reactivity worth of the absorber are evident, although based on the calculations shown in Table 4A.3, some of the B&W critical experiments seem to have unusually large experimental errors. B&W made an effort to report some of their experimental errors. Other laboratories did not evaluate their experimental errors.

To further confirm the absence of a significant trend with ^{10}B concentration in the absorber, a cross-comparison was made with MCNP4a and KENO5a (as suggested in Reg. Guide 3.41). Results are shown in Figure 4A.6 and Table 4A.4 for a typical geometry. These data substantiate the absence of any error (trend) in either of the two codes for the conditions analyzed (data points fall on a 45° line, within an expected 95% probability limit).

† The reactivity worth of the absorber panels was determined by repeating the calculation with the absorber analytically removed and calculating the incremental (Δk) change in reactivity due to the absorber.

4A.4 Miscellaneous and Minor Parameters

4A.4.1 Reflector Material and Spacings

PNL has performed a number of critical experiments with thick steel and lead reflectors.† Analysis of these critical experiments are listed in Table 4A.5 (subset of data in Table 4A.1). There appears to be a small tendency toward overprediction of k_{eff} at the lower spacing, although there are an insufficient number of data points in each series to allow a quantitative determination of any trends. The tendency toward overprediction at close spacing means that the rack calculations may be slightly more conservative than otherwise.

4A.4.2 Fuel Pellet Diameter and Lattice Pitch

The critical experiments selected for analysis cover a range of fuel pellet diameters from 0.311 to 0.444 inches, and lattice spacings from 0.476 to 1.00 inches. In the rack designs, the fuel pellet diameters range from 0.303 to 0.3805 inches O.D. (0.496 to 0.580 inch lattice spacing) for PWR fuel and from 0.3224 to 0.494 inches O.D. (0.488 to 0.740 inch lattice spacing) for BWR fuel. Thus, the critical experiments analyzed provide a reasonable representation of power reactor fuel. Based on the data in Table 4A.1, there does not appear to be any observable trend with either fuel pellet diameter or lattice pitch, at least over the range of the critical experiments applicable to rack designs.

4A.4.3 Soluble Boron Concentration Effects

Various soluble boron concentrations were used in the B&W series of critical experiments and in one PNL experiment, with boron concentrations ranging up to 2550 ppm. Results of MCNP4a (and one KENO5a) calculations are shown in Table 4A.6. Analyses of the very high boron concentration experiments (> 1300 ppm) show a tendency to slightly overpredict reactivity for the three experiments exceeding 1300 ppm. In turn, this would suggest that the evaluation of the racks with higher soluble boron concentrations could be slightly conservative.

† Parallel experiments with a depleted uranium reflector were also performed but not included in the present analysis since they are not pertinent to the Holtec rack design.

4A.5 MOX Fuel

The number of critical experiments with PuO_2 bearing fuel (MOX) is more limited than for UO_2 fuel. However, a number of MOX critical experiments have been analyzed and the results are shown in Table 4A.7. Results of these analyses are generally above a k_{eff} of 1.00, indicating that when Pu is present, both MCNP4a and KENO5a overpredict the reactivity. This may indicate that calculation for MOX fuel will be expected to be conservative, especially with MCNP4a. It may be noted that for the larger lattice spacings, the KENO5a calculated reactivities are below 1.00, suggesting that a small trend may exist with KENO5a. It is also possible that the overprediction in k_{eff} for both codes may be due to a small inadequacy in the determination of the Pu-241 decay and Am-241 growth. This possibility is supported by the consistency in calculated k_{eff} over a wide range of the spectral index (energy of the average lethargy causing fission).

4A.6 References

[4A.1] J.F. Briesmeister, Ed., "MCNP4a - A General Monte Carlo N-Particle Transport Code, Version 4A; Los Alamos National Laboratory, LA-12625-M (1993).

[4A.2] SCALE 4.3, "A Modular Code System for Performing Standardized Computer Analyses for Licensing Evaluation", NUREG-0200 (ORNL-NUREG-CSD-2/U2/R5, Revision 5, Oak Ridge National Laboratory, September 1995.

[4A.3] M.D. DeHart and S.M. Bowman, "Validation of the SCALE Broad Structure 44-G Group ENDF/B-Y Cross-Section Library for Use in Criticality Safety Analyses", NUREG/CR-6102 (ORNL/TM-12460) Oak Ridge National Laboratory, September 1994.

[4A.4] W.C. Jordan et al., "Validation of KENOV.a", CSD/TM-238, Martin Marietta Energy Systems, Inc., Oak Ridge National Laboratory, December 1986.

[4A.5] O.W. Hermann et al., "Validation of the Scale System for PWR Spent Fuel Isotopic Composition Analysis", ORNL-TM-12667, Oak Ridge National Laboratory, undated.

[4A.6] R.J. Larsen and M.L. Marx, An Introduction to Mathematical Statistics and its Applications, Prentice-Hall, 1986.

[4A.7] M.N. Baldwin et al., Critical Experiments Supporting Close Proximity Water Storage of Power Reactor Fuel, BAW-1484-7, Babcock and Wilcox Company, July 1979.

[4A.8] G.S. Hoovier et al., Critical Experiments Supporting Underwater Storage of Tightly Packed Configurations of Spent Fuel Pins, BAW-1645-4, Babcock & Wilcox Company, November 1991.

[4A.9] L.W. Newman et al., Urania Gadolinia: Nuclear Model Development and Critical Experiment Benchmark, BAW-1810, Babcock and Wilcox Company, April 1984.

[4A.10] J.C. Manaranche et al., "Dissolution and Storage Experimental Program with 4.75 w/o Enriched Uranium-Oxide Rods," Trans. Am. Nucl. Soc. 33: 362-364 (1979).

[4A.11] S.R. Bierman and E.D. Clayton, Criticality Experiments with Subcritical Clusters of 2.35 w/o and 4.31 w/o ^{235}U Enriched UO_2 Rods in Water with Steel Reflecting Walls, PNL-3602, Battelle Pacific Northwest Laboratory, April 1981.

[4A.12] S.R. Bierman et al., Criticality Experiments with Subcritical Clusters of 2.35 w/o and 4.31 w/o ^{235}U Enriched UO_2 Rods in Water with Uranium or Lead Reflecting Walls, PNL-3926, Battelle Pacific Northwest Laboratory, December, 1981.

[4A.13] S.R. Bierman et al., Critical Separation Between Subcritical Clusters of 4.31 w/o ^{235}U Enriched UO_2 Rods in Water with Fixed Neutron Poisons, PNL-2615, Battelle Pacific Northwest Laboratory, October 1977.

[4A.14] S.R. Bierman, Criticality Experiments with Neutron Flux Traps Containing Voids, PNL-7167, Battelle Pacific Northwest Laboratory, April 1990.

[4A.15] B.M. Durst et al., Critical Experiments with 4.31 wt % ^{235}U Enriched UO_2 Rods in Highly Borated Water Lattices, PNL-4267, Battelle Pacific Northwest Laboratory, August 1982.

[4A.16] S.R. Bierman, Criticality Experiments with Fast Test Reactor Fuel Pins in Organic Moderator, PNL-5803, Battelle Pacific Northwest Laboratory, December 1981.

[4A.17] E.G. Taylor et al., Saxton Plutonium Program Critical Experiments for the Saxton Partial Plutonium Core, WCAP-3385-54, Westinghouse Electric Corp., Atomic Power Division, December 1965.

[4A.18] M.G. Natrella, Experimental Statistics, National Bureau of Standards, Handbook 91, August 1963.

Table 4A.1

Summary of Criticality Benchmark Calculations

	Reference	Identification	Enrich.	Calculated k_{eff}		EALF [1] (eV)	
				MCNP4a	KENO5a	MCNP4a	KENO5a
1	B&W-1484 (4A.7)	Core I	2.46	0.9964 ± 0.0010	0.9898± 0.0006	0.1759	0.1753
2	B&W-1484 (4A.7)	Core II	2.46	1.0008 ± 0.0011	1.0015 ± 0.0005	0.2553	0.2446
3	B&W-1484 (4A.7)	Core III	2.46	1.0010 ± 0.0012	1.0005 ± 0.0005	0.1999	0.1939
4	B&W-1484 (4A.7)	Core IX	2.46	0.9956 ± 0.0012	0.9901 ± 0.0006	0.1422	0.1426
5	B&W-1484 (4A.7)	Core X	2.46	0.9980 ± 0.0014	0.9922 ± 0.0006	0.1513	0.1499
6	B&W-1484 (4A.7)	Core XI	2.46	0.9978 ± 0.0012	1.0005 ± 0.0005	0.2031	0.1947
7	B&W-1484 (4A.7)	Core XII	2.46	0.9988 ± 0.0011	0.9978 ± 0.0006	0.1718	0.1662
8	B&W-1484 (4A.7)	Core XIII	2.46	1.0020 ± 0.0010	0.9952 ± 0.0006	0.1988	0.1965
9	B&W-1484 (4A.7)	Core XIV	2.46	0.9953 ± 0.0011	0.9928 ± 0.0006	0.2022	0.1986
10	B&W-1484 (4A.7)	Core XV [11]	2.46	0.9910 ± 0.0011	0.9909 ± 0.0006	0.2092	0.2014
11	B&W-1484 (4A.7)	Core XVI [11]	2.46	0.9935 ± 0.0010	0.9889 ± 0.0006	0.1757	0.1713
12	B&W-1484 (4A.7)	Core XVII	2.46	0.9962 ± 0.0012	0.9942 ± 0.0005	0.2083	0.2021
13	B&W-1484 (4A.7)	Core XVIII	2.46	1.0036 ± 0.0012	0.9931 ± 0.0006	0.1705	0.1708

Table 4A.1

Summary of Criticality Benchmark Calculations

				Calculated k_{eff}		EALF [1] (eV)	
	Reference	Identification	Enrich.	MCNP4a	KENO5a	MCNP4a	KENO5a
14	B&W-1484 (4A.7)	Core XIX	2.46	0.9961 ± 0.0012	0.9971 ± 0.0005	0.2103	0.2011
15	B&W-1484 (4A.7)	Core XX	2.46	1.0008 ± 0.0011	0.9932 ± 0.0006	0.1724	0.1701
16	B&W-1484 (4A.7)	Core XXI	2.46	0.9994 ± 0.0010	0.9918 ± 0.0006	0.1544	0.1536
17	B&W-1645 (4A.8)	S-type Fuel, w/886 ppm B	2.46	0.9970 ± 0.0010	0.9924 ± 0.0006	1.4475	1.4680
18	B&W-1645 (4A.8)	S-type Fuel, w/746 ppm B	2.46	0.9990 ± 0.0010	0.9913 ± 0.0006	1.5463	1.5660
19	B&W-1645 (4A.8)	SO-type Fuel, w/1156 ppm B	2.46	0.9972 ± 0.0009	0.9949 ± 0.0005	0.4241	0.4331
20	B&W-1810 (4A.9)	Case 1 1337 ppm B	2.46	1.0023 ± 0.0010	NC	0.1531	NC
21	B&W-1810 (4A.9)	Case 12 1899 ppm B	2.46/4.02	1.0060 ± 0.0009	NC	0.4493	NC
22	French (4A.10)	Water Moderator 0 gap	4.75	0.9966 ± 0.0013	NC	0.2172	NC
23	French (4A.10)	Water Moderator 2.5 cm gap	4.75	0.9952 ± 0.0012	NC	0.1778	NC
24	French (4A.10)	Water Moderator 5 cm gap	4.75	0.9943 ± 0.0010	NC	0.1677	NC
25	French (4A.10)	Water Moderator 10 cm gap	4.75	0.9979 ± 0.0010	NC	0.1736	NC
26	PNL-3602 (4A.11)	Steel Reflector, 0 separation	2.35	NC	1.0004 ± 0.0006	NC	0.1018

Table 4A.1

Summary of Criticality Benchmark Calculations

				Calculated k_{eff}		EALF † (eV)	
	Reference	Identification	Enrich.	MCNP4a	KENO5a	MCNP4a	KENO5a
27	PNL-3602 (4A.11)	Steel Reflector, 1.321 cm sepn.	2.35	0.9980 ± 0.0009	0.9992 ± 0.0006	0.1000	0.0909
28	PNL-3602 (4A.11)	Steel Reflector, 2.616 cm sepn	2.35	0.9968 ± 0.0009	0.9964 ± 0.0006	0.0981	0.0975
29	PNL-3602 (4A.11)	Steel Reflector, 3.912 cm sepn.	2.35	0.9974 ± 0.0010	0.9980 ± 0.0006	0.0976	0.0970
30	PNL-3602 (4A.11)	Steel Reflector, infinite sepn.	2.35	0.9962 ± 0.0008	0.9939 ± 0.0006	0.0973	0.0968
31	PNL-3602 (4A.11)	Steel Reflector, 0 cm sepn.	4.306	NC	1.0003 ± 0.0007	NC	0.3282
32	PNL-3602 (4A.11)	Steel Reflector, 1.321 cm sepn.	4.306	0.9997 ± 0.0010	1.0012 ± 0.0007	0.3016	0.3039
33	PNL-3602 (4A.11)	Steel Reflector, 2.616 cm sepn.	4.306	0.9994 ± 0.0012	0.9974 ± 0.0007	0.2911	0.2927
34	PNL-3602 (4A.11)	Steel Reflector, 5.405 cm sepn.	4.306	0.9969 ± 0.0011	0.9951 ± 0.0007	0.2828	0.2860
35	PNL-3602 (4A.11)	Steel Reflector, Infinite sepn. ††	4.306	0.9910 ± 0.0020	0.9947 ± 0.0007	0.2851	0.2864
36	PNL-3602 (4A.11)	Steel Reflector, with Boral Sheets	4.306	0.9941 ± 0.0011	0.9970 ± 0.0007	0.3135	0.3150
37	PNL-3926 (4A.12)	Lead Reflector, 0 cm sepn.	4.306	NC	1.0003 ± 0.0007	NC	0.3159
38	PNL-3926 (4A.12)	Lead Reflector, 0.55 cm sepn.	4.306	1.0025 ± 0.0011	0.9997 ± 0.0007	0.3030	0.3044
39	PNL-3926 (4A.12)	Lead Reflector, 1.956 cm sepn.	4.306	1.0000 ± 0.0012	0.9985 ± 0.0007	0.2883	0.2930

Table 4A.1

Summary of Criticality Benchmark Calculations

				Calculated k_{eff}		EALF † (eV)	
	Reference	Identification	Enrich.	MCNP4a	KENO5a	MCNP4a	KENO5a
40	PNL-3926 (4A.12)	Lead Reflector, 5.405 cm sepn.	4.306	0.9971 ± 0.0012	0.9946 ± 0.0007	0.2831	0.2854
41	PNL-2615 (4A.13)	Experiment 004/032 - no absorber	4.306	0.9925 ± 0.0012	0.9950 ± 0.0007	0.1155	0.1159
42	PNL-2615 (4A.13)	Experiment 030 - Zr plates	4.306	NC	0.9971 ± 0.0007	NC	0.1154
43	PNL-2615 (4A.13)	Experiment 013 - Steel plates	4.306	NC	0.9965 ± 0.0007	NC	0.1164
44	PNL-2615 (4A.13)	Experiment 014 - Steel plates	4.306	NC	0.9972 ± 0.0007	NC	0.1164
45	PNL-2615 (4A.13)	Exp. 009 1.05% Boron-Steel plates	4.306	0.9982 ± 0.0010	0.9981 ± 0.0007	0.1172	0.1162
46	PNL-2615 (4A.13)	Exp. 012 1.62% Boron-Steel plates	4.306	0.9996 ± 0.0012	0.9982 ± 0.0007	0.1161	0.1173
47	PNL-2615 (4A.13)	Exp. 031 - Boral plates	4.306	0.9994 ± 0.0012	0.9969 ± 0.0007	0.1165	0.1171
48	PNL-7167 (4A.14)	Experiment 214R - with flux trap	4.306	0.9991 ± 0.0011	0.9956 ± 0.0007	0.3722	0.3812
49	PNL-7167 (4A.14)	Experiment 214V3 - with flux trap	4.306	0.9969 ± 0.0011	0.9963 ± 0.0007	0.3742	0.3826
50	PNL-4267 (4A.15)	Case 173 - 0 ppm B	4.306	0.9974 ± 0.0012	NC	0.2893	NC
51	PNL-4267 (4A.15)	Case 177 - 2550 ppm B	4.306	1.0057 ± 0.0010	NC	0.5509	NC
52	PNL-5803 (4A.16)	MOX Fuel - Type 3.2 Exp. 21	20% Pu	1.0041 ± 0.0011	1.0046 ± 0.0006	0.9171	0.8868

Table 4A.1

Summary of Criticality Benchmark Calculations

	Reference	Identification	Enrich.	Calculated k_{eff}		EALF † (eV)	
				MCNP4a	KENO5a	MCNP4a	KENO5a
53	PNL-5803 (4A.16)	MOX Fuel - Type 3.2 Exp. 43	20% Pu	1.0058 ± 0.0012	1.0036 ± 0.0006	0.2968	0.2944
54	PNL-5803 (4A.16)	MOX Fuel - Type 3.2 Exp. 13	20% Pu	1.0083 ± 0.0011	0.9989 ± 0.0006	0.1665	0.1706
55	PNL-5803 (4A.16)	MOX Fuel - Type 3.2 Exp. 32	20% Pu	1.0079 ± 0.0011	0.9966 ± 0.0006	0.1139	0.1165
56	WCAP-3385 (4A.17)	Saxton Case 52 PuO2 0.52" pitch	6.6% Pu	0.9996 ± 0.0011	1.0005 ± 0.0006	0.8665	0.8417
57	WCAP-3385 (4A.17)	Saxton Case 52 U 0.52" pitch	5.74	1.0000 ± 0.0010	0.9956 ± 0.0007	0.4476	0.4580
58	WCAP-3385 (4A.17)	Saxton Case 56 PuO2 0.56" pitch	6.6% Pu	1.0036 ± 0.0011	1.0047 ± 0.0006	0.5289	0.5197
59	WCAP-3385 (4A.17)	Saxton Case 56 borated PuO2	6.6% Pu	1.0008 ± 0.0010	NC	0.6389	NC
60	WCAP-3385 (4A.17)	Saxton Case 56 U 0.56" pitch	5.74	0.9994 ± 0.0011	0.9967 ± 0.0007	0.2923	0.2954
61	WCAP-3385 (4A.17)	Saxton Case 79 PuO2 0.79" pitch	6.6% Pu	1.0063 ± 0.0011	1.0133 ± 0.0006	0.1520	0.1555
62	WCAP-3385 (4A.17)	Saxton Case 79 U 0.79" pitch	5.74	1.0039 ± 0.0011	1.0008 ± 0.0006	0.1036	0.1047

Notes: NC stands for not calculated.

† EALF is the energy of the average lethargy causing fission.

†† These experimental results appear to be statistical outliers (>3σ) suggesting the possibility of unusually large experimental error. Although they could justifiably be excluded, for conservatism, they were retained in determining the calculational basis.

Table 4A.2

COMPARISON OF MCNP4a AND KENO5a CALCULATED REACTIVITIES[†] FOR VARIOUS ENRICHMENTS

Enrichment	Calculated $k_{eff} \pm 1\sigma$	
	MCNP4a	KENO5a
3.0	0.8465 ± 0.0011	0.8478 ± 0.0004
3.5	0.8820 ± 0.0011	0.8841 ± 0.0004
3.75	0.9019 ± 0.0011	0.8987 ± 0.0004
4.0	0.9132 ± 0.0010	0.9140 ± 0.0004
4.2	0.9276 ± 0.0011	0.9237 ± 0.0004
4.5	0.9400 ± 0.0011	0.9388 ± 0.0004

[†] Based on the GE 8x8R fuel assembly.

Table 4A.3

MCNP4a CALCULATED REACTIVITIES FOR
CRITICAL EXPERIMENTS WITH NEUTRON ABSORBERS

Ref.	Experiment		Δk Worth of Absorber	MCNP4a Calculated k_{eff}	EALF † (eV)
4A.13	PNL-2615	Boral Sheet	0.0139	0.9994±0.0012	0.1165
4A.7	B&W-1484	Core XX	0.0165	1.0008±0.0011	0.1724
4A.13	PNL-2615	1.62% Boron-steel	0.0165	0.9996±0.0012	0.1161
4A.7	B&W-1484	Core XIX	0.0202	0.9961±0.0012	0.2103
4A.7	B&W-1484	Core XXI	0.0243	0.9994±0.0010	0.1544
4A.7	B&W-1484	Core XVII	0.0519	0.9962±0.0012	0.2083
4A.11	PNL-3602	Boral Sheet	0.0708	0.9941±0.0011	0.3135
4A.7	B&W-1484	Core XV	0.0786	0.9910±0.0011	0.2092
4A.7	B&W-1484	Core XVI	0.0845	0.9935±0.0010	0.1757
4A.7	B&W-1484	Core XIV	0.1575	0.9953±0.0011	0.2022
4A.7	B&W-1484	Core XIII	0.1738	1.0020±0.0011	0.1988
4A.14	PNL-7167	Expt 214R flux trap	0.1931	0.9991±0.0011	0.3722

†EALF is the energy of the average lethargy causing fission.

Table 4A.4

COMPARISON OF MCNP4a AND KENO5a
CALCULATED REACTIVITIES† FOR VARIOUS ^{10}B LOADINGS

^{10}B, g/cm^2	Calculated $k_{eff} \pm 1\sigma$	
	MCNP4a	KENO5a
0.005	1.0381 ± 0.0012	1.0340 ± 0.0004
0.010	0.9960 ± 0.0010	0.9941 ± 0.0004
0.015	0.9727 ± 0.0009	0.9713 ± 0.0004
0.020	0.9541 ± 0.0012	0.9560 ± 0.0004
0.025	0.9433 ± 0.0011	0.9428 ± 0.0004
0.03	0.9325 ± 0.0011	0.9338 ± 0.0004
0.035	0.9234 ± 0.0011	0.9251 ± 0.0004
0.04	0.9173 ± 0.0011	0.9179 ± 0.0004

† Based on a 4.5% enriched GE 8x8R fuel assembly.

Table 4A.5

CALCULATIONS FOR CRITICAL EXPERIMENTS WITH THICK LEAD AND STEEL REFLECTORS†

Ref.	Case	E, wt%	Separation, cm	MCNP4a k_{eff}	KENO5a k_{eff}
4A.11	Steel Reflector	2.35	1.321	0.9980±0.0009	0.9992±0.0006
		2.35	2.616	0.9968±0.0009	0.9964±0.0006
		2.35	3.912	0.9974±0.0010	0.9980±0.0006
		2.35	∞	0.9962±0.0008	0.9939±0.0006
4A.11	Steel Reflector	4.306	1.321	0.9997±0.0010	1.0012±0.0007
		4.306	2.616	0.9994±0.0012	0.9974±0.0007
		4.306	3.405	0.9969±0.0011	0.9951±0.0007
		4.306	∞	0.9910±0.0020	0.9947±0.0007
4A.12	Lead Reflector	4.306	0.55	1.0025±0.0011	0.9997±0.0007
		4.306	1.956	1.0000±0.0012	0.9985±0.0007
		4.306	5.405	0.9971±0.0012	0.9946±0.0007

† Arranged in order of increasing reflector-fuel spacing.

Table 4A.6

CALCULATIONS FOR CRITICAL EXPERIMENTS WITH VARIOUS SOLUBLE BORON CONCENTRATIONS

Reference	Experiment	Boron Concentration, ppm	Calculated k_{eff}	
			MCNP4a	KENO5a
4A.15	PNL-4267	0	0.9974 ± 0.0012	-
4A.8	B&W-1645	886	0.9970 ± 0.0010	0.9924 ± 0.0006
4A.9	B&W-1810	1337	1.0023 ± 0.0010	-
4A.9	B&W-1810	1899	1.0060 ± 0.0009	-
4A.15	PNL-4267	2550	1.0057 ± 0.0010	-

Table 4A.7

CALCULATIONS FOR CRITICAL EXPERIMENTS WITH MOX FUEL

Reference	Case†	MCNP4a		KENO5a	
		k_{eff}	EALF††	k_{eff}	EALF††
PNL-5803 [4A.16]	MOX Fuel - Exp. No. 21	1.0041±0.0011	0.9171	1.0046±0.0006	0.8868
	MOX Fuel - Exp. No. 43	1.0058±0.0012	0.2968	1.0036±0.0006	0.2944
	MOX Fuel - Exp. No. 13	1.0083±0.0011	0.1665	0.9989±0.0006	0.1706
	MOX Fuel - Exp. No. 32	1.0079±0.0011	0.1139	0.9966±0.0006	0.1165
WCAP-3385-54 [4A.17]	Saxton @ 0.52" pitch	0.9996±0.0011	0.8665	1.0005±0.0006	0.8417
	Saxton @ 0.56" pitch	1.0036±0.0011	0.5289	1.0047±0.0006	0.5197
	Saxton @ 0.56" pitch borated	1.0008±0.0010	0.6389	NC	NC
	Saxton @ 0.79" pitch	1.0063±0.0011	0.1520	1.0133±0.0006	0.1555

Note: NC stands for not calculated

† Arranged in order of increasing lattice spacing.

†† EALF is the energy of the average lethargy causing fission.

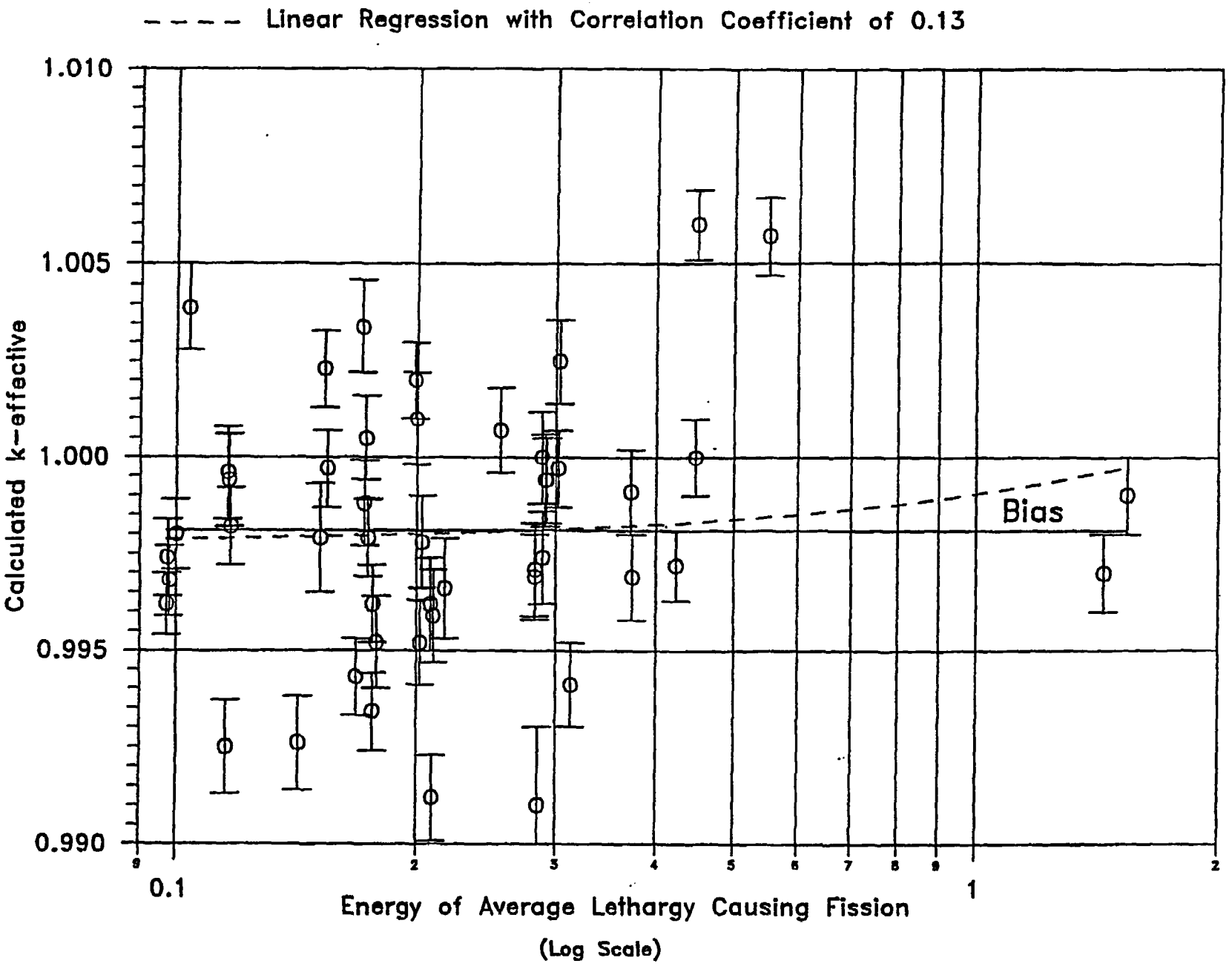

FIGURE 4A.1 MCNP CALCULATED k-eff VALUES for VARIOUS VALUES OF THE SPECTRAL INDEX

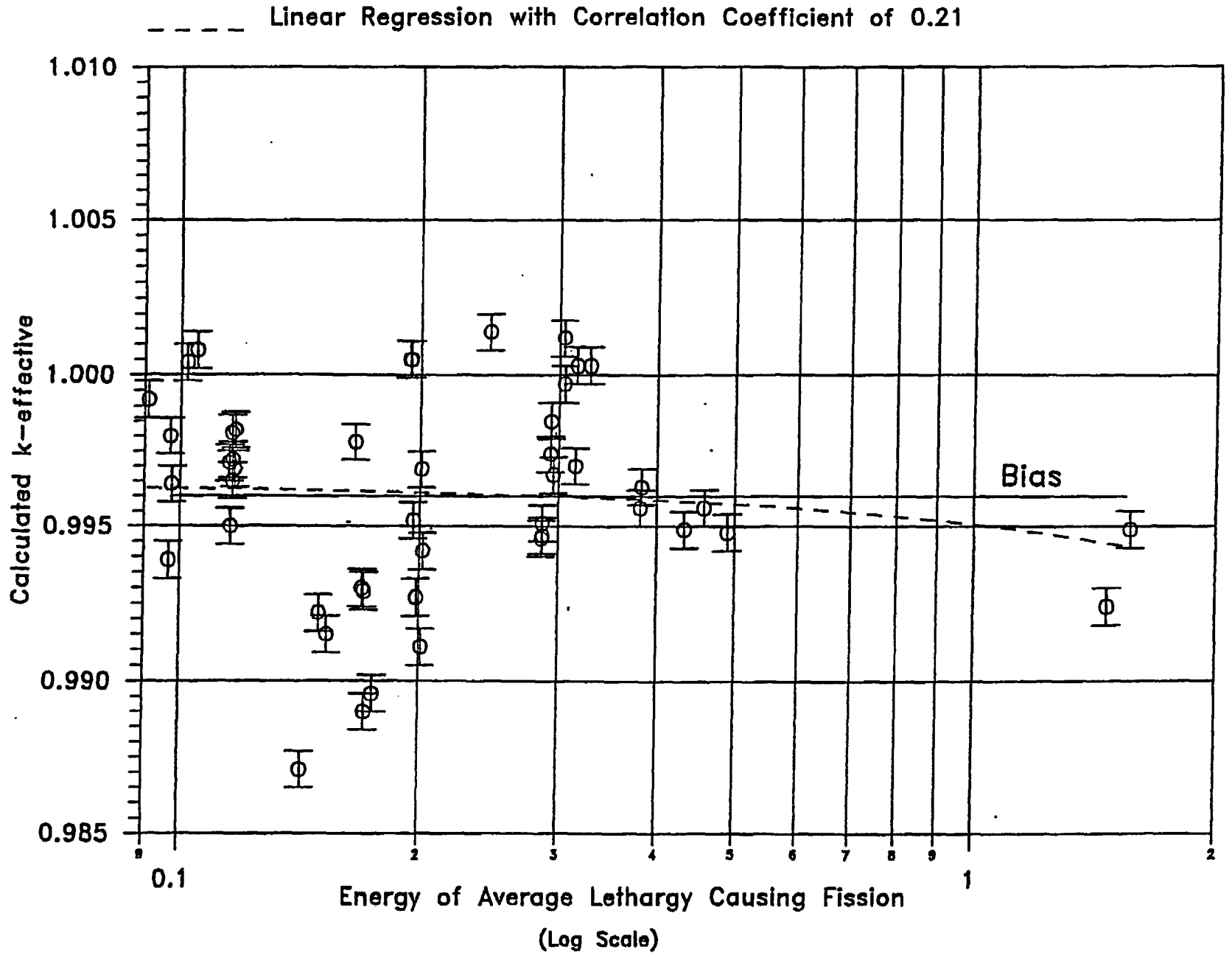

FIGURE 4A.2 KENO5a CALCULATED k-eff VALUES FOR VARIOUS VALUES OF THE SPECTRAL INDEX

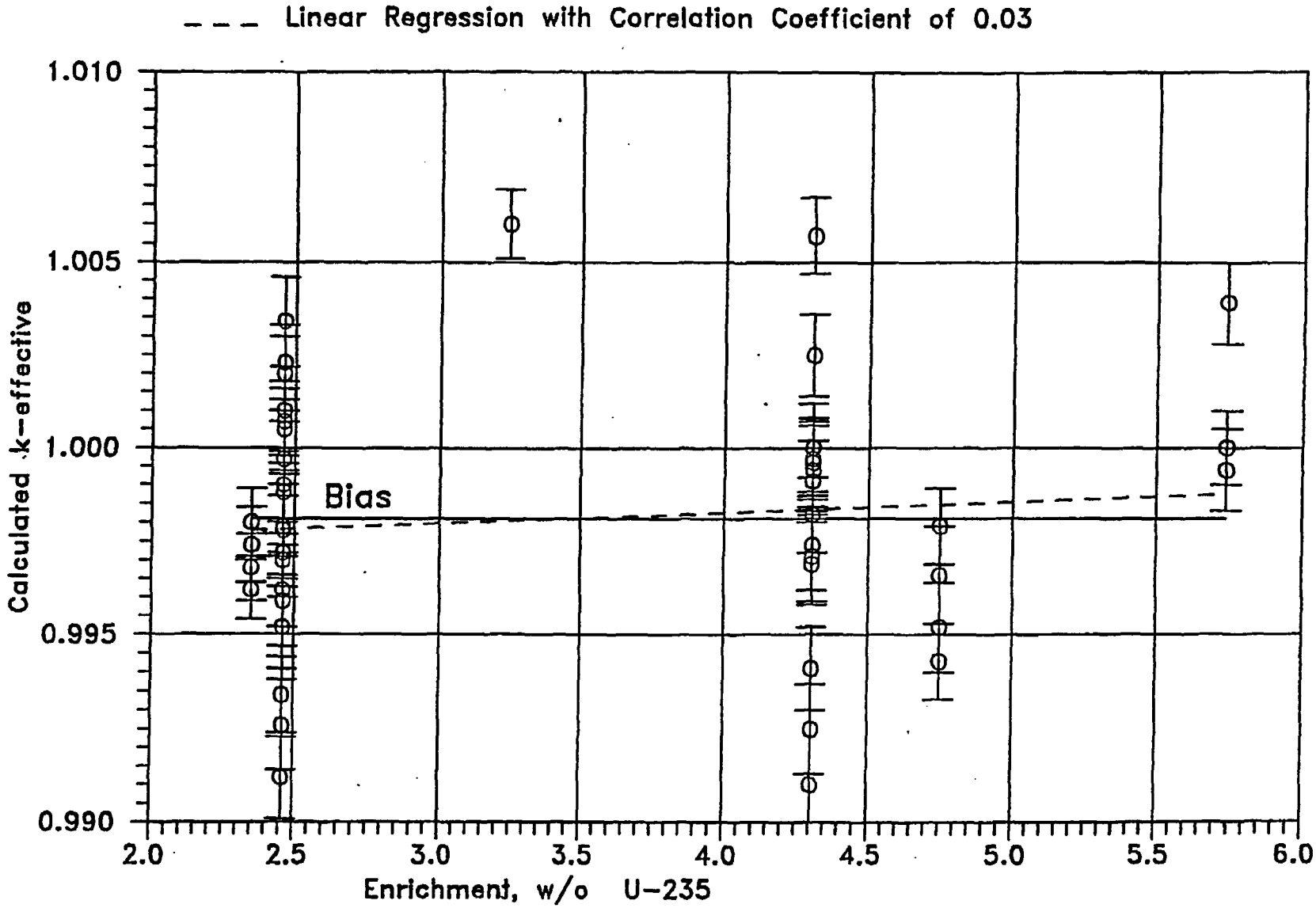

FIGURE 4A.3 MCNP CALCULATED k-eff VALUES AT VARIOUS U-235 ENRICHMENTS

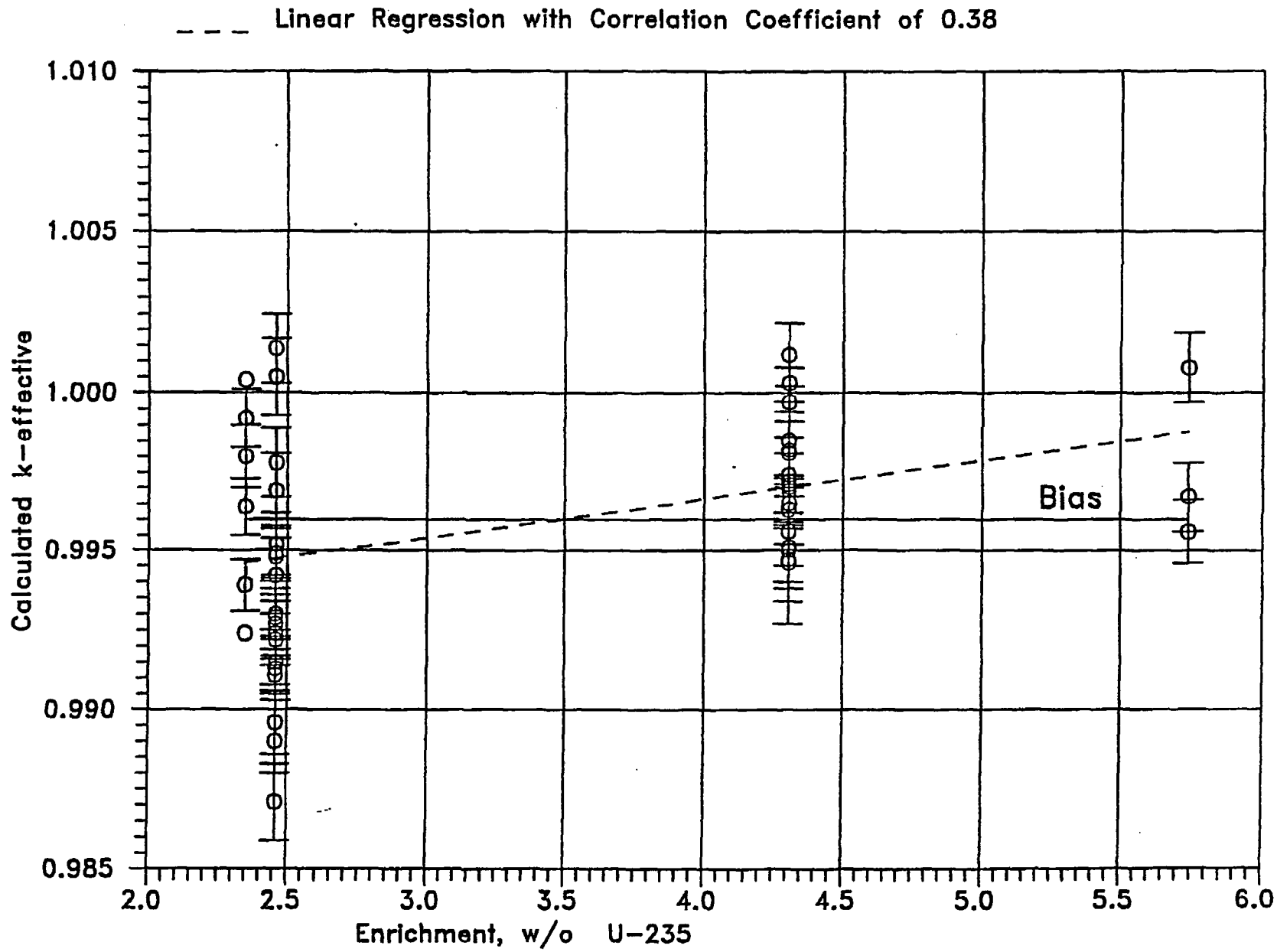

FIGURE 4A.4 KENO CALCULATED k-eff VALUES AT VARIOUS U-235 ENRICHMENTS

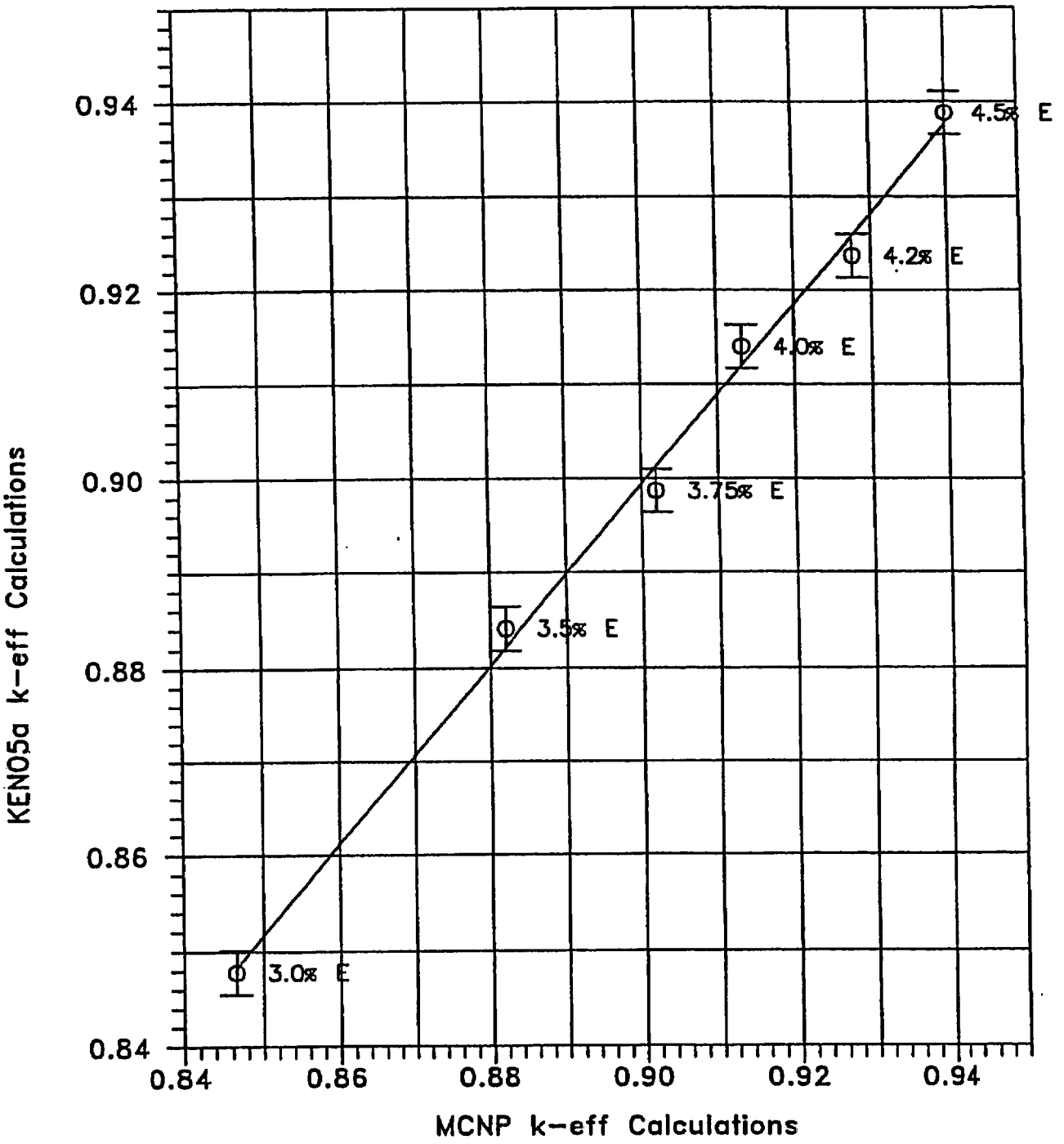

FIGURE 4A.5 COMPARISON OF MCNP AND KENO5A CALCULATIONS FOR VARIOUS FUEL ENRICHMENTS

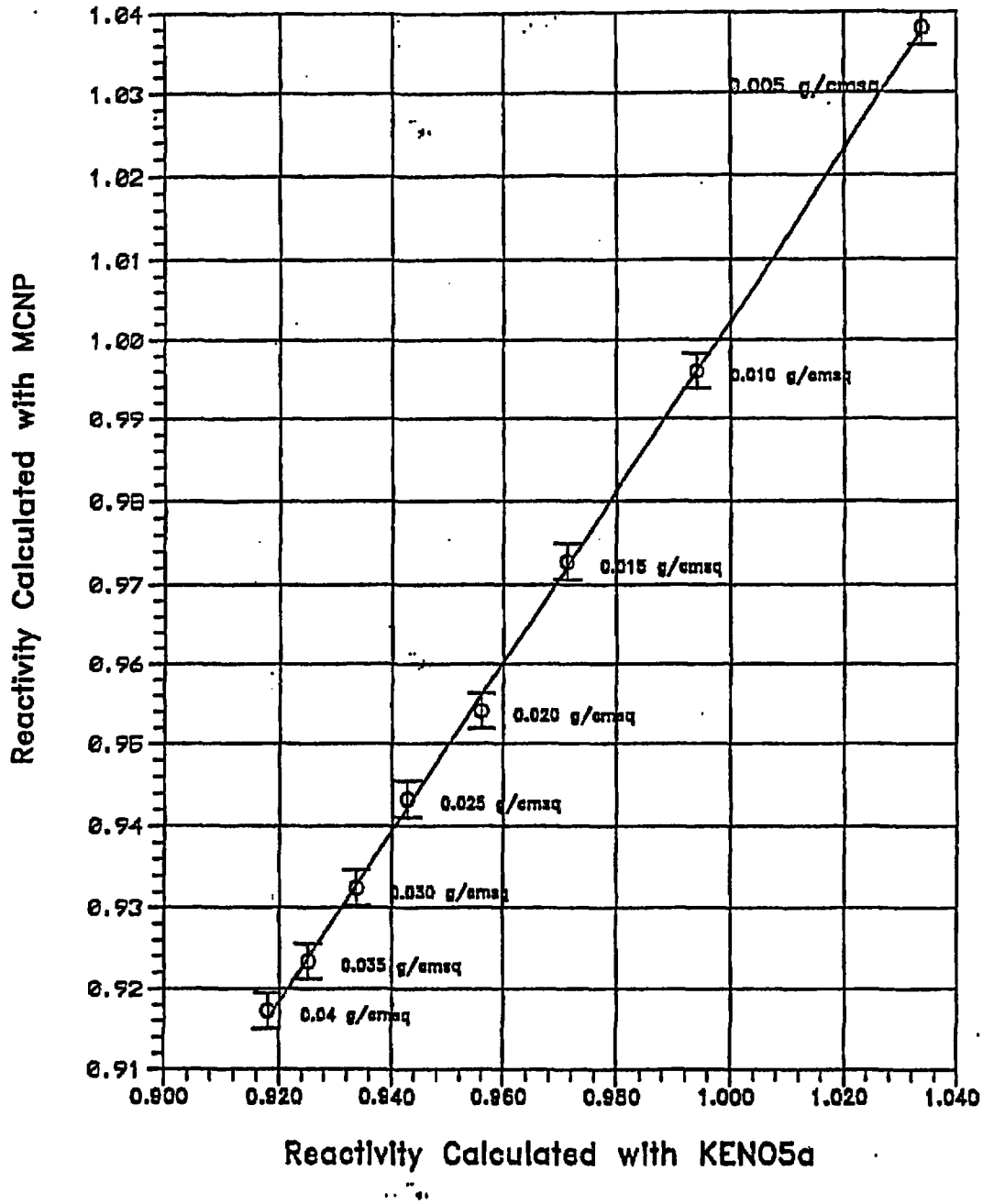

FIGURE 4A.6 : COMPARISON OF MCNP AND KENO5a CALCULATIONS FOR VARIOUS BORON-10 AREAL DENSITIES

5.0 THERMAL-HYDRAULIC CONSIDERATIONS

5.1 INTRODUCTION

This section provides a summary of the thermal-hydraulic analyses performed to demonstrate compliance of the SFP and its attendant cooling system with the provisions of USNRC Standard Review Plan (SRP) 9.1.3 (Spent Fuel Pool Cooling and Cleanup System, Rev. 1, July 1981) and Section III of the USNRC "OT Position Paper for Review and Acceptance of Spent Fuel Storage and Handling Applications," (April 14, 1978). Similar methods of thermal-hydraulic analysis have been used in the licensing evaluations for other SFP capacity expansion projects.

The thermal-hydraulic qualification analyses for the modified rack array may be broken down into the following categories:

i. Evaluation of bounding maximum decay heat versus time profiles, used as input to subsequent analyses.

ii. Evaluation of loss-of-forced cooling scenarios, to establish minimum times to perform corrective actions and the associated makeup water requirements.

iii. Determination of the maximum local water temperature, at the instant when the pool decay heat reaches its maximum value, to establish that localized boiling in the Spent Fuel Storage Racks (SFSRs) is not possible while forced cooling is operating. The bulk pool temperature is postulated to be at the maximum limit.

iv. Evaluation of the maximum fuel rod cladding temperature, at the instant when the pool decay heat reaches its maximum value, to establish that nucleate boiling is not possible while forced cooling is operating. The bulk pool temperature is postulated to be at the maximum limit.

The following sections present plant system descriptions, analysis methodologies and assumptions, a synopsis of the input data employed, and summaries of the calculated results.

5.2 COOLING SYSTEM DESCRIPTION

The Spent Fuel Cooling (SFC) System is designed to maintain the water quality and clarity and to remove the decay heat from the stored fuel in the SFP. It is designed to maintain the SFP water at less than or equal to approximately 150°F. This is accomplished by recirculating spent fuel coolant water from the SFP through the pumps and coolers and back to the pool. The SFP coolers reject heat to the nuclear intermediate cooling water system, which subsequently rejects its heat to the service water system. The spent fuel coolant pumps take suction from the SFP and deliver the water through the tube side of two coolers arranged in parallel back to the pool.

In addition to its primary function, a bypass purification loop is provided to maintain the purity of the water in the SFP. This loop is also utilized to purify the water in the Borated Water Storage Tank (BWST) following refueling and to maintain clarity in the fuel transfer canal during refueling. Water from the BWST or fuel transfer canal can be purified by using the borated water recirculation pump. The system also provides for filling the fuel transfer canal, the incore instrumentation tank, and the cask loading area from the BWST.

The SFP is provided with a makeup system design, which meets the intent of Safety Guide 13. That is, the BWST is a Seismic Category 1 vessel; all connecting piping is located in a Seismic Category 1 structure; a backup system for supplying water to the pool is provided through a temporary connection to the Seismic Category 1 service water system; and, there is sufficient time to rig a temporary makeup water supply to the pool in the event of failure of the normal source. The service water system can be supplied from either Lake Dardanelle or the emergency cooling pond.

5.3 SPENT FUEL POOL DECAY HEAT LOADS

The decay heat in the SFP is generated in the spent fuel assemblies stored therein. In order to conservatively simplify the decay heat calculations, the total decay heat is considered as coming from two different groups of assemblies:

i. Fuel assemblies from previous offloads already stored in the SFP
ii. Fuel assemblies that are being offloaded from the reactor to the SFP

The fuel assemblies in the first group are referred to as previously offloaded fuel. Over the relatively short transient evaluation periods of this report the heat generation rate of these assemblies reduces very slowly with time, due to the exponential nature of radioactive decay and their relatively long decay periods. The decay heat contribution of these assemblies can therefore be conservatively treated as constant, neglecting any reduction in their decay heat contribution during the evaluation period. The fuel assemblies in the second group are referred to as recently offloaded fuel. The heat generation rate of these assemblies reduces rapidly with time, so the decay heat contribution of these assemblies is treated as time varying. The following equation defines the total decay heat generation in the SFP.

$$Q_{GEN}(\tau) = Q_P + F(\tau) \times Q_R(\tau) \qquad (5\text{-}1)$$

where:

$Q_{GEN}(\tau)$ is the total time-varying decay heat generation rate in SFP, Btu/hr
Q_P is the decay heat contribution of the previously offloaded fuel, Btu/hr
$F(\tau)$ is the fraction of the recently offloaded fuel transferred to the SFP
$Q_R(\tau)$ is the decay heat contribution of the recently offloaded fuel, Btu/hr
τ is the fuel decay time after reactor shutdown, hrs

Prior to the start of fuel transfer from the reactor to the SFP, $F(\tau)$ is equal to zero and the total decay heat in the SFP will be equal to the invariant portion Q_P. During the fuel transfer, $F(\tau)$ will increase linearly from zero to one, and the total decay heat in the SFP will increase to $Q_P+Q_R(\tau)$. Following the completion of fuel transfer, the total decay heat in the SFP will decrease as $Q_R(\tau)$ decreases.

The decay heat contributions of both the previously and recently offloaded fuel are determined using the Holtec QA validated computer program DECOR [5.3.1]. This computer program incorporates the Oak Ridge National Laboratory (ORNL) ORIGEN2 computer code [5.3.2] for

performing decay heat calculations. The use of ORIGEN2 code has previously been accepted by the NRC for SFP decay heat calculations on multiple dockets [e.g. USNRC Dockets 50-461 and 50-395].

Based on the input data provided in Tables 5.3.1 and 5.3.2, the fuel decay heat is determined for the following two offload scenarios:

1. Partial Core Offload - A refueling batch of 76 assemblies is offloaded from the plant's reactor into the SFP, completely filling all available storage locations. The total SFP inventory prior to the offload is 912 fuel assemblies, for a final post-offload inventory of 988 fuel assemblies. This slightly exceeds the storage capacity of the ANO-1 SFP (and the ANO-1 TS 4.3.3 limit of 968 assemblies) and is used for calculation of decay heat loads, which is conservative.

2. Full Core Offload - The full core of 177 assemblies is offloaded from the plant's reactor into the SFP, completely filling all available storage locations. The total SFP inventory prior to the offload is 836 fuel assemblies, for a final post-offload inventory of 1013 fuel assemblies. This slightly exceeds the storage capacity of the ANO-1 SFP (and the ANO-1 TS 4.3.3 limit of 968 assemblies) and is used for calculation of decay heat loads, which is conservative.

There are two types of fuel assemblies to be stored in the SFP: non-high thermal performance and high thermal performance (HTP) assemblies. While most of the differences between these two assembly types are minor from a heat-generation standpoint, the HTP fuel contains 10 kg more uranium that will result in higher decay heat loads. As such, all fuel assemblies discharged from 2007 onward are assumed to be the higher heat generating HTP fuel.

5.4 MINIMUM TIME-TO-BOIL AND MAXIMUM BOILOFF RATE

The following conservatisms and assumptions are applied in the time-to-boil and boiloff rate calculations:

- The initial SFP bulk temperature is assumed to be equal to the bulk temperature limit of 150 °F for the full core offload and 120 °F for the partial core offload.

- The thermal inertia (thermal capacity) of the SFP is based on the net water volume only. This conservatively neglects the considerable thermal inertia of the fuel assemblies, stainless steel racks and stainless steel SFP liners.

- During the loss of forced cooling evaluations, it is assumed that makeup water is not available. This minimizes the thermal capacity of the SFP as water is boiled off, thus increasing the water level drop rate.

- The loss of forced cooling is assumed to occur coincident with the peak SFP bulk temperature and the maximum pool decay heat. Maximizing the initial temperature and the pool decay heat conservatively minimizes the calculated time-to-boil.

The governing enthalpy balance equation for this condition, subject to these conservative assumptions, can be written as:

$$C(\tau)\frac{dT}{d\tau} = Q_{gen}(\tau + \tau_0) \tag{5-2}$$

where:

$C(\tau)$ = Time-varying SFP thermal capacity (BTU/°F)
τ = Time after cooling is lost (hr)
τ_0 = Loss of cooling time after shutdown (hr)
T=Pool water temperature, (°F)

Equation 5-2 is solved to obtain the bulk pool temperature as a function of time, the time-to-boil, boil-off rate and water depth versus time. Once boiling begins, the ongoing evaporation of water will cause the water level of the SFP to decrease. The maximum water boil-off rate is determined by dividing the heat load by the latent heat of water at 212°F. The time required to drain the SFP to the top of the fuel racks is determined by computing the amount of water above the racks and dividing by the boil-off rate. The major input values for these analyses are summarized in Table 5.4.1.

5.5 MAXIMUM SFP LOCAL WATER TEMPERATURE

In order to determine an upper bound on the maximum SFP local water temperature, a series of conservative assumptions are made. The most important of these assumptions are:

- The walls and floor of the SFP are all modeled as adiabatic surfaces, thereby neglecting conduction heat loss through these items. This conservatively maximizes the net heat load, thereby maximizing both global and local temperatures.
- Heat losses by thermal radiation and natural convection from the hot SFP surface to the environment are neglected.
- No downcomer flow is assumed to exist between the rack modules.
- The hydraulic resistance parameters for the rack cells, permeability and inertial resistance, are conservatively adjusted by 10%. The conservatism bounds any small deviations in fuel assembly and rack geometry.

- The bottom plenum heights used in the model are less than the actual heights. This ensures that the effects of additional flow restrictions around rack pedestals and bearing pads are bounded in the model.

- The hydraulic resistance of every SFSR cell includes the effects of blockage due to an assumed dropped fuel assembly lying horizontally on top of the SFSRs. This conservatively increases the total rack cell hydraulic resistance and bounds the thermal-hydraulic effects of a fuel assembly dropped anywhere in the spent fuel storage area.

The objective of this study is to demonstrate that the thermal-hydraulic criterion of ensuring local subcooled conditions in the SFP is met for all postulated fuel offload scenarios. The local thermal-hydraulic analysis is performed such that slight fuel assembly variations are bounded. An outline of the Computational Fluid Dynamics (CFD) approach is described in the following.

There are several significant geometric and thermal-hydraulic features of the ANO-1 SFP that need to be considered for a rigorous CFD analysis. From a fluid flow modeling standpoint, there are two regions to be considered. One region is the SFP bulk region where the classical Navier-Stokes equations [5.5.1] are solved, with turbulence effects included. The other region is the SFSRs containing heat generating fuel assemblies, located near the bottom of the SFP. In this region, water flow is directed vertically upwards due to buoyancy forces through relatively small flow channels formed by the B&W 15x15 fuel assemblies in each SFSR cell. This situation is modeled as a porous region with pressure drop in the flowing fluid governed by Darcy's Law as:

$$\frac{\partial P}{\partial X_i} = -\frac{\mu}{K(i)} V_i - C \rho |V| \frac{V_i}{2} \qquad (5\text{-}3)$$

where $\partial P/\partial X_i$ is the pressure gradient, $K(i)$, V_i and C are the corresponding permeability, velocity and inertial resistance parameters, ρ is the fluid density, and μ is the fluid viscosity. These terms are added as sink terms to the classic Navier-Stokes equations. The permeability and inertial resistance parameters for the rack cells loaded with B&W 15x15 fuel assemblies are determined based on friction factor correlations for the laminar flow conditions that would exist due to the low buoyancy induced velocities and the small size of the flow channels.

The ANO-1 SFP geometry requires an adequate portrayal of both large scale and small scale features, spatially distributed heat sources in the SFSRs and water inlet/outlet piping. Relatively cooler bulk water normally flows down between the perimeter of the fuel rack array and wall

liner, a clearance known as the downcomer. Near the bottom of the racks the flow turns from a vertical to horizontal direction into the bottom plenum, supplying cooling water to the rack cells. Heated water flowing out of the top of the racks mixes with the bulk water. An adequate modeling of these features in the CFD program involves meshing the large scale bulk SFP region and small scale downcomer and bottom plenum regions with sufficient number of computational cells to capture both the global and local features of the flow field.

The distributed heat sources in the SFP racks are modeled by identifying distinct heat generation zones considering recently offloaded fuel, bounding peaking effects, and the presence of background decay heat from previous offloads. Two heat generating zones are modeled. The first consists of background fuel from previous offloads. The second zone consists of fuel from recently offloaded fuel assemblies. This is a conservative model, since all of the hot fuel assemblies from the recent offload are placed in a contiguous area. A uniformly distributed heat generation rate was applied throughout each distinct zone (i.e., there were no variations in heat generation rate within a single zone).

The CFD analysis was performed on the commercially available FLUENT [5.5.2] Computational Fluid Dynamics program, which has been benchmarked under Holtec's QA program. The FLUENT code enables buoyancy flow and turbulence effects to be included in the CFD analysis. Buoyancy forces are included by specifying a temperature-dependent density for water and applying an appropriate gravity vector. Turbulence effects are modeled by relating time-varying Reynolds' Stresses to the mean bulk flow quantities with the standard k-ε turbulence model.

Some of the major input values for this analysis are summarized in Table 5.5.1. An isometric view of the assembled CFD model is presented in Figure 5.5.1.

5.6 FUEL ROD CLADDING TEMPERATURE

The maximum fuel rod cladding temperature is determined to establish that nucleate boiling is not possible while forced cooling is operating. This requires demonstrating that the highest fuel rod cladding temperatures are less than the local saturation temperature of the adjacent SFP water. The maximum fuel cladding superheat above the local water temperature is calculated for two different peak fuel rod heat emission rates.

A fuel rod can produce F_z times the average heat emission rate over a small length, where F_z is the axial peaking factor. The axial heat distribution in a rod is generally a maximum in the central region, and tapers off at its two extremities. Thus, peak cladding heat flux over an infinitesimal rod section is given by the equation:

$$q_c = \frac{Q \times F_z}{A_c} \tag{5-4}$$

where Q is the rod average heat emission and A_c is the total cladding external heat transfer area in the active fuel length region. The axial peaking factor is given in Table 5.5.1.

As described previously, the maximum local water temperature was computed. Within each fuel assembly sub-channel, water is continuously heated by the cladding as it moves axially upwards under laminar flow conditions. Rohsenow and Hartnett [5.6.1] report a Nusselt-number for laminar flow heat transfer in a heated channel. The film temperature driving force (ΔT_f) at the peak cladding flux location is calculated as follows:

$$\Delta T_f = \frac{q_c}{h_f}$$
$$h_f = Nu\frac{Kw}{D_h} \tag{5-5}$$

where h_f is the waterside film heat transfer coefficient, D_h is sub-channel hydraulic diameter, Kw is water thermal conductivity and Nu is the Nusselt number for laminar flow heat transfer.

In order to introduce some additional conservatism in the analysis, we assume that the fuel cladding has a crud deposit resistance R_c (equal to 0.0005 ft^2-hr-°R/Btu) that covers the entire surface. Thus, including the temperature drop across the crud resistance, the cladding to water local temperature difference (ΔT_c) is given by the equation $\Delta T_c = \Delta T_f + R_c \times q_c$.

5.7 RESULTS

This section contains results from the analyses performed for the postulated offload scenarios.

5.7.1 Decay Heat

For the offload scenarios described in Section 5.3, the calculated SFP decay heat loads are summarized in Table 5.7.1. Given the conservatisms incorporated into the calculations, actual decay heat loads will be lower than these calculated values. Figures 5.7.1 and 5.7.2 each present profiles of net decay heat load versus time for the evaluated transient scenarios.

5.7.2 Minimum Time-to-Boil and Maximum Boiloff Rate

For the offload/cooling described in Section 5.4, the calculated times-to-boil and maximum boil-off rates are summarized in Table 5.7.2. These results show that, in the extremely unlikely event of a failure of forced cooling to the SFP, there would be at least 3.18 hours available for corrective actions prior to SFP boiling. Given the conservatisms incorporated into the calculations, actual times-to-boil will be higher than these calculated values. It is noted that a complete failure of forced cooling is extremely unlikely. The maximum water boiloff rate is less than 87 gpm.

5.7.3 Local Water and Fuel Cladding Temperatures

Consistent with our approach to make conservative assessments of temperature, the local water temperature calculations described in Section 5.5 are performed for a SFP with a total decay heat generation equal to the calculated decay heat load coincident with the maximum SFP bulk temperature. Thus, the local water temperature evaluation is a calculation of the temperature increment over the theoretical spatially uniform value due to local hot spots (due to the presence of highly heat emissive fuel assemblies). As described in Subsection 5.6, the peak fuel clad superheats (i.e., the maximum clad-to-local water temperature difference) are determined. The resultant bounding superheat values were used to calculate bounding maximum fuel clad temperatures.

The numeric results of the maximum local water temperature and the bounding fuel cladding temperature evaluations are presented in Table 5.7.3. Figure 5.7.3 presents converged temperature contours in a vertical slice through the hot fuel region. Figure 5.7.4 presents converged velocity vectors in a vertical slice through the hot fuel region.

Both the maximum local water temperatures and the bounding fuel cladding temperatures are substantially lower than the 240°F local boiling temperature at the top of the SFSRs. These results demonstrate that boiling, including nucleate boiling on clad surfaces, cannot occur anywhere within the ANO-1 SFP.

Under a postulated accident scenario of the loss of all cooling, the water temperature will rise. Assuming a temperature of 212°F at the inlet to the rack cells, and conservatively using the bounding bulk-to-local and local-to-clad temperature differences from Table 5.7.3, the maximum possible cladding temperature will be 261.5°F, which is greater than the saturation temperature at the top of the active fuel length. Due to the low maximum assembly heat flux (approximately 7300 W/m^2) and the critical heat flux required for departure from nucleate boiling (on the order of 10^6 W/m^2), it can be concluded that the fuel cladding will not be subjected to departure from nucleate boiling even under the postulated accident scenario of the loss of all SFP cooling and the cladding integrity would be maintained.

5.8 REFERENCES

[5.3.1] "QA Documentation for DECOR," Holtec Report HI-971734, Revision 0.

[5.3.2] A.G. Croff, "ORIGEN2 - A Revised and Updated Version of the Oak Ridge Isotope Generation and Depletion Code," ORNL-5621, Oak Ridge National Laboratory, 1980.

[5.5.1] Batchelor, G.K., "An Introduction to Fluid Dynamics," Cambridge University Press, 1967.

[5.5.2] "Validation of FLUENT Version 5.1," Holtec Report HI-992276, Revision 0.

[5.6.1] Rohsenow, N.M., and Hartnett, J.P., "Handbook of Heat Transfer," McGraw Hill Book Company, New York, 1973.

Table 5.3.1

Key Input Data for Decay Heat Computations

Input Data Parameter	Value
Reactor Thermal Power (MWt)	2800
Number of Assemblies in Reactor Core	177
Maximum Number of Storage Cells in SFP	968
Bounding Discharge Schedule	Table 5.3.2
Minimum In-Core Hold Time (hr)	100
Fuel Discharge Rate	5 per hour

Table 5.3.2

Offload Schedule

Cycle Number	Offload Date (mm/dd/yyyy)	Number of Assemblies	Average Burnup (MWd/MTU)	Initial ^{235}U Enrichment (wt.%)[4]	Assembly U Weight (kgU)
1	01/01/2002[1]	76	75,000	4.00	487
2	01/01/2004	76	75,000	4.00	487
3	01/01/2006	76	75,000	4.00	487
4	01/01/2008	76	75,000	4.00	497
5	01/01/2010	76	75,000	4.00	497
6	01/01/2012	76	75,000	4.00	497
7	01/01/2014	76	75,000	4.00	497
8	01/01/2016	76	75,000	4.00	497
9	01/01/2018	76	75,000	4.00	497
10	01/01/2020	76	75,000	4.00	497
11	01/01/2022	76	75,000	4.00	497
12	01/01/2024	76 or 177[2]	75,000	4.00	497
13	01/01/2026	76 or 0[3]	75,000	4.00	497

Table Notes:

(1) Dates are arbitrarily set to yield two years between offloads. While historic (ca. 2002) offloads were on 18-month cycles, the use of the longer 24-month cycle will have a negligible impact on the total SFP heat load. This is due to the use of bounding burnups and initial enrichments for the historic offloads, as well as the extremely long cooling times for these fuel assemblies at the point in time where the SFP becomes filled.

(2) 76 assemblies for partial core offload (previously discharged fuel), 177 assemblies for full core offload (recently discharged fuel).

(3) 76 assemblies for partial core offload (recently discharged fuel), 0 assemblies for full core offload.

(4) Initial enrichments may be as high as 5.0 wt.%. For a given burnup, a lower enrichment will yield a higher calculated decay heat. Thus, the use of 4.0 wt.% is conservative for the purposes of the thermal analysis.

Table 5.4.1

Key Input Data for Time-To-Boil Evaluation

SFP Surface Area	1012 ft^2
Minimum Pool Water Depth	37.0 feet
SFP Net Water Volume	34,340 ft^3

Note: The net water volume is the gross water volume (i.e., area times depth) minus the volume displaced by the fuel racks and stored fuel assemblies.

Table 5.5.1

Key Input Data for Local Temperature Evaluation

Axial Peaking Factor	1.65
Number of Fuel Assemblies	968
Cooled SFP Water Flow Rate through SFC Heat Exchanger	1000 gpm*
Fuel Assembly Type	B&W 15x15
Fuel Rod Outer Diameter	0.430 inches
Active Fuel Length**	140.6 inches
Number of Rods per Assembly	208 rods
Rack Cell Inner Dimension	8.97 inches
Rack Cell Length	162 inches
Modeled Bottom Plenum Height	3 inches

* Conservatively, only one pump flow is credited in the analysis.

** Conservatively, the lowerbound value for the active fuel length for ANO-1 fuel assemblies is used in the analysis.

Table 5.7.1

Result of SFP Decay Heat Calculations

Heat Load Component	Partial Core Offload Value (Btu/hr)	Full Core Offload Value (Btu/hr)
Previously Discharged Fuel	6.064×10^6	5.766×10^6
Recently Discharged Fuel at End of Transfer	15.760×10^6	34.400×10^6
Total Bounding Decay Heat	21.824×10^6	40.166×10^6
SFP Pump Heat (2 operating)	0.204×10^6	0.204×10^6
Total Bounding SFP Heat	22.028×10^6	40.370×10^6

Table 5.7.2

Results of Loss-of-Forced Cooling Evaluations

Calculate Result Parameter	Partial Core Offload Value	Full Core Offload Value
Minimum Time-to-Boil	8.67 hours	3.18 hours
Maximum Boiloff Rate	46.88 gallons per minute	86.28 gallons per minute
Minimum Time for Water to Drop to Top of Racks	62.1 hours	33.7 hours

Table 5.7.3

Results of Maximum Local Water and Fuel Cladding Temperature Evaluations

Parameter	Value
Peak Local Water Temperature	168°F
Peak Cladding Superheat	31.5°F
Peak Local Fuel Cladding Temperature	199.5°F

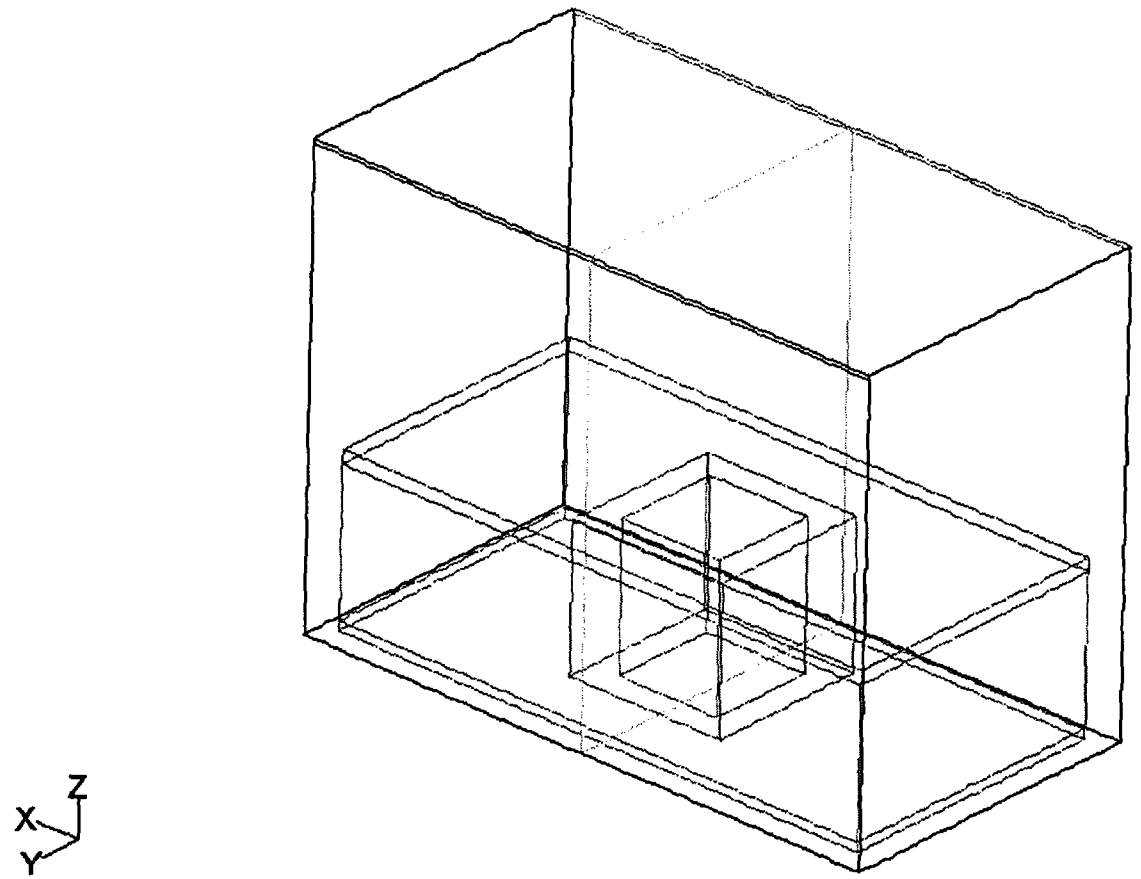

Grid

Feb 15, 2002
FLUENT 5.1 (3d, segregated, ke)

Figure 5.5.1 Schematic of the CFD Model of the ANO-1 SFP.

Figure 5.7.1 - Partial Core Offload Bounding Spent Fuel Pool Heat Load (including previously and recently discharged fuel and 2 SFP pumps)

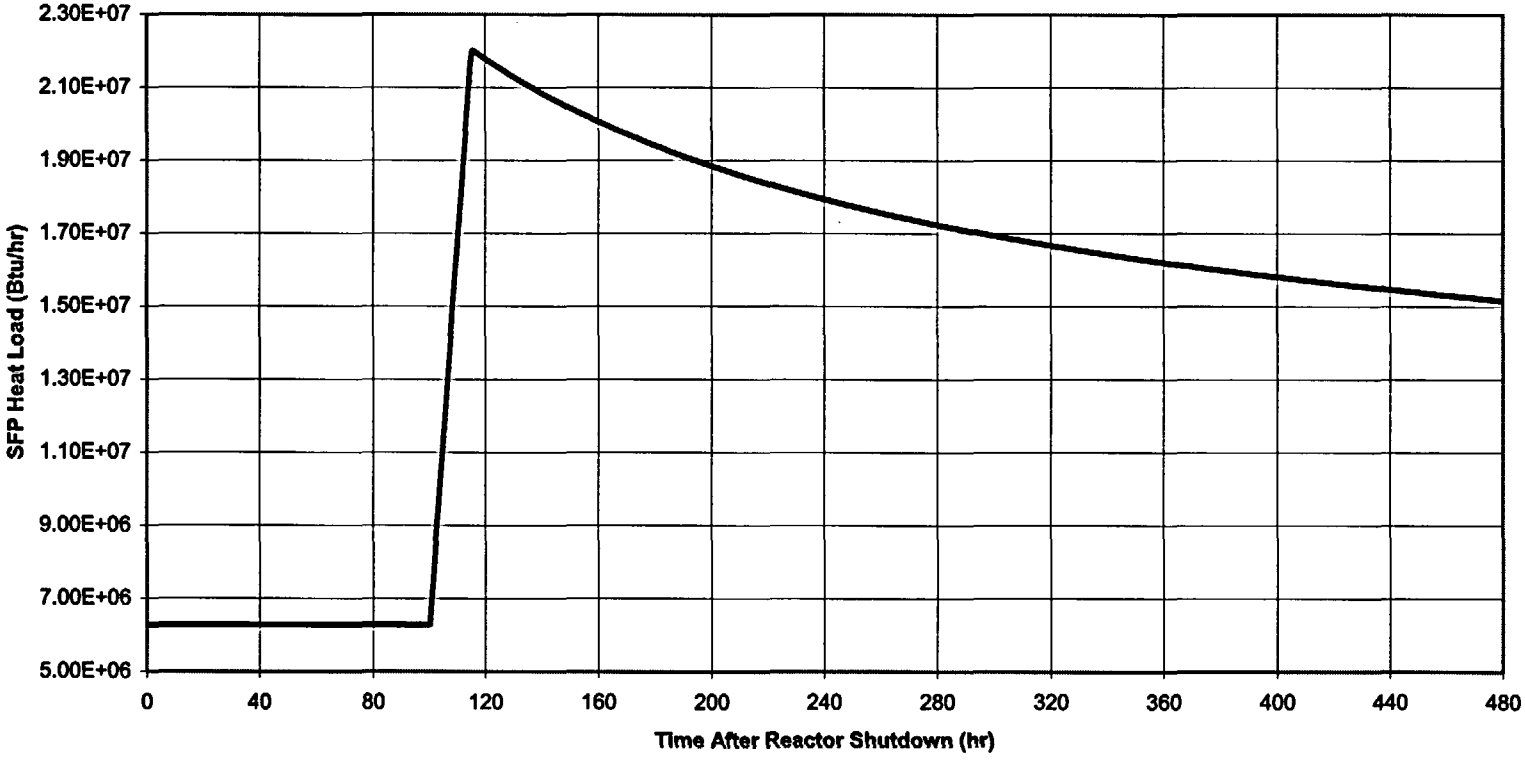

Figure 5.7.2 - Full Core Offload Bounding Spent Fuel Pool Heat Load (including previously and recently discharged fuel and 2 SFP pumps)

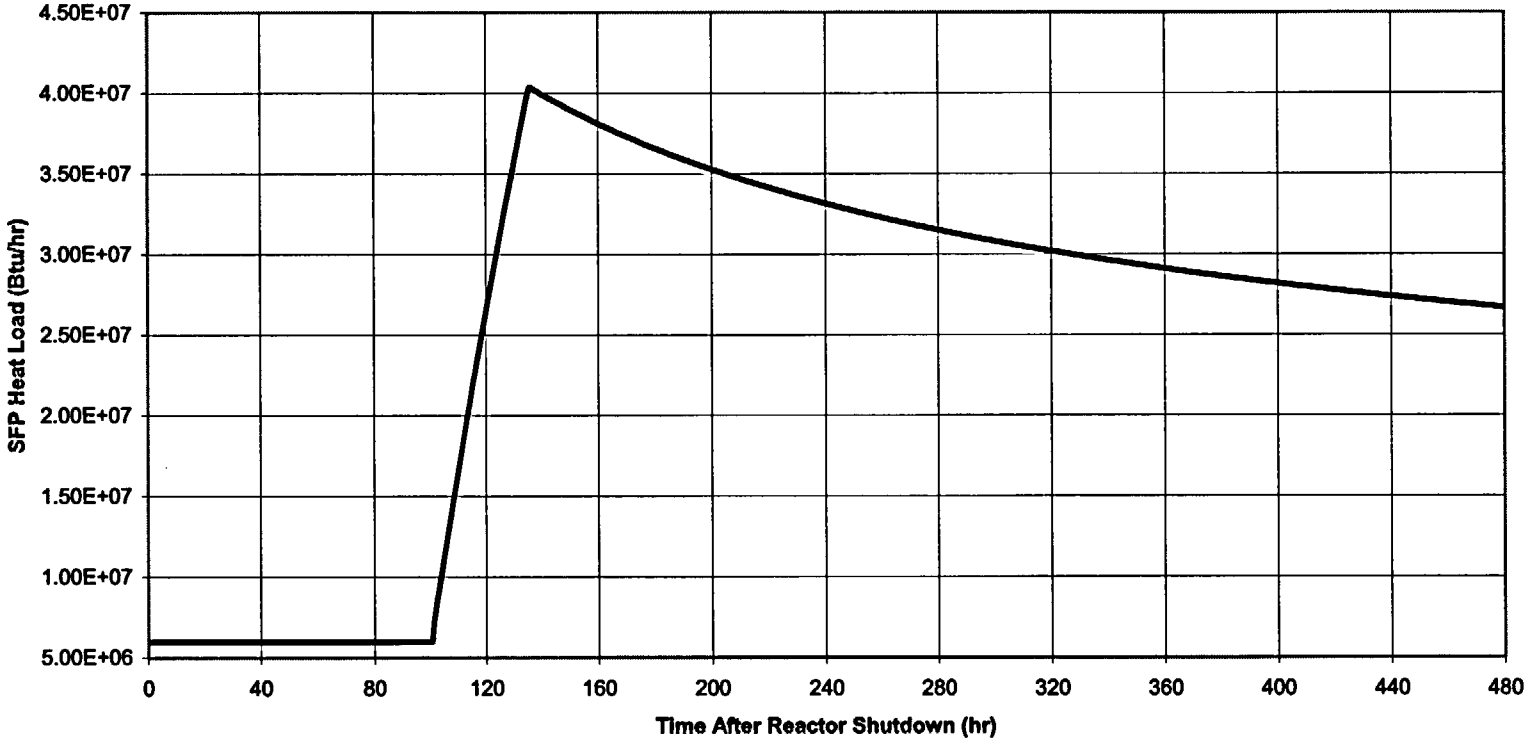

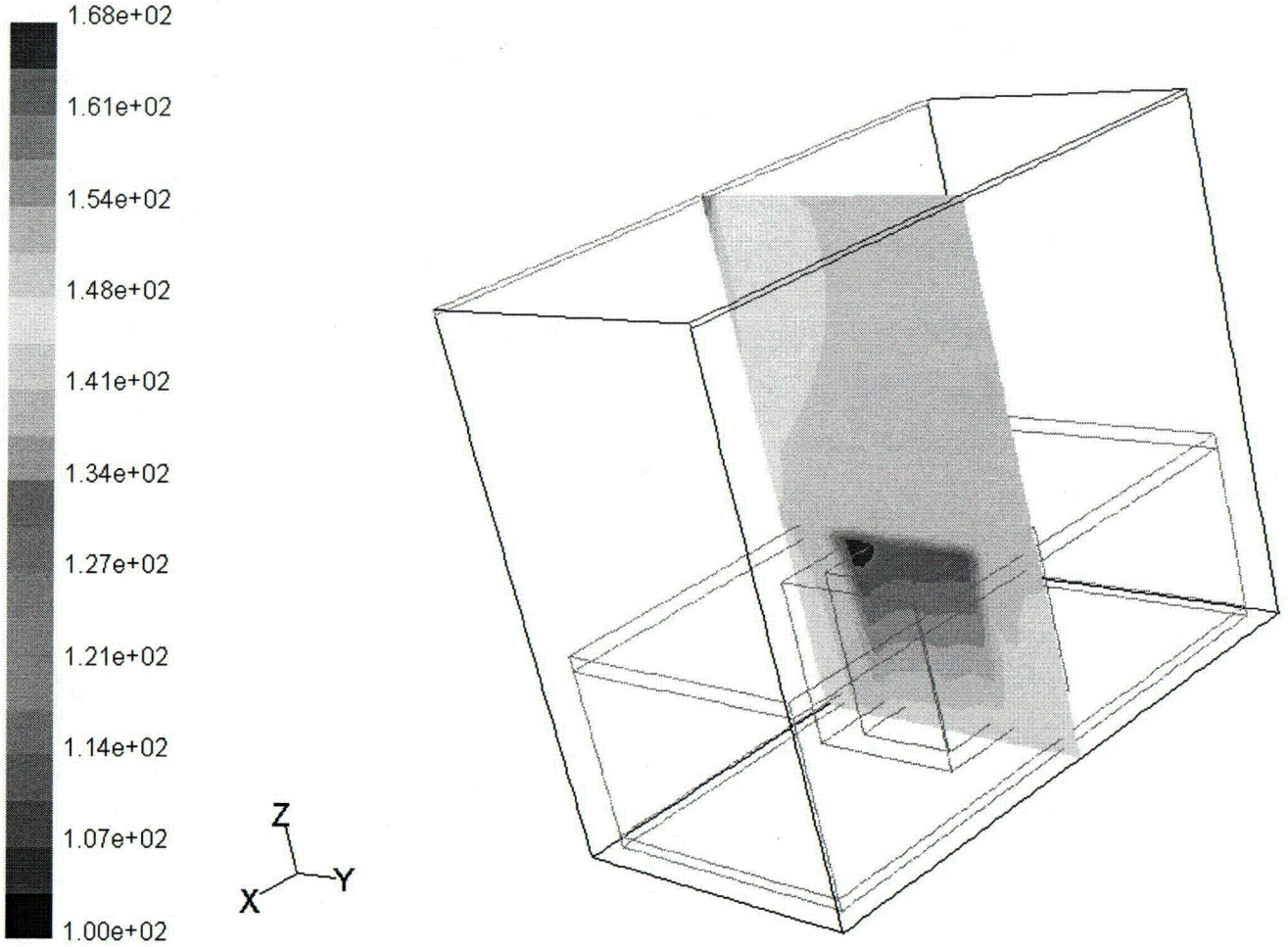

Figure 5.7.3. Contours of Static Temperature In a Vertical Plane Through the Center of the SFP.

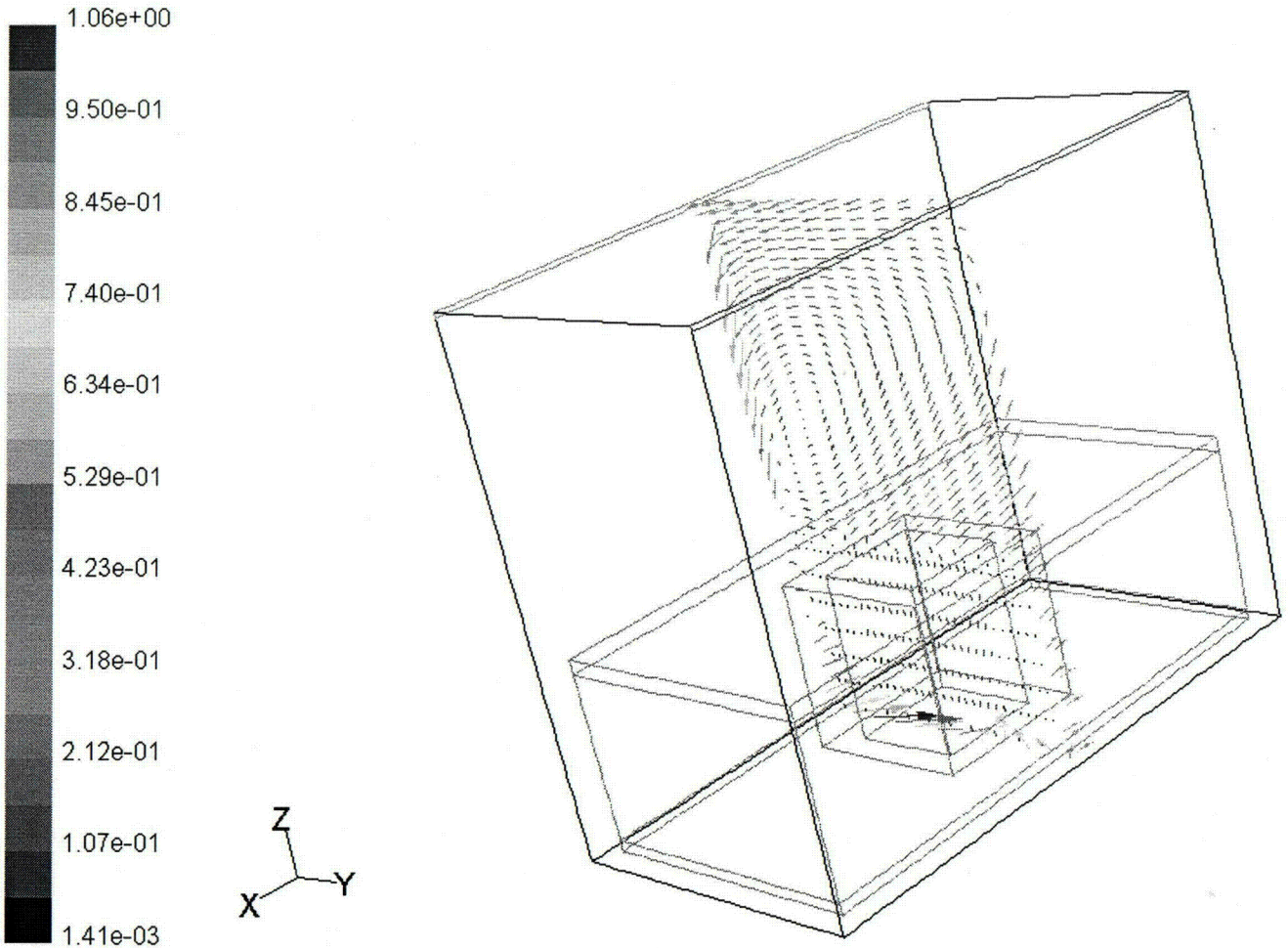

Velocity Vectors Colored By Velocity Magnitude (ft/s)

Jan 26, 2006
FLUENT 5.5 (3d, dp, segregated, ke)

Figure 5.7.4: Velocity Vector Plot In a Vertical Plane Through the Center of the SFP.

6.0 MECHANICAL ACCIDENTS

6.1 INTRODUCTION

The USNRC OT position paper [6.1.1] specifies that the design of the rack must ensure the functional integrity of the spent fuel racks under all credible drop events.

The postulated fuel drop events on the ANO-1 SFP Region 3 racks, which will be inserted with Metamic® material in the rack flux traps with lead-ins installed on the top of flux traps, were evaluated. The principal effect of this postulated drop accident would be damages to the poison material in the Region 3 racks, which would increase reactivity in those storage racks. In this report, the Region 1 racks have been analyzed for criticality safety under the assumption that they do not contain any poison material. The Region 2 racks in the ANO-1 SFP do not contain any poison material. Therefore, the reactivity effects of the postulated fuel drop accident for the Region 3 racks are bounding.

6.2 DESCRIPTION OF MECHANICAL ACCIDENTS

The postulated drop accidents assume that a fuel assembly, along with a portion of the handling tool, will drop vertically and hit the top of the rack at one of two enveloping locations: the cell wall edge or the cell wall corner intersection.

6.3 EVALUATION OF MECHANICAL ACCIDENTS

To obtain conservative results, the postulated mechanical drop accidents were evaluated based on the maximum impact energy, a thinner rack wall thickness, weakest weld size and configuration, and worst case fabrication tolerance for the ANO-1 Region 3 racks. The evaluation of the postulated drop events demonstrated that, with the previously described conservative considerations, the postulated mechanical drop accidents would result in significant damage to the impacted cell wall down into the active fuel region of the racks, leading to the failure of Metamic® inserts inside the flux trap.

6.4 CONCLUSION

The fuel assembly drop events postulated for the ANO-1 spent fuel pool Region 3 racks were conservatively evaluated and found that the poison inserts, as well as the cell wall, of the impacted rack cell could be significantly damaged under the postulated accidental events. To ensure the functional integrity of the rack, the criticality safety evaluation (reported in Section 4.0) conservatively analyzed the Region 3 racks under the postulated assumption that all poison inserts are damaged. The racks were determined to remain subcritical even under this extremely conservative postulated scenario, when credit was taken for a conservative value of 1600 ppm soluble boron in the pool. The minimum technical specification requirement for soluble boron concentration in the pool water is greater than 2000 ppm.

6.5 REFERENCES

[6.1.1] "OT Position for Review and Acceptance of Spent Fuel Storage and Handling Applications," dated April 14, 1978, and addendum dated 1979.